NOVEL APPROACHES TO IMPROVING OPIOID ANALGESIC THERAPY

by

David Isaiah Duron

A Dissertation Submitted to the Faculty of the

DEPARTMENT OF PHARMACOLOGY

In Partial Fulfillment of the Requirements
For the Degree of

DOCTOR OF PHILOSOPHY

In the Graduate College

THE UNIVERSITY OF ARIZONA

2020

THE UNIVERSITY OF ARIZONA
GRADUATE COLLEGE

As members of the Dissertation Committee, we certify that we have read the dissertation prepared by David I. Duron titled Novel approaches to improving opioid analgesic therapy and recommend that it be accepted as fulfilling the dissertation requirement for the Degree of Doctor of Philosophy

Prof. John M. Streicher — Date 2/11/2020

Prof. Patrick Ronaldson — Date 7 FEB 2020

Prof. Nam Lee — Date 10 Feb 2020

Prof. Ronald Lynch — Date 11 Feb, 2020

Prof. Todd Vanderah — Date 10 Feb 2020

Final approval and acceptance of this dissertation is contingent upon the candidate's submission of the final copies of the dissertation to the Graduate College.

I hereby certify that I have read this dissertation prepared under my direction and recommend that it be accepted as fulfilling the dissertation requirement.

Dissertation Director: John M. Streicher — Date 2/11/2020

ACKNOWLEDGEMENTS

I first want to acknowledge my mentor John Streicher, PhD for giving me the opportunity to work within his lab and promoting free expression of thoughts and ideas within his lab. I would like to acknowledge my committee members as well for providing me with direction and furthering my academic development. I would also like to thank Wei Lei, PhD for providing the scientific basis for my initial project and also for his training and troubleshooting assistance of various procedures within the lab. I would next like to thank the other graduate students within my lab Justin LaVigne and Seph Palomino for their intellectual contributions and also for their friendship. I would like to also thank the rest of my current/former lab members namely Atilla Keresztes, PhD, Carrie Stine, and Gaby Molnar for their assistance and support within the lab. Finally, I would like to thank my friends and family for their emotional support.

DEDICATION

I dedicate this to my parents who despite their differences have always supported me throughout my life in all my endeavors.

TABLE OF CONTENTS

LIST OF FIGURES

LIST OF TABLES

ABSTRACT

Despite their extensive side effect profile and potential for abuse, clinically used opioids such as morphine are still the most effective analgesics for most chronic pain patients. A negative stigma has been cast over opioids due to the recent opioid epidemic, which has claimed hundreds of thousands of lives over the past few decades in the United States alone. Despite this, there is still great potential for the use of these drugs if negative side effect profiles, especially reward and addiction, can be reduced or eliminated. Here we identify a pharmacological and non-pharmacological means for enhancing analgesic potency while reducing side effect profiles attributed to systemic morphine. We have uncovered a novel regulator of downstream mu opioid receptor (MOR) signaling within the spinal cord, heat shock protein 90 (HSP90). Within the spinal cord, HSP90 prevents MOR induced ERK MAPK phosphorylation which otherwise activates RSK2 and subsequent translation, leading to enhanced morphine induced anti-nociception. By selectively inhibiting HSP90 within the spinal cord, morphine induced anti-nociception is elevated without impacting side effects, and therefore allows for a dose reduction strategy while achieving equi-efficacious anti-nociception. Additionally, we have uncovered a novel consequence of dietary intervention on opioid pharmacology. Through daily intermittent fasting (IF), morphine induced anti-nociception is enhanced and prolonged, while several side effects including reward, constipation, and tolerance are reduced. MOR functionality but not expression within various brain regions is altered due to daily IF which may account for the behavioral differences in systemic morphine treatments seen with IF. These two approaches attempt to alter opioid pharmacology not by modifications to new drugs, but by altering opioid physiology to maximize the desired effect of anti-nociception while reducing side effects. Together these novel approaches

may allow for rapid translation into the clinic and lead to additional research efforts to improve existing opioids with the aim of treating chronic pain in patients while reducing side effects and abuse.

CHAPTER 1: INTRODUCTION TO PAIN

In recent years, acute and chronic pain have had an economic burden in the United States of more than 600 billion U.S. dollars every year [1, 2]. This economic burden stems primarily from lost productivity of workers suffering from pain conditions and the cost of health care to treat these individuals [3]. It is estimated that a minimum of 50 million American adults suffer from chronic pain on a current yearly basis, equating to roughly 20% of the entire American adult population [4]. This growing pain population within the United States is tied to a variety of factors including an increasing elderly population, high prevalence of physical and mental pathologies, and decline in general health potentially linked to poor nutrition and/or physical upkeep [5-8]. The chronic pain epidemic, along with an inadequate analgesic repertoire, has spurred a substantial surge in research efforts toward pain management strategies and analgesic drug discovery. Much is known about the basic mechanisms of acute pain sensation, but much less is known about chronic pain, the mechanisms of specific chronic pain states, and molecular mechanisms which can be used for the development of novel therapeutic strategies.

Pain is characterized by a distressful sensory, emotional, and cognitive experience. This experience is often evoked through a noxious external stimulus which may elicit tissue damage, though many pain conditions and disorders (e.g. migraine) lack this external stimulus. From an evolutionary perspective, pain is a critical sensory component for alerting the body to a potentially harmful stimulus. Nociceptive pain or nociception is a term which refers to the sensory component of pain alone. The majority of analgesic compounds prevent neuronal action potentials within these nociceptive sensory circuits and thus prevent the perception of pain. Many pain conditions such as

migraine and neuropathic pain may elicit pain through alternative circuits and mechanisms to the general dogma and thus classical medications have minimal efficacy [9, 10]. Despite these exceptions, the most efficacious clinical analgesics such as opioids act on these classical nociceptive circuits (Fig. 1), and a complete understanding of these circuits and signal transduction events are critical for the development of novel analgesics and pain management strategies.

Noxious stimuli often begin externally but can have central and/or visceral origins as well. These noxious stimuli include mechanical, temperature, and chemical varieties. Noxious mechanical stimuli examples include sharp puncture, pressure, and other direct physical tissue trauma. Noxious temperature stimuli include excess heat and cold. Noxious chemical stimuli include strong acids, strong bases, and other chemical irritants. Despite the physical differences in these stimuli, they all lead to the depolarization of primary afferents of the Aδ and C fiber types. Aδ are typically activated by mechanical and temperature stimuli, while polymodal C fibers can be activated through mechanical, temperature, and/or chemical stimuli [11]. The depolarization of these free nerve endings is achieved through a variety of mechanisms. Mechanical stimuli activate mechanosensitive Piezo channels which allow for a direct non-selective influx of cations including Na^{+}, Ca^{++}, and Mg^{++} [12]. Hot and cold stimuli activate temperature sensitive transient receptor potential (TRP) channels which similarly allow for a direct influx of cations [13]. Chemical stimuli include a variety of different subtypes which elicit neuronal depolarization. These can include the opening of ion channels for the influx of cations in the case of ATP and protons, which open the ligand gated ion channels P2X and acid-sensing ion channels (ASICs) respectively [14, 15]. Other chemical stimuli activate G-protein coupled receptors (GPCRs) such as subsets of EP receptors activated by prostaglandins and P2Y receptors activated by ATP [16, 17]. These GPCRs are typically

Figure 1

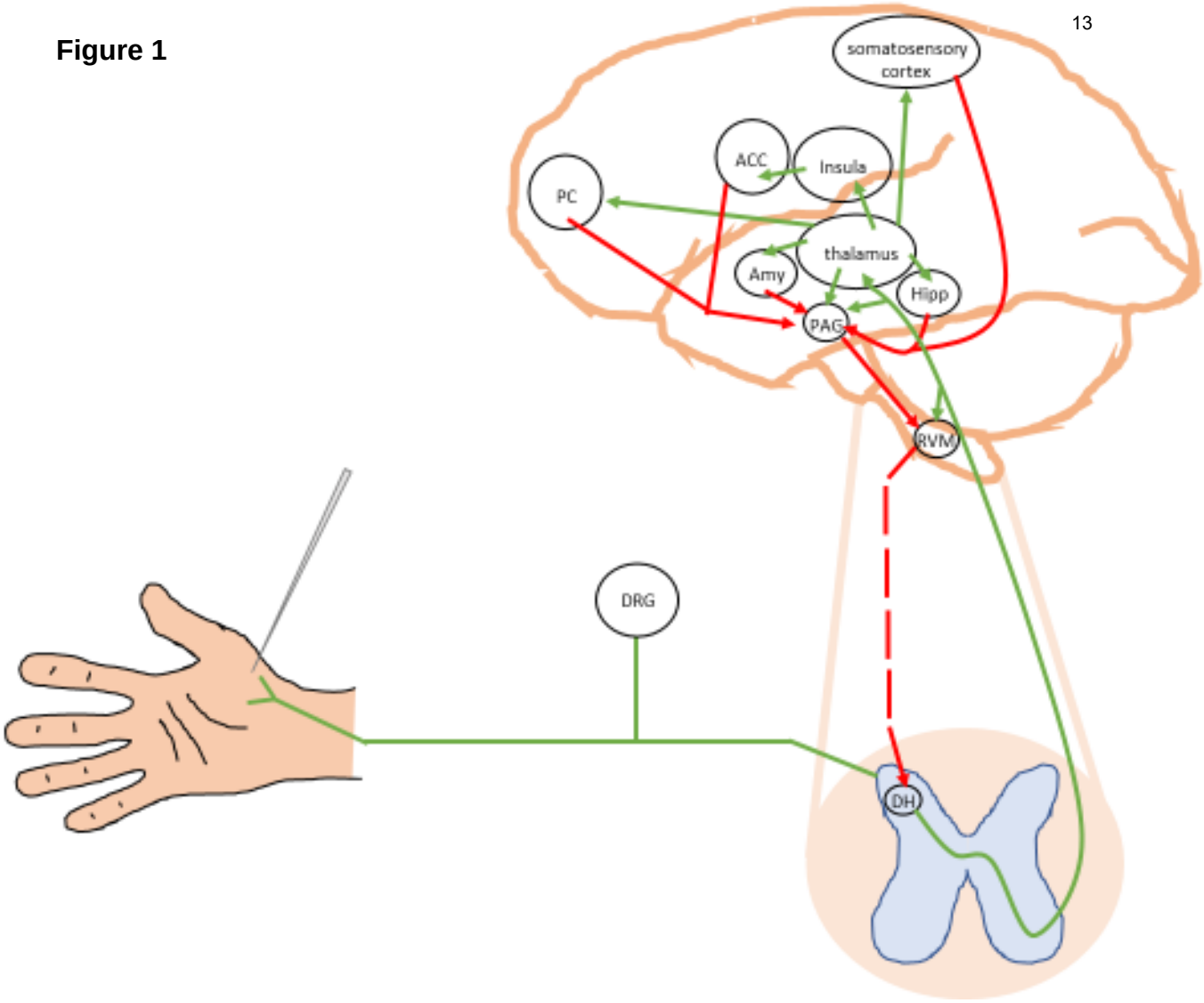

Figure. 1 - Diagram of classical nociceptive circuitry

Nociceptive input begins in the periphery with a noxious stimulus. This stimulus results in an action potential from nociceptive free nerve endings in the periphery. That signal is transmitted to the dorsal horn of the spinal cord via first order nociceptors. Secondary neurons in the spinal cord dorsal horn then transmit their signal up to the thalamus, with input into the periaqueductal PAG and RVM as well. The thalamus then projects third order inputs into various areas of the brain. Descending nociceptive modulation occurs primarily through the PAG and RVM from various regions ultimately resulting in inhibitory input within the dorsal horn of the spinal cord. ACC, anterior cingulate cortex; PC, prefrontal cortex; Amy, amygdala; Hipp, hippocampus; PAG, periaqueductal gray; RVM, rostral ventromedial medulla; DH, spinal cord dorsal horn; DRG,

dorsal root ganglion. Green arrows indicate ascending circuitry, red arrows indicate descending circuitry. Not meant to be anatomically accurate.

either $G\alpha_s$ or $G\alpha_q$ coupled and therefore indirectly elicit depolarization through kinase activity on ion channels. The more recognized kinases activated by these GPCRs are Protein Kinase A (PKA) and C (PKC) which may directly or indirectly lead to the phosphorylation of ion channels allowing for the influx of cations [18]. If the threshold for action potential is reached, these depolarization events will allow for the opening of voltage-gated (VG) Na^+ channels and initiation of an action potential, concluding the first step in nociception.

The cell bodies of Aδ and C fibers are located within dorsal root ganglia (DRG) adjacent to the spinal cord [11]. Aδ fibers are heavily myelinated and therefore action potentials are transmitted quicker than the less myelinated C-fiber, resulting in quick “sharp” pain versus slow “burning” pain sensations respectively [19]. The electrical signal travels up the primary afferent to the pseudo-unipolar neurons within the DRG which then projects primarily to lamina I-II of the dorsal horn of the spinal cord. Within these lamina primary neurons synapse onto second order neurons which will project to either motor neurons for a muscle reflex or up the spinothalamic tract [20]. This synapse between primary and secondary afferents involves several known excitatory neurotransmitters and receptors. Some of the more well-known neurotransmitters released in this synapse are glutamate, substance P (SP), and calcitonin gene related peptide (CGRP) which act on various channels and receptors post-synaptically [20]. Glutamate elicits depolarization through the ligand gated cation channels α-amino-3-hydroxy-5-methyl-4-isoxazolepropionic acid receptor (AMPAR) and N-methyl-D-aspartate receptor (NMDAR), and through the GPCR metabotropic glutamate receptor (mGluR) [21]. SP activates an excitatory GPCR, the Neurokinin 1 (NK1) receptor [22]. CGRP also activates an excitatory GPCR, the CGRP receptor, which is typically

composed of a multi-protein complex of the calcitonin receptor-like receptor (CLR), receptor activity-modifying protein (RAMP), and receptor component protein (RCP) [23].

Second order neurons which receive excitatory input from primary nociceptors project up through the spinothalamic tract and eventually transmit excitatory signals to third order neurons wither in the thalamus for further distribution to higher cortical areas to provide affective processing to the initial sensory pain stimulus or to the periaqueductal grey region (PAG) for descending modulation of pain [24]. The PAG is a region within the midbrain which is highly involved in the descending modulation of pain through mechanisms like the endogenous opioid systems [25]. While some of the cortical areas projected to from the thalamus include: the insula which provides the feeling of disgust, the somatosensory cortex which provides the localization of the pain stimulus, the amygdala which provides emotional context to the pain stimulus, the cingulate cortex which adds motivational context to the pain stimulus, the prefrontal cortex which adds decision making and empathy aspects to the stimulus, and the hippocampus which provides the memory and learning components to the stimulus.

Although pain is a critical sensory warning for a potentially threatening stimulus, it can become debilitating if left unchecked. Therefore, natural selection has resulted in a descending pain modulatory circuit which endogenously inhibits pain. Second order neurons within the classical nociceptive circuit projecting from the thalamus to the PAG are involved in this descending modulation of pain. Descending circuits may also originate from higher cortical brain regions such as the ACC, amygdala, insula, cortex, and hypothalamus [26]. Neurons within the PAG then project to the nucleus raphe magnus (NRM) located within the rostral ventral medulla (RVM), which in turn project to laminas I and II of the dorsal horn where they can inhibit the transmission of the nociceptive signals between primary and secondary afferents [24, 27]. This inhibition

occurs through a variety of neurotransmitters including norepinephrine, serotonin (5-HT), endorphins, and enkephalins, which act on several $G\alpha_i$ coupled GPCRs including α2 adrenergic receptors (α2R), several subsets of 5-HT1 receptors, mu opioid receptors (MOR), and delta opioid receptors (DOR), both pre- and post-synaptically [28, 29]. Typically, this descending circuitry is thought to be inhibited via gamma-aminobutyric acid (GABA)-ergic interneurons within the PAG and RVM which can be inhibited through the release of endogenous endorphins acting at the MOR within these GABAergic neurons, resulting in disinhibition of the descending pain modulatory circuit and the promotion of anti-nociception [30]. Within the RVM, there is the presence of “on” and “off’ cells which are named based on their response to nociceptive input. “On” cells demonstrate increased activity when presented with nociceptive input, which is thought to promote nociception. “Off” cells demonstrate a reduction of firing rate under the same conditions, and are thus thought to be anti-nociceptive. Activation of “off” cells with a MOR agonist yields an anti-nociceptive effect, and it has been proposed that the inhibition of “on” cells may also yield anti-nociception [31].

The above described circuitry, both pro- and anti-nociceptive, has mostly been studied in the context of acute pain sensation, which is relatively well-understood. In contrast, much less is known about the mechanisms of chronic pain, and how or when acute pain states (injury, etc.) transition to chronic pain. Chronic pain in humans is generally classified as a pain state which persists for 3 months or more [32]. This general classification can be further broken down into more specific pain types which include headache, post-trauma pain, arthritic pain, cancer pain, neuropathic pain, and psychogenic pain, to name a few [32]. These pain types can then be broken down even further to address the initial cause of pain which can be due to various disease/disorders, age, medication use, and other physiological factors [33]. These

subclassifications make the research and treatment of chronic pain extremely complex and difficult. Due to these difficulties, many have turned their attention toward personalized medicine for the treatment of these various pain types, but drugs which have a more generalized application allow for are more cost effective and therefore more desirable within clinics [34]. For the case of chronic pain, opioid analgesics have been heavily prescribed due in large part to a lack of better options. The various negative properties of these opioid drugs have synergized with heavy and increasing prescription rates over the past 20 years, which has now culminated in a new opioid abuse and overdose epidemic.

CHAPTER 2: TREATMENT OF PAIN: OPIOIDS

Opiates have been used by human civilizations to treat pain for thousands of years [35, 36]. There is even evidence for the use of opium poppy plants discovered in Neolithic culture sites in the Iberian Peninsula [37]. Opiates are classically defined as drugs derived from the opium poppy plant, while modern day pharmacology and drug discovery efforts have yielded a variety of both natural and synthetically derived compounds which bind to opioid receptors [38]. The modern term “opioid” describes this more comprehensive category of drugs. Opioids can be effective for the treatment of several pain states in humans, but they also have a large negative side effect profile. The side effect profile for opioids includes, among others: constipation, analgesic tolerance, addiction/dependence, and respiratory depression [39]. Constipation and analgesic tolerance become an increasing issue in the treatment of chronic pain when continuous opioid administration is necessary [40, 41]. Constipation can be incredibly debilitating to quality of life for patients, while analgesic tolerance requires escalating doses to achieve an equal analgesic effect and therefore enhances negative side effect complications. Addiction stems from the rewarding properties of opioids, can further increase the odds for developing physical dependence, and are at the root of the cause for the current opioid epidemic which plagues the United States [42, 43]. Respiratory depression is the primary cause of death with opioid overdose and significantly reduces the therapeutic window of opioids as analgesics [44]. These negative side effects make opioids extremely dangerous medications which should be used with extreme care.

Several alternatives to opioid analgesics exist in the clinic today. Some of the pharmacological options include cannabinoids, nonsteroidal anti-inflammatory drugs (NSAIDs) and acetaminophen. Other non-pharmacological options include physical

therapy, acupuncture, and diet/exercise. Experimental drugs and therapeutics include gene therapies, drug delivery systems, and novel small molecules and peptide drugs targeting ion channels and receptors within the above-mentioned nociceptive circuit. The issue with these options is that the currently available drugs and therapies are simply limited by their efficacy and the experimental drugs and therapies are still limited by a lack of preclinical and clinical progress. With this said, opioids are already used clinically and have demonstrated high efficacy in the treatment of several pain states.

Unfortunately, opioids throughout history have been significantly abused. This abuse potential paired with external factors such as false advertisement, a careless healthcare system, and significant over prescription have now led to the modern-day opioid epidemic [45-48]. This epidemic burdens millions of Americans with opioid abuse disorder and worse still, claims thousands of lives on a yearly basis [49]. Despite this, opioids remain our most effective pain medications and a significant portion of research has been designated to the study of opioid receptor systems and discovery of novel drugs and methods to achieve a safer and more effective opioid based treatment for pain [50].

At the molecular level, opioid agonists produce their effects through activation of a specific subset of $G\alpha_i$ coupled GPCRs deemed opioid receptors. There are multiple types of opioid receptors; the three most extensively studied receptors are the mu (MOR), delta (DOR) and kappa (KOR) opioid receptors. The majority of clinically used opioid analgesics are either full or partial agonists at MOR. Efforts for the use of DOR and KOR agonists as analgesics have been made but these drugs generally have limited efficacy and can produce seizures and dysphoria/hallucinations respectively [51, 52]. Therefore, our lab focuses on modulating MOR signal transduction to enhance opioid analgesic activity while reducing side effects.

From a physiological perspective, activation of MOR by an agonist prevents action potential propagation within neuronal nociceptive circuits; therefore the location of the MOR within these circuits is critical for changes in behavioral output [53]. MOR is expressed in a variety of locations, but the locations thought to be primarily involved in the anti-nociceptive effects of opioid agonists are those involved in descending modulation of pain, namely the PAG, RVM, and spinal cord [54]. Activation of MOR within these locations can directly inhibit the firing of neurons within nociceptive circuits, which can be activated by exogenous drugs as well as descending modulatory neurons leading to a release of endogenous opioids [55, 56].

Side effects such as euphoria/reward, constipation, and respiratory depression exhibit their effects in other regions. Euphoria occurs due to the disinhibition of GABAergic neurons in the ventral tegmental area (VTA) allowing for dopamine release into the nucleus accumbens (NAc) [57]. Constipation occurs within the enteric nervous system whereby the inhibitory effects of MOR activation prevents peristalsis and promotes water absorption within the gastrointestinal system [58]. Respiratory depression occurs within the pre-Bötzinger complex in the medulla of the brainstem where MOR activation inhibits autonomic firing of neurons responsible for rhythmic respiration [59, 60]. The location of MOR activation is therefore critical for a specific analgesic response to opioid agonists; but equally important is the molecular signaling mechanisms that link MOR activation to neuronal activity changes in MOR-expressing neurons.

Like all GPCRs, the binding of an opioid agonist to this 7 transmembrane domain protein causes a conformational shift which promotes the release of GDP from the alpha subunit of the heterotrimeric G protein [61, 62]. Once released, GTP is then able to bind and causes a dissociation of the alpha subunit from the beta/gamma subunits [63]. Once

dissociated, both subunits are now in their active state and produce respective downstream signaling [64, 65]. In the case of the MOR, the alpha subunit is of the i subclass and upon dissociation will inactivate adenyl cyclase (AC). Once inactivated, AC is prevented from activating cyclic adenosine monophosphate (cAMP) production and subsequent kinase activation including protein kinase A (PKA) [66-68]. It is thought that this PKA inactivation and beta/gamma subunit activation are the primary driving factors for the inactivation of N-type voltage gated (VG) Ca^{++} channels and the activation of G protein-coupled inwardly-rectifying potassium channels (GIRKs) respectively [69-71]. It should also be noted that the activated beta/gamma subunit has also been shown to have several other direct and indirect effector molecules including but not limited to p21-activated protein kinase, PI3K, Raf-1, and phospholipase A and C [72-76]. The inactivation of VG Ca^{++} channels in a presynaptic terminal will prevent Ca^{++} dependent neurotransmitter release [77]. The activation of GIRKs will cause an efflux of K^{+} ions and subsequent hyperpolarization [78]. Hyperpolarization will decrease the odds of an action potential occurring both pre and post synaptically [79]. When these mechanisms occur within nociceptive circuits mentioned above, there is a suppression of the nociceptive neuronal transmission which results in pain relief.

In addition to the MOR signaling mentioned above, there are a variety of other MOR signaling mechanisms which have been investigated to an extent. After activation, MOR is then rapidly desensitized [80]. Desensitization begins with the phosphorylation of MOR by G protein-coupled receptor kinases (GRKs) [81]. The phosphorylation of MOR then promotes the binding of β-arrestins (β-Arr), formation of clathrin coated pits, and internalization of endosomes containing the MOR complex [82]. The relatively acidic pH of these endosomes reduces the ligands affinity for MOR and allows for the dissociation of β-Arr [83]. MOR can then be dephosphorylized by phosphatases, and

either reinserted into the membrane or transferred to lysosomes for degradation [84]. This desensitization mechanism is critical in downstream signaling events as well. β-Arr is thought to produce diverse mitogen-activated protein kinase (MAPK) pathways including ERK, p38, and JNK signaling thought to lead to modifications to transcription [85]. Among these effectors, it is also thought that additional β-Arr effectors may be involved in opioid side effects such as constipation, respiratory depression, and tolerance [86]. Evidence for differential behavioral effects based on specific molecular signaling has led to a significant drug discovery effort into biased opioid agonists which lack β-Arr signaling activation [87]. Despite this, downstream MOR signaling events and their subsequent effectors have not been extensively studied and therefore there is a need for further research into these areas which could potentially lead to further drug discovery efforts.

CHAPTER 3: IMPROVING OPIOID TREATMENT

Many strategies are currently under investigation to improve the treatment of pain. Some groups have opted to investigate non-opioid targets including cannabinoid receptors, the neurokinin-1 (NK-1) receptor, and pain related subsets of ion channels such as Nav1.7 [88]. Other groups have focused their efforts towards biased opioid agonists or bivalent molecules to produce specific molecular signal cascades that produce analgesia without side effects [89, 90]. Additionally, efforts are also being made for drug delivery systems to specific tissues to avoid regions which produce side effects [91]. Finally, there are also a few groups which aim to modulate opioid agonist pharmacodynamics through alternative approaches. Two examples of this are through the modulation of MOR signaling with additional compounds to lead to a preferred analgesic specific outcome, and non-pharmacological modulation of endogenous opioid systems through practices such as diet modification [92, 93].

OPIOID SIGNALING MODULATION: HEAT SHOCK PROTEIN 90

Many aspects of MOR physiology and molecular signaling are still poorly understood. One previous study performed a meta-analysis from available proteomic reports from animal and human brain tissue to identify protein expression changes after morphine and/or heroin exposure [94]. This study suggested heat shock protein 70/90 organizing protein (Hop) as a potential target in morphine induced signaling, as it was increased in response to chronic opioid treatment in the brain. Although there are very few specific inhibitors for this protein, it’s known to modulate the function of heat shock protein 90 (HSP90) which could serve as the most suitable target considering the variety of available inhibitors.

HSP90 is a chaperone protein which makes up roughly 2% of the total protein pool in a given cell [95]. This expression can then be increased up to 6% of the total protein pool upon stress conditions [96]. HSP90 has been found to be involved in numerous cellular processes which can be regulated by several factors including: the HSP90 isoform, the formation of specific co-chaperone complexes, and other ongoing cellular functions [97, 98]. Identified functions in which HSP90 is involved includes: protein folding, kinase modulation, transcription factor activation, and many others [99, 100]. HSP90's ability to modulate kinase function makes it a promising candidate as a signal transduction modulation target [101, 102]. Despite this, due to the high expression of HSP90 in tumor cells, HSP90 has been primarily researched within the context of cancer pathology [103]. Therefore, there is a need for further investigation of HSP90 function within receptor-mediated signal transduction such as in the case of MOR signaling.

Previous research within our lab has demonstrated that the inhibition of HSP90 in the brain with either the N-terminal inhibitor 17-(Allylamino)-17-demethoxygeldanamycin (17-AAG) or the C-terminal inhibitor KU-32 prevents systemic morphine induced anti-nociception in mice. Additionally, the inhibition of HSP90 in the brain prevents DAMGO-induced ERK phosphorylation within the PAG, and the inhibition of ERK within the brain recapitulates the loss of morphine induced anti-nociception seen with HSP90 inhibition. Therefore, HSP90 activity and ERK phosphorylation within the brain are necessary for systemic morphine induced anti-nociception [104]. Along with these findings, the use of selective HSP90 isoform and co-chaperone inhibitors, and CRISPR verification, has attributed this promotion of morphine induced anti-nociception to a co-chaperone complex involving HSP90-alpha, p23, and Cdc37 within the brain [105].This study was restricted to HSP90's role in MOR signaling within the brain and PAG. Further

investigations for HSP90 in MOR signaling within the brain, PAG and other MOR expressing regions such as the RVM, VTA, and spinal cord may yield additional insights into MOR signaling and gain a more comprehensive understanding of HSP90s role as a downstream GPCR signaling modulator. We hypothesized that similar to the brain, spinal cord HSP90 inhibition would result in a loss of morphine induced anti-nociception through a prevention of ERK phosphorylation. Exploring the signaling regulation of the MOR by HSP90 could lead to future drug discovery strategies to utilize selective HSP90 inhibitors or modulators to improve the therapeutic index of opioid treatment.

NON-PHARMACOLOGICAL OPIOID MODULATION: DIET AND INTERMITTENT FASTING

Today's United States culture has grown accustomed to the convenience of modern medicine and pharmacology which has exponentially surged over the past few centuries [106]. This surge has allowed for an extension of life span, growth in the economy, and increased quality of life [107-109]. In general, both the therapeutic benefits and negative side effects of drugs act on existing physiological processes in the human body. Historically, pharmacological research has been focused on the synthesis of drugs with the aim of improving or correcting normal/abnormal physiological processes. This has led to a vast library of compounds which are now available for clinical use and seemingly boundless libraries of compounds which have yet to be fully investigated. With the development of these massive libraries of drugs, we can now begin to approach pharmacological research from a different perspective. Namely, is it possible to change the existing physiology of an individual through non-pharmacological means to alter the pharmacodynamics and/or kinetics of a drug for a safer and more effective therapy? Some of these non-pharmacological processes which shape human physiology include: diet, exercise, and sleep quality [110-112]. Modulating therapy

through these means has the further benefit of being low-cost, relatively high compliance, with no or essentially no side effects.

With respect to opioids in particular, there have been numerous studies aimed at how several positive and negative dietary archetypes might impact certain opioid physiological processes and subsequent pharmacology. Mediterranean diets have been shown to reduce mesolimbic neuroplasticity and relapse after chronic morphine use in mice. [113]. The high fat western diet has been demonstrated to increase morphine anti-nociceptive tolerance, reduce morphine antinociception, and cause dysregulation of endogenous opioid systems in mice [114, 115]. Additionally, rats who are fed more “palatable” substances demonstrate enhanced analgesic properties of exogenous opioids [116]. These findings may not necessarily be surprising considering numerous studies which have demonstrated the role of endogenous opioids in food reward and selection [117]. Therefore, opioids likely have impacts on food related processes and vice versa.

With several diets demonstrating positive and negative impacts on exogenous opioid pharmacology, we can begin the process of identifying diets which enhance desired properties of opioids and reduce negative properties. One such candidate for this is intermittent fasting (IF). Intermittent fasting is a time restriction feeding strategy which has recently grown in popularity as a weight management strategy. The idea behind this diet is to mimic the hypothesized eating patterns of our ancestors [118]. There is a general consensus that our ancestors routinely went through periods of fasts due to limitations in food availability and storage [119]. There are several IF methods which have yielded physiological benefits in both human and rodent studies [120]. The more common methods are: monthly fasting (2-5 days once a month), weekly fasting (2 days per week), alternate day fasting, and daily time restricted feeing (16-22 hours per

day) [121, 122]. Some of the benefits of these IF methods include: reduction in proinflammatory cytokines, positive alterations in hormones, increased life span, and prevention and/or mitigation of pathologies such as cardiovascular disease, gastrointestinal disorders, metabolic disorders, and neurodegenerative disorders [118, 120, 121, 123, 124]. To date there are several studies which suggest that acute fasting can impact opioid systems, but there are only two studies which investigate the impacts of continuous IF on opioid systems. The first of which suggests an anti-nociceptive effect of IF through the kappa opioid system, and the second suggests circadian dependent increased morphine induced anti-nociception with IF mice [125, 126]. While intriguing, these studies did not examine the impact of IF on opioid therapy itself; the impact on analgesia vs. side effects (therapeutic index). The literature does suggest that such a link exists, but has not been experimentally tested [127]. The research carried out within this study aims to assess IF as an adjunct therapy to opioid treatment, and the mechanisms by which any benefits and/or adverse effects might occur. We hypothesized an enhancement in morphine induced anti-nociception in IF mice and a reduction of side effects, which may allow for an opioid dose reduction strategy to improve the therapeutic index of opioid treatment.

CHAPTER 4: HSP90 MODULATION OF OPIOID SIGNALING IN THE SPINAL CORD

INTRODUCTION

The current available therapeutics for the treatment of chronic pain are largely limited by their efficacy and undesired side effects. With over 100 million individuals suffering from chronic pain, and an economic burden exceeding $600 billion in the United States alone, chronic pain remains an area of critical and growing medical need [128, 129]. One of the more efficacious therapeutic options for the treatment of a variety of pain states are opioid analgesics, such as morphine. Although these drugs can be very effective acutely, their side effects such as tolerance, addiction, and respiratory depression make them a high-risk choice when dealing with continuous medication regimens [130, 131]. Accompanying these negative side effects is a growing social awareness of the potential dangers of opioids that have begun to negatively stigmatize their use, abetted by a growing opioid abuse and addiction crisis, despite their great potential as analgesics [132].

Intensive research over decades has revealed a complex signaling network evoked by opioid treatment downstream of the μ-opioid receptor (MOR)[133]. Increased understanding of the complexity of MOR signal transduction has resulted in new efforts for drug discovery and development, such as biased agonism to reduce opioid side effects [134-136]. These efforts have produced new biased ligands, as well as additional drugs targeting key proteins such as mTOR or receptors such as PAR2 relevant to MOR signaling, to either augment or reduce key behavioral outputs such as anti-nociception [137-141]. These efforts illuminate the relevant MOR signaling cascades beyond the “classical” $G\alpha_i$ cascade, and show the value in elucidation of key signaling regulators downstream of MOR activation.

Heat shock protein 90 (Hsp90) is a molecular chaperone protein which is upregulated in response to stress. It regulates its client proteins via several molecular mechanisms, including protein folding, kinase modulation, protein complex formation, and subcellular localization [97, 142]. Hsp90 makes up roughly 2% of the total protein pool in a given cell, highlighting its centrality to cell biology, but its functions have primarily been investigated in the context of cancer models and treatments [143-145]. Although less studied, Hsp90 has been shown to have a key role in regulating signal transduction at the receptor and downstream cascade levels in a number of different tissues and physiological contexts, suggesting this protein could play a key role in MOR signal transduction [146].

We tested this hypothesis in our earlier work, in which we selectively inhibited Hsp90 in the brain using intracerebroventricular (i.c.v.) administration of 17-N-allylamino-17-demethoxygeldanamycin (17-AAG). We found that Hsp90 inhibition in the brain completely suppressed systemically administered morphine-induced anti-nociception in a variety of murine pain models [104]. In addition, we showed that i.c.v. administration of 17-AAG blocked ERK phosphorylation in response to the selective MOR agonist DAMGO, and that this loss of ERK phosphorylation was responsible for the loss of morphine anti-nociception. These findings demonstrated that Hsp90 regulates MOR signaling in the brain, and identified new signaling pathways to explore. However this work was just the first step, leaving many mechanistic details unknown, such as the contribution of other regions of the central nervous system.

In this work we thus began our investigation of tissue differences in Hsp90 modulation of MOR signal transduction by testing the spinal cord. To do this we inhibited spinal cord Hsp90 by performing 24-hour pretreatments of intrathecal (i.t.) Hsp90 inhibitors 17-AAG or KU-32. We then assessed the impact of spinal Hsp90 inhibition on morphine anti-nociception using tail flick and post-surgical paw incision pain models in CD-1 mice.

Contrary to what was observed in our previous study in the brain, we found an amplified morphine anti-nociceptive response with spinal cord Hsp90 inhibition. We were also able to demonstrate that these effects were elicited in an ERK MAPK dependent manner within the spinal cord dorsal horn, and also required rapid protein translation and p90-Ribosomal S6 kinase (RSK) activation. These findings identify a novel molecular ERK/RSK circuit in the spinal cord that can promote opioid anti-nociception, which is normally repressed by local Hsp90. These findings may also allow for an opioid dose reduction strategy using spinal Hsp90 inhibitors to avoid negative opioid side effects while maintaining analgesia.

METHODS AND MATERIALS

Materials

17-AAG (#AAJ66960MC), DAMGO (#11711), Fmk (#46-901-0), cycloheximide (#AC357420010), and U0126 (#11-445) were all purchased from Fisher Scientific (Waltham, MA). Morphine sulfate pentahydrate was obtained through the National Institute on Drug Abuse Drug Supply Program and distributed through the Research Triangle Institute. KU-32 was synthesized using published protocols, and purity (>95%) and identity confirmed by HPLC and mass spectrometry [147]. 17-AAG, U0126, Fmk, KU-32, and cycloheximide were prepared as stock solutions in DMSO, and DAMGO was prepared as a stock solution in water. Morphine was prepared fresh for each experiment in USP saline. Powders were stored as recommended by the manufacturer, and stock solutions stored at -20°C. Appropriate vehicle controls were used for each experiment: 10% DMSO in water for KU-32, Fmk, and cycloheximide i.t. injections; water for DAMGO i.t. injections; USP saline for systemic morphine injections; and 10% DMSO, 10% Tween-80, and 80% USP saline for the 17-AAG and U0126 i.t., i.c.v., and i.p. injections.

Animals

Male and female CD-1 mice in age-matched controlled cohorts from 4–8 weeks of age were used for all experiments and were obtained from Charles River Laboratories (Wilmington, MA). Male and female mice were used in approximately equal numbers in each experiment; no sex differences were observed, so the male and female cohorts were combined for all data shown. CD-1 (a.k.a. ICR) mice are commonly used in opioid research and in our previous work as a line with a strong response to opioid drugs ([104, 148], etc.). Mice were recovered for a minimum of 5 days after shipment before being used in experiments. The mice were kept in an AAALAC-accredited vivarium at the University of Arizona under temperature control and 12-h light/dark cycles with food (standard lab chow) and water available *ad libitum*. No more than five mice were kept in a cage. The animals were monitored daily, including after surgical procedures, by trained veterinary staff. All experiments performed were in accordance with IACUC-approved protocols at the University of Arizona and according to the guidelines of the NIH Care and Use of Laboratory Animals handbook.

Behavioral experiments

Prior to any behavioral experiment or testing, the animals were brought to the testing room in their home cages for at least 1 hr for acclimation. Testing always occurred within the same approximate time of day between experiments, and environmental factors (noise, personnel, and scents) were minimized. All testing apparatus (cylinders, grid boxes, etc.) were cleaned between uses. The experimenter was blinded to treatment group by another laboratory member delivering coded drug vials, which were then decoded after collection of all data.

Paw incision and mechanical allodynia

Mechanical thresholds were determined prior to surgery using calibrated Von Frey filaments (Ugo Basile, Varese, Italy) with the up-down method and four measurements after the first response per mouse [104, 149]. The mice were housed in a homemade apparatus with Plexiglas walls and ceiling and a wire mesh floor (3”W x 4”L x 3”H with 0.25” wire mesh). The surgery was then performed by anesthesia with ~2% isoflurane in standard air, preparation of the left plantar hind paw with iodine and 70% ethanol, and a 5-mm incision made through the skin and fascia with a no. 11 scalpel. The muscle was elevated with curved forceps leaving the origin and insertion intact, and the muscle was split lengthwise using the scalpel. The wound was then closed with 5-0 polyglycolic acid sutures. All i.c.v. and i.t. injections were performed as described in our previous work [104]. For the 17-AAG/KU-32 experiments, the mice were then injected i.t. and left to recover for 24 hrs. The next day, the mechanical threshold was again determined as described above, and i.t. injections took place for the U0126 experiments with a 15-min treatment time. Both the 17-AAG and the U0126 mice were then injected with 3.2 mg/kg morphine s.c., and mechanical thresholds were determined over a 3-hour time course. No animals were excluded from these studies.

Tail-flick assay

Pre-injection tail-flick baselines were determined in a 52 °C warm water tail-flick assay with a 10 sec cutoff time [104]. The mice were then injected i.t. with 17-AAG, KU-32, cycloheximide, Fmk, or U0126 with a 24-hr (17-AAG and KU-32), 30-min (cycloheximide and Fmk), or 15-min (U0126) treatment time. 24 hr post-injection baselines

were determined for the 17-AAG experiments. The mice were then injected s.c. with 3.2 mg/kg of morphine, and tail-flick latencies were determined over a 2-hour time course. No animals were excluded from these studies.

Rotarod test

Mice were subjected to three training trials of 3 min each on a Rotarod device, with the machine off for trial 1, the machine on but not rotating for trial 2, and the machine rotating at 4 rpm for trial 3 [104]. An automatic timer in the unit was used to record fall latencies with a 3-min maximum time. The mice were then injected i.t. with 17-AAG or vehicle and allowed to recover for 24 hr, and another 3-min Rotarod trial was performed without additional treatments or interventions. This trial was done with an accelerating 4–16 rpm task over the 3-min trial time. No mice were excluded from these studies.

Western blotting and analysis

Mouse spinal cord or PAG protein lysates were prepared using our previously published protocol [104] and quantified with a BCA protein quantitation assay using the manufacturer's protocol (Bio-Rad). The protein was run on precast 10% Bis-Tris Bolt gels (Fisher Scientific #NW00100BOX) using the Bolt gel apparatus and following the manufacturer's instructions. The gels were transferred to nitrocellulose membrane (Bio-Rad) using a wet transfer system (30 V, minimum of 1 hr on ice). The blots were blocked with 5% nonfat dry milk in TBS and incubated with primary antibody in 5% BSA in TBS + 0.1% Tween-20 (TBST) overnight rocking at 4 °C. The blots were then washed three times for 5 min in TBST, incubated with secondary antibody (see below) in 5% milk in TBST for 1 hr of rocking at room temperature, washed again, and imaged with a LiCor Odyssey

infrared imaging system (LiCor, Lincoln, NE). Some blots were then stripped with 25 mM glycine-HCl and 1% SDS, pH 2.0, for 30–60 min of rocking at room temperature prior to being washed and re-exposed to primary antibody. The resulting image bands were quantified using Scion Image (based on NIH Image). All images were quantified in the linear signal range, which is easier to ensure because the Odyssey imager is a dynamic imager that allows for fine control of exposure. The pERK signal was normalized to the tERK signal, and pRSK1 and 2 were normalized to tRSK1 and 2 respectively, with both measured from the same blot as the primary target. The normalized intensities were further normalized to a vehicle control present on the same blot.

Immunohistochemistry

Perfusions were performed on drug treated mice with cold PBS, followed with cold 4% paraformaldehyde in PBS. Shortly after the perfusions were complete, fixed spinal cords were extracted and immediately placed in cold 4% paraformaldehyde for ~6 hours. Spinal cords were then placed in 15% sucrose in PBS overnight, followed by 30% sucrose in PBS overnight. Spinal cords were then flash frozen in O.C.T. Compound using liquid nitrogen and sectioned with a Microm HM 525 cryostat at a thickness of 20 µm between the L5 and L6 vertebrae and mounted on Surgipath X-tra microscope slides. Spinal cord sections were rehydrated in PBS in preparation for free float staining. Samples were incubated in an endogenous peroxidase blocking buffer consisting of 60% methanol and 0.3% H2O2 in PBS at RT for 30 minutes and then washed with PBST. They were then incubated in 5% goat serum, 1% BSA in PBST at RT for 1 hour. Samples were then incubated with 1:5000 primary pERK antibody in 1.5% goat serum, 1% BSA in PBST at 4˚C overnight. Samples were then washed with PBST and then incubated with a 1:400 biotinylated secondary goat anti-rabbit IgG antibody in 1.5% goat serum, 1% BSA in PBST

at RT for 1 hour. Samples were prepared as instructed using the Vectastain Elite ABC HRP Kit (#PK-6101) and TSA Plus Fluorescein Evaluation Kit (#NEL741E001KT), both from PerkinElmer. NeuN and MAP2 primary antibodies were used at 1:1000 and 1:500 respectively during the pERK primary incubation. The secondary for NeuN and MAP2 was Alexa Flour goat anti-mouse IgG 594 which was used at 1:500 for both which was added during the pERK secondary incubation mentioned above. Stained spinal cord sections were then mounted onto slides with Novus FluorEver. Sections were imaged at 4x, 10x, and 63x using an Olympus BX51 microscope equipped with a Hamamatsu C8484 digital camera. Images were analyzed using ImageJ. Dorsal horn regions were selected, and average mean intensities were measured and normalized to no primary Ab and vehicle controls within experimental groups.

Antibodies

The antibodies used were: Hsp70 (Cell Signaling 4872S, lot 4, rabbit, 1:1000), GAPDH (ThermoFisher MA5-15738, lot PI209504, mouse, 1:1000), pERK (Cell Signaling 4370S, lot 12, rabbit, 1:1000 for Westerns and 1:5000 for IHC), tERK (Cell Signaling 4696S, lot 16, mouse, 1:1000), pRSK1 (Cell Signaling 11989S, lot 4, rabbit 1:1000), tRSK1 (Cell Signaling 8408S, lot 5, rabbit 1:1000), pRSK2 (Cell Signaling 3556S, lot 4, rabbit, 1:1000), tRSK2 (Cell Signaling 5528S, lot 1, rabbit 1:1000), MAP2 (Invitrogen 13-1500, lot TJ275359, mouse, 1:500), NeuN (Abcam ab104224, lot GR3247200-1, mouse, 1:1000), secondary GαM680 (LiCor 926-68020, lot C50721-02, goat, 1:10,000–1:20,000), secondary GαR800 (LiCor 926-32211, lot C50602–05, goat, 1:10,000–1:20,000), and secondary Alexa Fluor goat anti-mouse IgG 594 (Invitrogen A11032, lot 1985396, mouse, 1:500).

Proteomics - In-gel digestion

Mouse spinal cord protein lysates (100 µg) were prepared as for Western blot from animals that were treated with either 17-AAG or vehicle (N = 3 each) and were separated on a 10% SDS-PAGE gel and stained with Bio-Safe Coomassie G-250 Stain. Each lane of the SDS-PAGE gel was cut into six slices and the gel slices were subjected to trypsin digestion. The resulting peptides were purified by C18-based desalting exactly as previously described [150, 151].

Proteomics - Mass spectrometry and database search

HPLC-ESI-MS/MS was performed in positive ion mode on a Thermo Scientific Orbitrap Fusion Lumos tribrid mass spectrometer fitted with an EASY-Spray Source (Thermo Scientific, San Jose, CA). NanoLC was performed exactly as previously described [150, 151]. Tandem mass spectra were extracted from Xcalibur 'RAW' files and charge states were assigned using the ProteoWizard 3.0 msConvert script using the default parameters. The fragment mass spectra were searched against the *Mus musculus* SwissProt_2018_01 database (16965 entries) using Mascot (Matrix Science, London, UK; version 2.6.0) using the default probability cut-off score. The search variables that were used were: 10 ppm mass tolerance for precursor ion masses and 0.5 Da for product ion masses; digestion with trypsin; a maximum of two missed tryptic cleavages; variable modifications of oxidation of methionine and phosphorylation of serine, threonine, and tyrosine. Cross-correlation of Mascot search results with X! Tandem was accomplished with Scaffold (version Scaffold_4.8.7; Proteome Software, Portland, OR, USA). Probability assessment of peptide assignments and protein identifications were made using Scaffold. Only peptides with ≥ 95% probability were considered. The mass spectrometry proteomics data have been deposited to the ProteomeXchange Consortium via the PRIDE [152, 153]

partner repository with the dataset identifier PXD015060 and 10.6019/PXD015060. The reviewer account details are Username: reviewer97855@ebi.ac.uk and Password: 8AM00kfd.

Label-free quantitative proteomics

Progenesis QI for proteomics software (version 2.4, Nonlinear Dynamics Ltd., Newcastle upon Tyne, UK) was used to perform ion-intensity based label-free quantification as previously described [151]. In an automated format, .RAW files were imported and converted into two-dimensional maps (y-axis = time, x-axis = m/z) followed by selection of a reference run for alignment purposes. An aggregate data set containing all peak information from all samples was created from the aligned runs, which was then further narrowed down by selecting only +2, +3, and +4 charged ions for further analysis. The samples were then grouped and a peak list of fragment ion spectra from only the top eight most intense precursors of a feature was exported to a Mascot generic file (.MGF) format and searched using Mascot (Matrix Science, London, UK; version 2.4) with the same search variables as described above. The resulting Mascot .XML file was then imported into Progenesis, allowing for peptide/protein assignment, while peptides with a Mascot Ion Score of <25 were not considered for further analysis. Protein quantification was performed using only non-conflicting peptides and precursor ion-abundance values were normalized in a run to those in a reference run (not necessarily the same as the alignment reference run)

Statistical analysis

All data were reported as the mean ± SEM and normalized where appropriate as described above to total protein and/or Vehicle control groups. SEM is justified as it indicates the impact of sample size on data set variability. The behavioral data were reported raw without maximum possible effect (MPE) or other normalization. Biological and technical replicates are described in the Figure Legends. Comparisons between two groups (HSP70 protein expression) were performed by unpaired 2-tailed *t* tests. Comparisons of more than two groups (ERK and RSK signaling, paw incision, tail flick, and rotarod) were performed by two-way ANOVA with Sidak's (behavior) or Tukey's (Western) post hoc tests. In all cases, significance was defined as $p < 0.05$. All graphing and statistical analyses were performed using GraphPad Prism 8.1 (San Diego, CA).

RESULTS

Spinal inhibition of Hsp90 enhances morphine-induced anti-nociception

We previously showed that intracerebroventricularly (i.c.v.) administered Hsp90 inhibitors completely ablated morphine-induced anti-nociception in multiple pain models [104]. In addition, Hsp90 has a considerable number of client proteins, which differ in various tissue, cellular, and environmental contexts [154-156]. This suggests the potential for context specific roles for Hsp90 within downstream MOR signaling. We began to test this question for Hsp90 in MOR signaling by considering the contribution of Hsp90 to morphine induced anti-nociception within the spinal cord. CD-1 mice were treated with 0.5 nmol of intrathecal (i.t.) 17-AAG, a geldanamycin derivative which competitively binds the N-terminal ATP binding domain of Hsp90. 24 hours post-injection mice were then treated with 3.2 mg/kg morphine subcutaneously (s.c.), and behavioral pain assays were performed.

Contrary to our previous report with i.c.v. administered 17-AAG, we found that spinally inhibited Hsp90 resulted in an elevated anti-nociceptive response due to morphine

in both thermal tail flick and mechanical post-operative paw incision pain models (**Fig. 1A-B**). To verify the Hsp90 selectivity of these results, we utilized a C-terminal inhibitor of Hsp90, KU-32, that binds to an alternate site than 17-AAG, and would be highly unlikely to share off-target interactions [147, 157]. KU-32 was administered at 0.01 nmol i.t. followed by s.c. morphine 24 hrs later. Enhanced morphine-induced anti-nociception was also observed with KU-32 treatment, confirming the Hsp90 selectivity of our results (**Fig. 1C**).

We next confirmed that these findings were not due to off-target motor or sedative effects using the Rotarod test. Spinal 17-AAG treatment had no impact on Rotarod performance in the mice, suggesting that our findings reflect *bona fide* changes to the opioid pain modulatory system (**Fig. 1D**). Lastly, in our previous report, we tested the brain role of Hsp90 in tail flick pain using i.c.v. DAMGO instead of morphine, showing that inhibition of brain Hsp90 had no impact on tail flick pain [104]. To confirm that our tail flick results here were due to changes in Hsp90 location (brain vs. spinal cord) rather than drug and route (i.c.v. DAMGO vs. s.c. morphine), we tested i.c.v. 17-AAG combined with s.c. morphine. We found that at both 3.2 and 10 mg/kg s.c., morphine had no impact on tail flick response, the same as for i.c.v. DAMGO in our earlier study (**Fig. 1E**, [104]).

Brain Hsp90 inhibition overrides spinal cord Hsp90 inhibition

With behavioral differences identified in brain vs. spinal cord Hsp90 inhibition, we next tested the interaction of these two regions using systemic Hsp90 inhibition, which would impact both brain and spinal cord. To do this we injected mice with intraperitoneal (i.p.) 17-AAG and assessed its effects on morphine induced anti-nociception after a 24 hr period. We tested for increased Hsp70 expression levels as a marker of Hsp90 inhibition

Figure 1

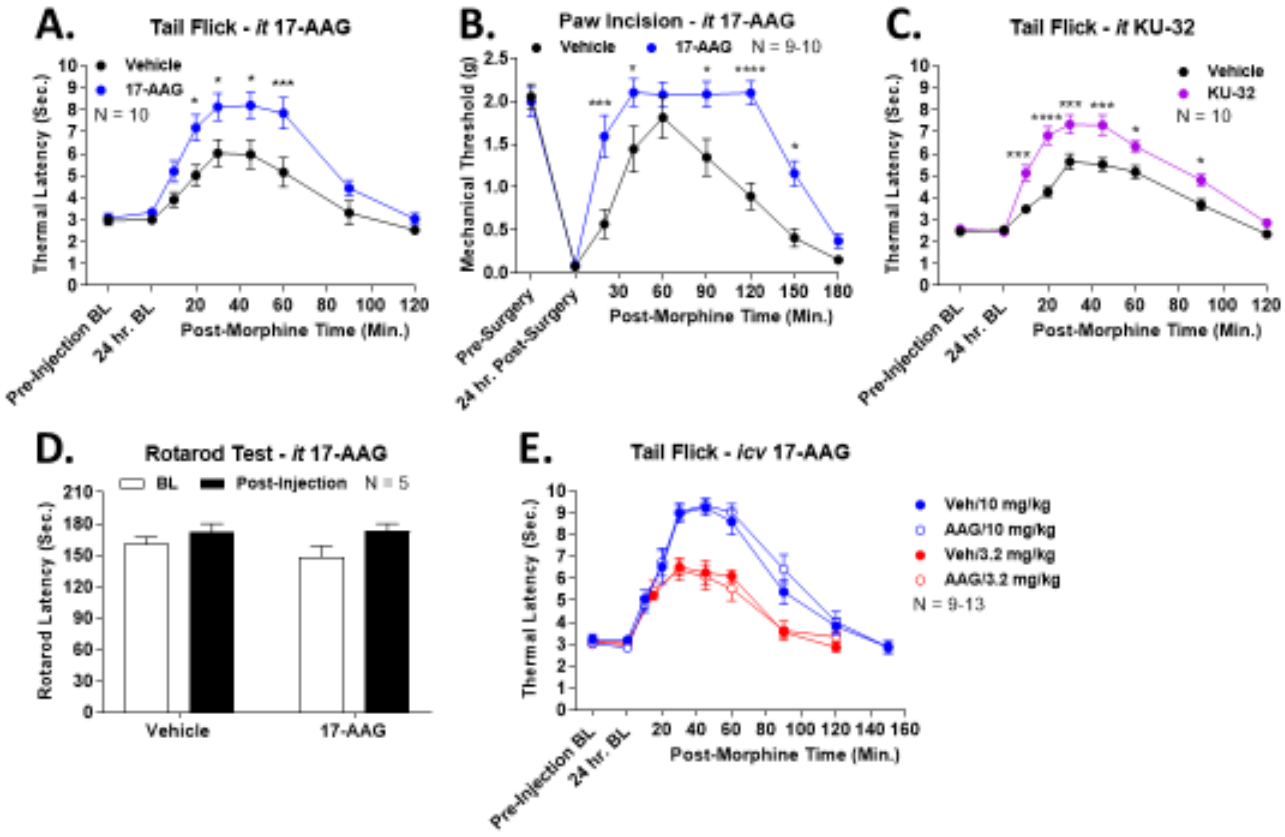

Figure 1 – Spinal cord Hsp90 inhibition enhances morphine anti-nociception. Male and female CD-1 mice were injected as indicated with 17-AAG (0.5 nmol) or KU-32 (0.01 nmol) or Vehicle control by the i.c.v. or i.t. route, followed by 24 hr recovery and then behavioral testing with or without morphine injection. Data reported as the mean ± SEM, with the sample size in mice/group noted on each graph. *, ***, **** = $p < 0.05$, 0.001, 0.0001 vs. same time point Vehicle group by 2 Way ANOVA with Sidak's post hoc test. **A)** Mice tested using the 52°C warm water tail flick assay with i.t. 17-AAG and 3.2 mg/kg morphine s.c.; 17-AAG caused a significant increase in anti-nociception. Two independent technical replicates. **B)** Mice tested using a post-surgical paw incision model with i.t. 17-AAG and 3.2 mg/kg morphine s.c.; 17-AAG caused a significant increase in anti-nociception. Two independent technical replicates. **C)** Mice tested using the tail

flick assay with i.t. KU-32 instead of 17-AAG along with 3.2 mg/kg morphine s.c., which caused a similar significant elevation in anti-nociception. Two independent technical replicates. **D)** Mice tested using the Rotarod test after i.t. 17-AAG injection with no morphine injection; 17-AAG had no effect ($p > 0.05$). One technical replicate. **E)** Mice tested using the tail flick assay with i.c.v. 17-AAG and 3.2 or 10 mg/kg morphine s.c.; i.c.v. 17-AAG treatment had no effect on morphine anti-nociception at either dose ($p > 0.05$). Three independent technical replicates.

as expected, validating our treatment regimen as effective in inhibiting CNS Hsp90 (**Fig. 2A-B**). Interestingly, we were unable to detect an increase in spinal cord Hsp70 (**Fig. 2A-B**). The 17-AAG is likely reaching the spinal cord since we've shown it can reach the PAG, thus this result may represent different molecular mechanisms for Hsp90 in brain vs. spinal cord. Now validated, we tested the impact of systemic 17-AAG on morphine anti-nociception. We observed that systemic 17-AAG had no impact on anti-nociception in tail flick pain, and very strongly reduced anti-nociception in paw incision pain (**Fig. 2C-D**); these results are very similar to what was observed with i.c.v. 17-AAG treatment (**Fig. 1E**, [104]).

The effects on morphine anti-nociception seen with systemic Hsp90 inhibition suggest that the signaling events within the brain may override that of the spinal cord. To directly test this hypothesis and rule out peripheral mechanisms, we performed dual i.c.v. and i.t. injections of 17-AAG. We found that dual brain and spinal cord injections recapitulated systemic injection in both the tail flick and paw incision pain models (**Fig. 2E-F**). These results suggest that the signaling events regulated by Hsp90 within the brain override MOR signaling within the spinal cord, which would otherwise allow for amplified pain relief in these models.

ERK MAPK is activated by spinal Hsp90 inhibition and is necessary for enhanced anti-nociception

Our previous study within the brain demonstrated that blocked activation of ERK MAPK in the PAG by 17-AAG treatment is a mechanism for the reduction in morphine induced anti-nociception [104]. We thus tested ERK signaling activation within the spinal cord after i.t. 17-AAG and DAMGO (selective MOR agonist) treatment using Western blot.

Figure 2

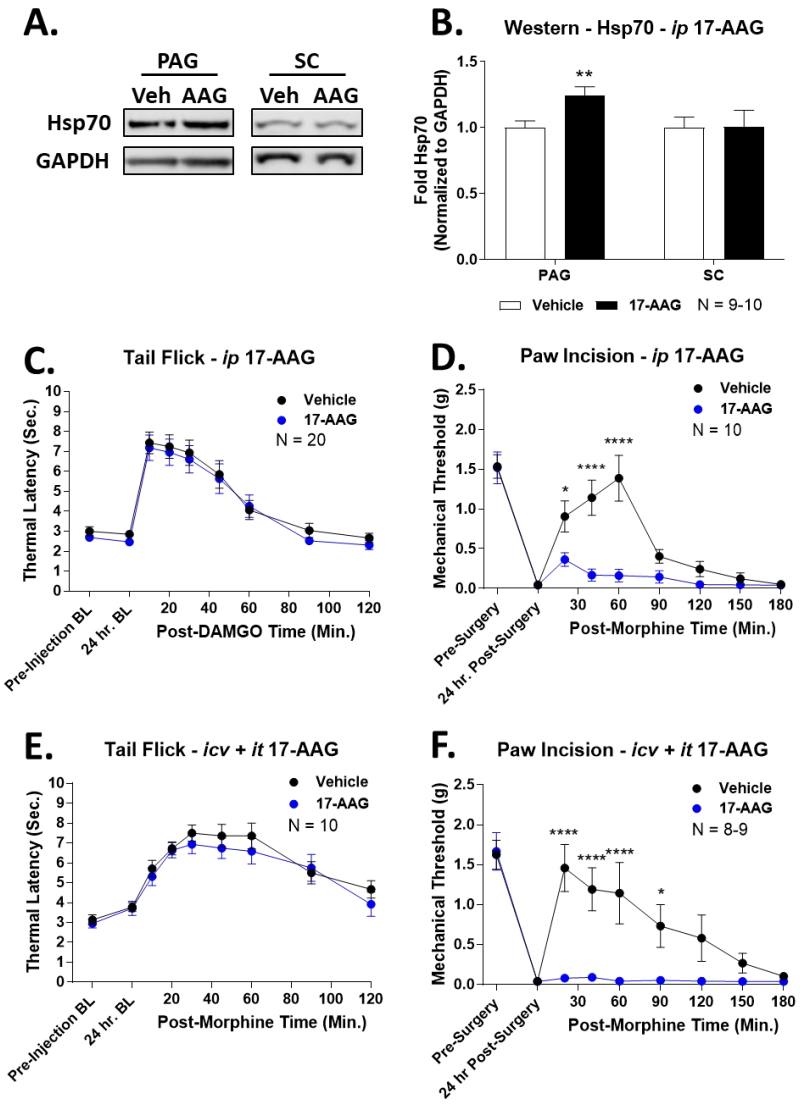

Figure. 2 – Brain Hsp90 inhibition overrides spinal cord Hsp90 inhibition with respect to opioid anti-nociception. Male and female CD-1 mice were treated as indicated with 17-AAG or Vehicle with a 24 hour recovery time. Data reported as the mean ± SEM with sample sizes in mice/group noted on each graph. **A)** Mice injected with 50 mg/kg 17-AAG or Vehicle i.p., and Hsp70 levels analyzed in brain (PAG) and spinal cord by Western blot. Representative blots shown for Hsp70 and GAPDH loading control. **B)** Quantitation of the Western data from **A**. Hsp70 density normalized to GAPDH from each sample, and further normalized to the Vehicle group within each tissue. ** = $p < 0.01$ vs. same tissue Vehicle group by unpaired 2-tailed *t* test. Two independent technical replicates. **C-D)** Mice injected with 50 mg/kg 17-AAG or Vehicle i.p., followed by 3.2 mg/kg morphine in the tail flick (**C**) and paw incision (**D**) models. *, **** = $p < 0.05$, 0.0001 vs.

same time point 17-AAG group by 2 Way ANOVA with Sidak's post-hoc test. Four (**C**) or two (**D**) independent technical replicates. **E-F)** Mice injected both i.c.v. and i.t. with 0.5 nmol 17-AAG or Vehicle, followed by 3.2 mg/kg morphine s.c. in the tail flick (**E**) or paw incision (**F**) models. *, **** = $p < 0.05$, 0.0001 vs. same time point 17-AAG group by 2 Way ANOVA with Sidak's post-hoc test. Two independent technical replicates for each model.

DAMGO was used as a high efficacy selective agonist, increasing our ability to observe kinase changes in tissue vs. the partial agonist morphine; our results above (**Fig. 1E**) and experiments below validate this choice. Interestingly, DAMGO alone showed no ERK activation relative to vehicle treatment; in contrast, 17-AAG induced an elevated ERK baseline with a further increase in ERK phosphorylation when combined with DAMGO (**Fig. 3A-B**). As in our systemic inhibition studies above, we also sought to confirm Hsp90 inhibition by 17-AAG by testing for Hsp70 upregulation [104, 158, 159]. We again found no Hsp70 upregulation, even with direct i.t. injection of inhibitor, confirming our systemic results above and further suggesting that Hsp90 molecular mechanisms may differ in spinal cord vs. brain (**Fig. 3A, C**).

To localize the observed increases in ERK phosphorylation within the spinal cord, we performed immunohistochemical (IHC) analysis of spinal cord tissue from mice treated with i.t. 17-AAG and DAMGO as for our Western studies. Our findings confirmed the Western results, with very low phospho-ERK signal observed in Vehicle/Vehicle and Vehicle/DAMGO groups; we observed some increase in signal in the 17-AAG/Vehicle group, and a large increase in specific phospho-ERK signal in the 17-AAG/DAMGO group (**Fig. 3D**). We particularly noted an apparent increase in ERK phosphorylation in the lamina I/II region of the dorsal horn, a region rich in nociceptive input and opioid receptors (**Fig. 3D** white arrows). We also performed co-localization studies with NeuN, a marker for neuronal cell bodies, and MAP2, a neuronal cytoskeletal protein enriched in dendrites; we found that the pERK signal co-localized with MAP2 but not NeuN, suggesting ERK activation in post-synaptic dendrites (**Fig. 3E**). This was confirmed using high magnification imaging in **Fig. 3F**, showing substantial but not complete pERK/MAP2 overlap. We also quantitated the phospho-ERK signal in the dorsal horn region, which confirmed a significant increase with 17-AAG and DAMGO co-treatment (**Fig. 3G**).

Figure 3

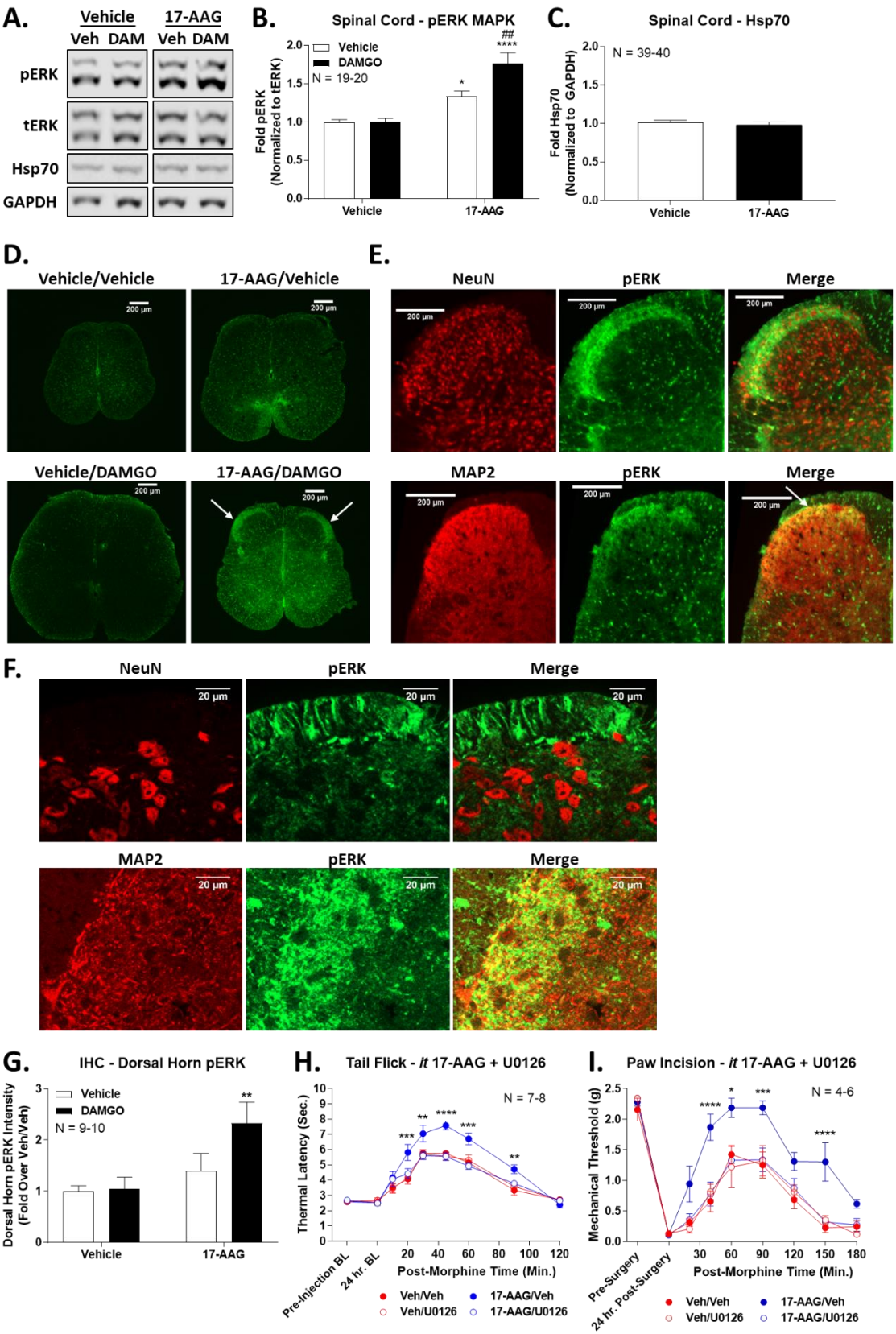
A.
Vehicle
17-AAG
Veh DAM Veh DAM
pERK
tERK
Hsp70
GAPDH
B.
Spinal Cord - pERK MAPK
Vehicle
DAMGO
N = 19-20
Fold pERK (Normalized to tERK)
Vehicle
17-AAG
C.
Spinal Cord - Hsp70
N = 39-40
Fold Hsp70 (Normalized to GAPDH)
Vehicle
17-AAG
D.
Vehicle/Vehicle
17-AAG/Vehicle
Vehicle/DAMGO
17-AAG/DAMGO
200 µm
E.
NeuN
pERK
Merge
MAP2
pERK
Merge
200 µm
F.
NeuN
pERK
Merge
MAP2
pERK
Merge
20 µm
G.
IHC - Dorsal Horn pERK
Vehicle
DAMGO
N = 9-10
Dorsal Horn pERK Intensity (Fold Over Veh/Veh)
Vehicle
17-AAG
H.
Tail Flick - it 17-AAG + U0126
N = 7-8
Thermal Latency (Sec.)
Pre-Injection BL
24 hr. BL
Post-Morphine Time (Min.)
Veh/Veh
17-AAG/Veh
Veh/U0126
17-AAG/U0126
I.
Paw Incision - it 17-AAG + U0126
N = 4-6
Mechanical Threshold (g)
Pre-Surgery
24 hr. Post-Surgery
Post-Morphine Time (Min.)
Veh/Veh
17-AAG/Veh
Veh/U0126
17-AAG/U0126

Figure 3 – Spinal Hsp90 inhibition enables opioid activation of ERK MAPK, leading to enhanced anti-nociception. Male and female CD-1 mice were treated as indicated with 17-AAG or Vehicle with a 24 hour recovery time. Data reported as the mean ± SEM with sample sizes in mice/group noted on each graph. **A)** Mice injected with 0.5 nmol 17-AAG or Vehicle i.t., followed by 0.1 nmol DAMGO or Vehicle i.t. for 10 minutes. Spinal cord tissue was then analyzed by Western blot. Representative blots shown for phospho-ERK (pERK), total ERK (tERK), Hsp70, and GAPDH. **B)** Quantitation of pERK and tERK signal from **A**. pERK density normalized to tERK density within each sample, and further normalized to the Vehicle:Vehicle group. *, **** = $p < 0.05$, 0.0001 vs. Vehicle:Vehicle group; ## = $p < 0.01$ vs. 17-AAG:Vehicle group; both by 2 Way ANOVA with Tukey's post hoc test. Four independent technical replicates. **C)** Quantitation of Hsp70 signal from **A**. Hsp70 density normalized to GAPDH within each sample, and further normalize to the Vehicle group. $P > 0.05$ by unpaired 2-tailed *t* test. Four independent technical replicates. **D)** IHC for pERK (green) performed from treated spinal cords as for **A** in the L4-L6 region. Representative images shown. Increased pERK signal was most obviously apparent in the lamina I/II region of the dorsal horn in the 17-AAG/DAMGO group (white arrows), matching the Western data in **B**. **E)** Colocalization IHC experiments were performed in the dorsal horn region from 17-AAG/DAMGO treated spinal cords. pERK (green) was separately tested for co-localization with the neuronal markers NeuN or MAP2 (red). pERK/MAP2 co-localization is visible as a yellow signal in the merged image (white arrow). $N \geq 3$ individual spinal cords per target; representative images shown; two independent technical replicates. **F)** Higher magnification images (63x) from **E** are shown. These images further confirm substantial but not complete pERK/MAP2 colocalization. **G)** Quantitation of the pERK signal in the dorsal horn region from all four groups in **D**. Intensity values normalized to the Vehicle:Vehicle group. ** = $p < 0.01$ vs. Vehicle:Vehicle group by 2 Way ANOVA with Tukey's post hoc test. Four independent technical replicates. **H-I)** Mice injected with 0.5 nmol 17-AAG or Vehicle i.t., 24 hrs, followed by 5 μg U0126 or Vehicle i.t., 15 min, followed by 3.2 mg/kg morphine s.c. in the tail flick (**H**) or paw

incision (**I**) assays. *, **, ***, **** = $p < 0.05$, 0.01, 0.001, 0.0001 vs. same time point Vehicle:Vehicle group by 2 Way ANOVA with Sidak's post hoc test. U0126 returns the enhanced anti-nociception caused by 17-AAG back to baseline while causing no effect on its own. Four (**H**) or three (**I**) independent technical replicates.

To investigate whether these differences in ERK signaling contribute to the enhanced morphine induced anti-nociception observed, we performed behavioral analysis with co-treatment of i.t. 17-AAG and i.t. 5 μg U0126, a MEK/ERK inhibitor [104]. In both tail flick and paw incision models, U0126 treatment brought the enhanced morphine induced anti-nociceptive profile back to the baseline morphine response (**Fig. 3H-I**). In addition, mice treated with U0126 alone without 17-AAG showed no difference in morphine induced anti-nociception (**Fig. 3H-I**). These results demonstrate that ERK phosphorylation within the spinal cord is necessary for increased morphine induced anti-nociception via spinal cord Hsp90 inhibition; they also support our Western and IHC results suggesting that ERK is not activated by opioids without Hsp90 inhibition.

Rapid protein translation after ERK activation is necessary for enhanced morphine anti-nociception through spinally inhibited Hsp90

Hsp90 and ERK MAPK signaling pathways have been previously connected to translational initiation [160-163]. To evaluate the possibility of these pathways altering translation and subsequently contributing to the behavioral differences observed here, we administered the translational inhibitor cycloheximide (CX) i.t. in the context of our behavioral experiments. In a very similar pattern to the ERK inhibitor experiments above, we found that 85 nmol i.t. CX, 24 hours post-17AAG and 30 minutes prior to morphine, reduced the enhancement of morphine induced anti-nociception back to baseline in the tail flick model (**Fig. 4A**). CX alone without 17-AAG treatment did not change morphine-induced anti-nociception (**Fig. 4A**). These findings suggest that rapid translation within 30 minutes of opioid treatment is necessary for the enhanced morphine anti-nociception seen through spinally inhibited Hsp90.

Figure 4

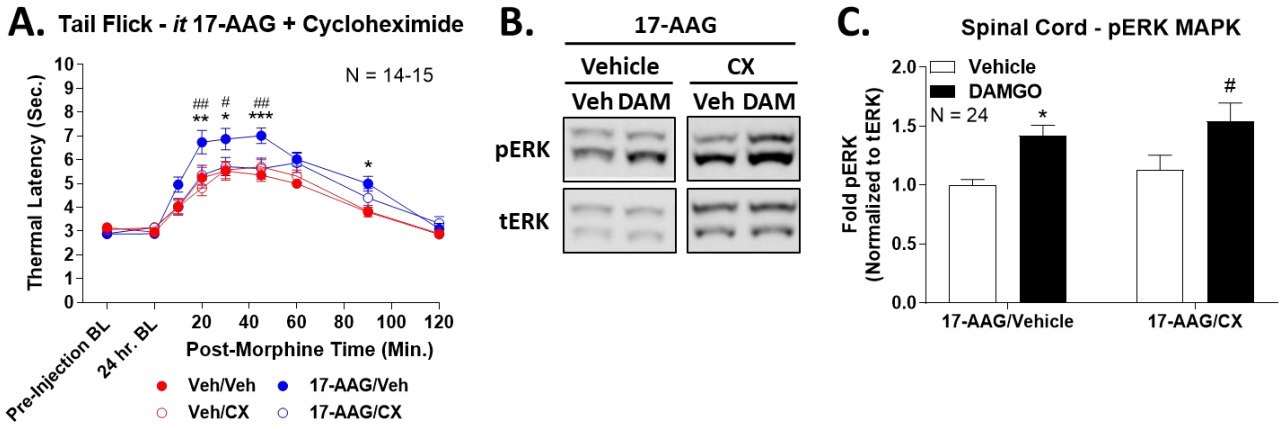

Figure 4 – Spinal Hsp90 inhibition evokes rapid protein translation that is necessary for enhanced morphine anti-nociception. Male and female CD-1 mice injected as noted below. Data reported as the mean ± SEM with the sample size of mice/group noted in each graph. **A)** Mice injected with 0.5 nmol 17-AAG or Vehicle i.t., 24 hrs, then 85 nmol CX or Vehicle i.t., 30 minutes, then 3.2 mg/kg morphine s.c. in the tail flick assay. *, **, *** = $p < 0.05$, 0.01, 0.001 vs. same time point Vehicle:Vehicle group; #, ## = $p < 0.05$, 0.01 vs. same time point 17-AAG:CX group; both by 2 Way ANOVA with Sidak's post hoc test. Four independent technical replicates. **B)** Mice treated with 17-AAG and CX (or Vehicle control) as in **A**, followed by 0.1 nmol DAMGO or Vehicle i.t. for 10 minutes and spinal cords analyzed by Western blot for p/tERK. Representative blots shown. **C)** The p/tERK data from **B** was quantitated. pERK density was normalized to tERK density within each sample, and further normalized to the 17-AAG:Vehicle:Vehicle group. * = $p <$ 0.05 vs. 17-AAG:Vehicle:Vehicle; # = $p < 0.05$ vs. 17-AAG:CX:Vehicle; both by 2 Way ANOVA with Tukey's post hoc test. ERK activation by 17-AAG and DAMGO was not altered by CX treatment. Six independent technical replicates.

To identify the position of translation within the Hsp90/ERK molecular cascade, we performed Western blot analysis on spinal cord tissues harvested from mice treated with 17-AAG and combinations of CX and DAMGO. 17-AAG paired with DAMGO treatment stimulated ERK phosphorylation as above; CX treatment 30 minutes prior to DAMGO had no effect on this stimulation (**Fig. 4B-C**). These results suggest that translational initiation is a downstream event from ERK phosphorylation after Hsp90 inhibition.

Proteomic analysis reveals a protein network altered by spinal Hsp90 inhibition

Our results above suggest that protein translation is altered by spinal Hsp90 inhibition; these changes should thus in principle be measurable by quantitative proteomics. We treated mice with 0.5 nmol i.t. 17-AAG or Vehicle control as above for 24 hours, and removed their spinal cords for analysis. We followed a protocol of protein extraction, SDS-PAGE gel separation with 6 equal bands excised, tryptic digest, and an MS-MS analysis workflow (**Fig. 5A**). We detected 116 proteins significantly downregulated by 17-AAG treatment and 69 proteins significantly upregulated; unbiased hierarchical clustering analysis showed that the individual mice in each sample group (Vehicle vs. 17-AAG) clustered together, validating a consistent effect of 17-AAG treatment (**Fig. 5B**). The full data sets for the significantly altered proteins in the whole analysis and in the sub-analyses shown in this Figure are available in the Supplementary Data. Of the proteins in this data set, we noted that the kinase RSK2 was significantly upregulated by 17-AAG treatment (**Fig. 5C**). RSK2 has been shown to promote acute opioid anti-nociception, highlighting this protein as a potential mechanism for spinal Hsp90 inhibition impacting opioid anti-nociception [164].

We next performed additional analyses to validate the proteomic data set and explore the network of protein changes evoked by Hsp90 inhibition. Principal component analysis (PCA) showed that the individual mice in each treatment group (Vehicle vs. 17-

Figure 5

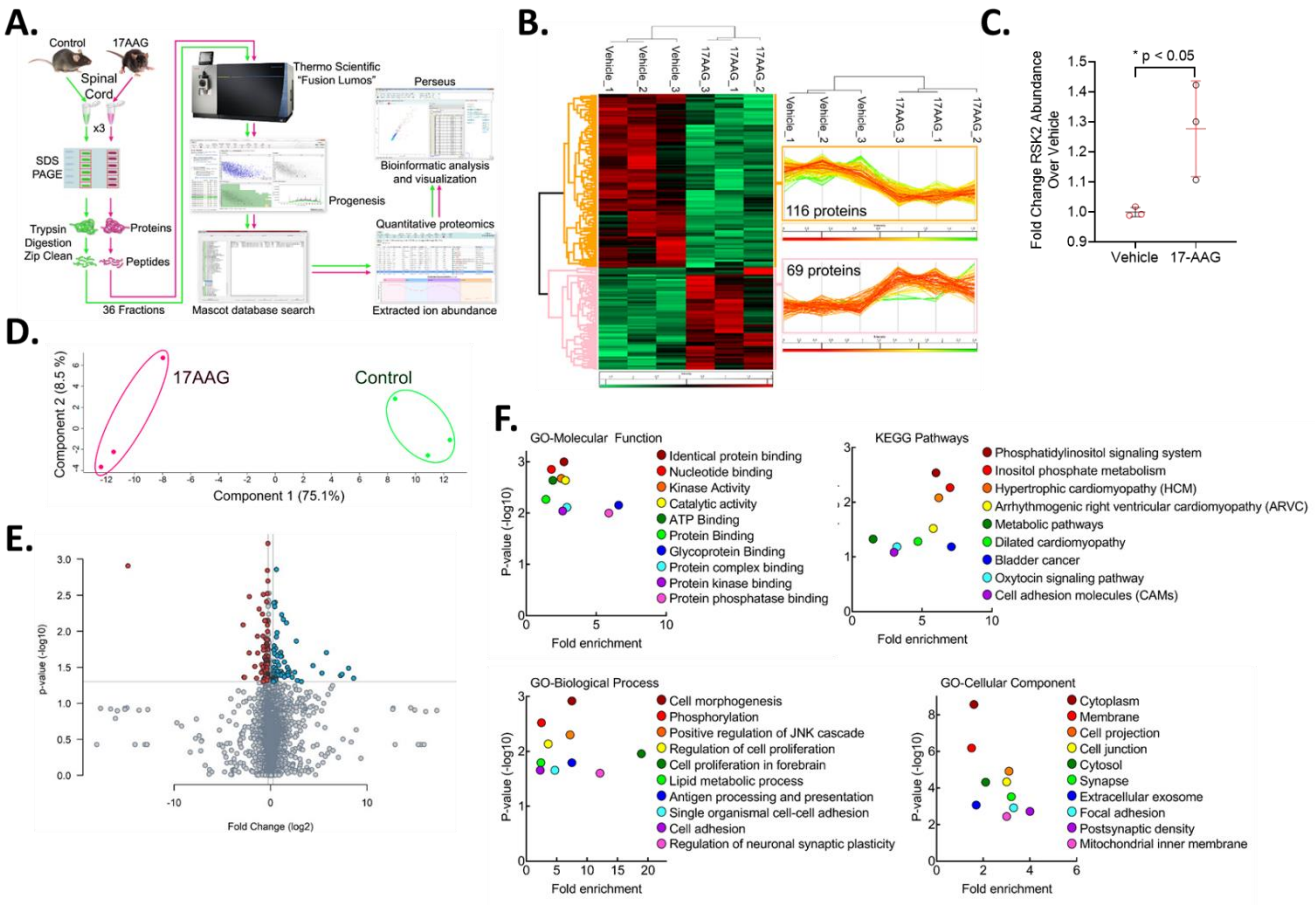

Figure 5 – Quantitative proteomic analysis reveals a protein network altered by spinal Hsp90 inhibition. Female CD-1 mice, N=3/group, 1 technical replicate, were injected with 0.5 nmol 17-AAG or Vehicle i.t. for 24 hrs. Spinal cords removed for proteomic analysis; protein extracted as for Western blot above. **A)** Sample preparation and proteomic analysis workflow (see Methods for more details). **B)** Unbiased hierarchical clustering and heat map analysis of proteins significantly altered by 17-AAG treatment ($p < 0.05$). All 3 Vehicle and 17-AAG samples cluster together. Red = increased, green = decreased, rows = individual proteins, columns = individual samples. 116 proteins were significantly downregulated and 69 significantly upregulated; protein quantity traces for all proteins in each sample shown (*inset*). **C)** Protein quantity data for the protein kinase RSK2 shown, data reported as the mean ± SEM. * = $p < 0.05$ vs. Vehicle group by unpaired 2-tailed *t* test.

D) Principal component analysis of the data set performed. Both treatment groups cluster together and are well-separated along Component 1, accounting for 75.1% of the variance. Within-group variance only occurs along Component 2, accounting for only 8.5% of the variance. **E)** Volcano plot of all proteins plotting p-value vs. fold change. Red = significantly downregulated; blue = significantly upregulated; grey = not significant. **F)** Gene ontology (GO) and KEGG pathway analysis of significantly altered proteins (see Methods for details). Molecular Function, Pathways, Biological Process, and Cell Compartment are all shown, and plot significance vs. fold enrichment.

AAG) clustered together; the groups were strongly separated from each other on Component 1, accounting for 75.1% of the variance, while within treatment the samples were much closer together along Component 2, accounting for only 8.5% of the variance (**Fig. 5D**). We also represented our data in a volcano plot, permitting an overall visualization of significance and fold-change (**Fig. 5E**). Together these analyses further confirm the quality of our data and analysis.

Lastly we performed Gene Ontology and KEGG Pathways analysis of the significantly changed proteins using Database for Annotation, Visualization, and Integrated Discovery (DAVID) to identify broad themes in functions and processes altered by Hsp90 inhibition (**Fig. 5F**). We identified proteins heavily represented in molecular functions such as kinase activity, protein kinase binding, and protein phosphatase binding; pathways including metabolic pathways and oxytocin signaling; processes such as phosphorylation, cell proliferation, lipid metabolism, and synaptic plasticity; and cell components including synapse, exosome, focal adhesion, and postsynaptic density (**Fig. 5F**). This network analysis begins to identify an overall role for Hsp90 in regulating protein networks in the spinal cord, which has not been previously reported.

RSK signaling is required for enhanced anti-nociception through spinally inhibited Hsp90

Cytosolic RSK1 and RSK2 have both been implicated in translational initiation through several substrates, suggesting a potential link to our translation findings above [165-171]. RSK2 has also been implicated in acute morphine induced analgesia within the medial habenula [164]. Our proteomic analysis demonstrated altered expression levels of RSK2 within the spinal cord due to Hsp90 inhibition. Therefore, we aimed to probe both RSK1 and RSK2 as a potential mechanism within this molecular path

To evaluate the necessity of RSK activation within our behavioral model, we utilized the irreversible RSK 1/2 inhibitor 1-[4-Amino-7-(3-hydroxypropyl)-5-(4-methylphenyl)-7H-pyrrolo[2,3-d] pyrimidin-6-yl]-2-fluoroethanone (Fmk). In a similar design to the U0126 and CX experiments above, 24 hr i.t. 17-AAG was combined with i.t. 10 nmol Fmk 30 minutes before morphine treatment in the tail flick model. Fmk treatment returned the enhanced morphine anti-nociception caused by 17-AAG treatment back to baseline, while Fmk alone without 17-AAG treatment had no effect on morphine anti-nociception (**Fig. 6A**). These results show the same pattern as the U0126 and CX experiments above, and strongly suggest that RSK promotes morphine anti-nociception after spinal Hsp90 inhibition. Notably, Fmk is non-selective between RSK1 and RSK2, so either or both isoforms could promote anti-nociception.

To confirm and extend these findings, we evaluated phosphorylation levels of both isoforms by Western blot in treated spinal cords as above. We found that both RSK1 and RSK2 demonstrate a similar phosphorylation pattern to that of ERK. 17-AAG treatment alone elicits increases in both RSK1 and RSK2 phosphorylation that rises to the level of significance for RSK2; 17-AAG and DAMGO co-treatment significantly increases phosphorylation of both proteins vs. the Vehicle/Vehicle control group, and over the 17-AAG/Vehicle group for RSK2 (**Fig. 6B-D**). These results show that both RSK1 and RSK2 are activated by 17-AAG and DAMGO co-treatment, and may both promote morphine anti-nociception after spinal cord Hsp90 inhibition.

DISCUSSION

In this study, we've identified a novel molecular ERK/RSK signaling circuit in the spinal cord which can promote acute opioid anti-nociception; this circuit is normally suppressed by Hsp90, and is only uncovered by spinal Hsp90 inhibition. Our results place

Figure 6

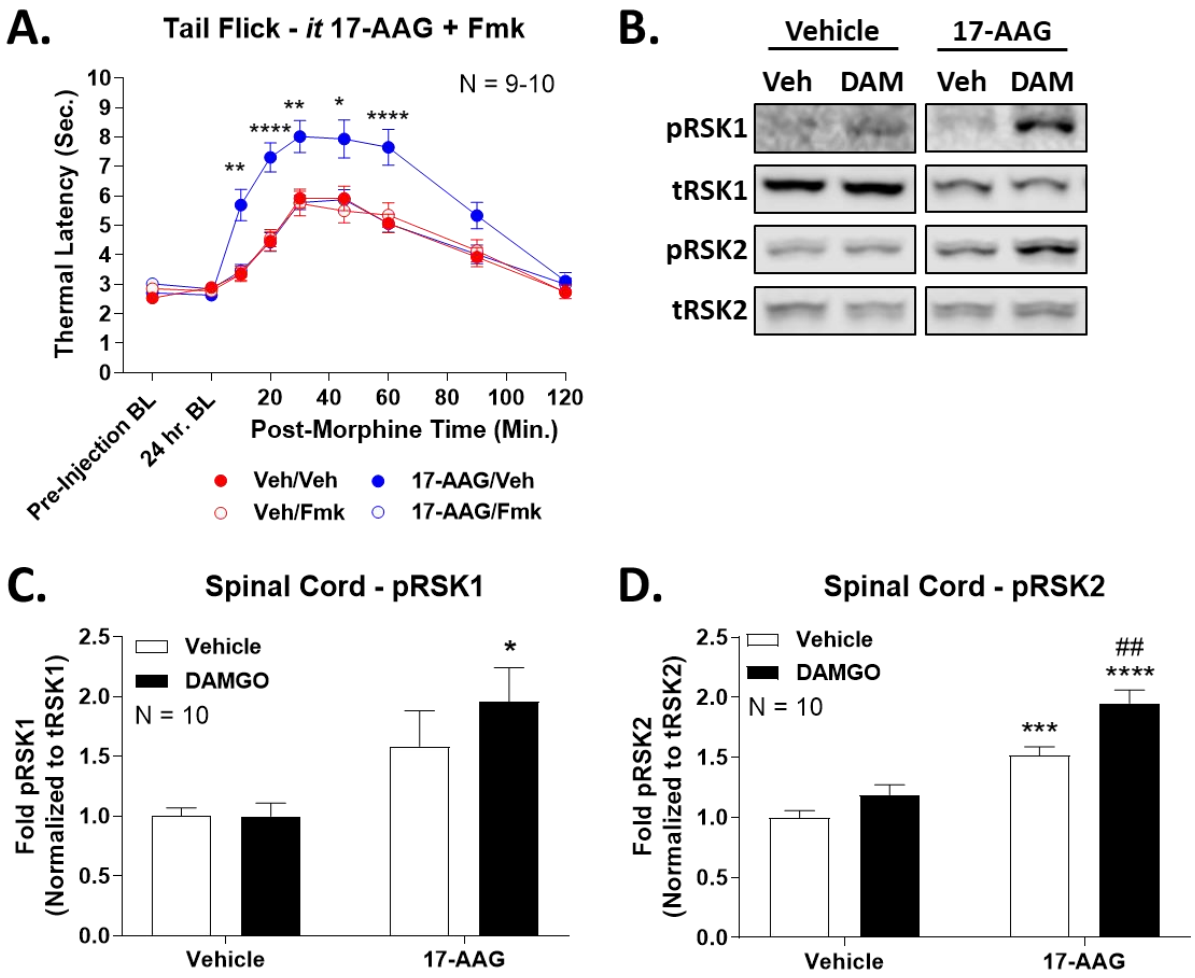

Figure 6 – Spinal Hsp90 inhibition activates RSK1/2 phosphorylation, which is necessary for enhanced morphine anti-nociception. Male and female CD-1 mice injected as noted below. Data reported as the mean ± SEM with sample sizes in mice/group noted in the graphs. **A)** Mice injected with 0.5 nmol 17-AAG or Vehicle i.t., 24 hrs, followed by 10 nmol Fmk or Vehicle i.t., 30 minutes, followed by 3.2 mg/kg morphine s.c. and the tail flick assay. **, ***, **** = $p < 0.01$, 0.001, 0.0001 vs. same time point Vehicle:Vehicle group by 2 Way ANOVA with Sidak's post hoc test. Three independent technical replicates. **B)** Mice injected with 0.5 nmol 17-AAG or Vehicle i.t., 24 hrs, followed by 0.1 nmol DAMGO or Vehicle i.t., 10 min, and spinal cords removed for Western analysis of p/tRSK1/2 signaling. Representative blots shown. **C)** The data from **B** was quantitated

for phosphorylation of RSK1 (**C**) and RSK2 (**D**). pRSK was normalized to tRSK within each sample, and further normalized to the Vehicle:Vehicle group. *, ***, **** = $p < 0.05, 0.001, 0.0001$ vs. Vehicle:Vehicle group; ## = $p < 0.01$ vs. 17-AAG:Vehicle group; both by 2 Way ANOVA with Tukey's post hoc test. Three independent technical replicates.

rapid protein translation as a downstream event of ERK activation; due to extensive literature which has shown an ERK/RSK/translation cascade [165-171], we propose a model by which Hsp90 inhibition relieves repression of ERK activation by the MOR, resulting in an ERK/RSK/translation/anti-nociception cascade after opioid treatment (**Fig. 7**).

Our results provide strong support that spinal ERK, RSK, and translation are not active at baseline for acute opioid anti-nociception. The inhibitors U0126, Fmk, and CX all had no effect on their own without 17-AAG treatment; we also showed that neither ERK nor RSK phosphorylation was stimulated by opioid treatment in vehicle-treated control mice using both Western blot and IHC methods. Notably, we could find no literature reports showing acute activation of these kinases by opioids in the spinal cord. This is in sharp contrast to the brain, where our results and others show that ERK and RSK are phosphorylated by baseline opioid treatment, and contribute to opioid anti-nociception [104, 164, 172-175]. This is not to say that ERK can have no impact on the opioid system in the spinal cord. Spinal ERK has been shown to have a role in mediating chronic opioid treatment side effects, particularly tolerance [176]. ERK also has a well-established role in promoting chronic pain states after activation in the dorsal horn by strong and chronic pain stimuli [177]. These contrasting findings show the importance of context in the function of signaling kinases. ERK is downstream of numerous receptor systems in the same cell, and must be able to carry out diverse functions in the same cell when stimulated by these different systems. We propose that ERK is organized uniquely within the spinal cord so that it does not respond to acute MOR activation, but is free to act in response to chronic MOR activation and in response to other receptor systems; our results suggest that Hsp90 could be this organizing factor preventing acute activation by the MOR. Removing this blockade enables ERK activation, leading to RSK activation, translation of

Figure 7

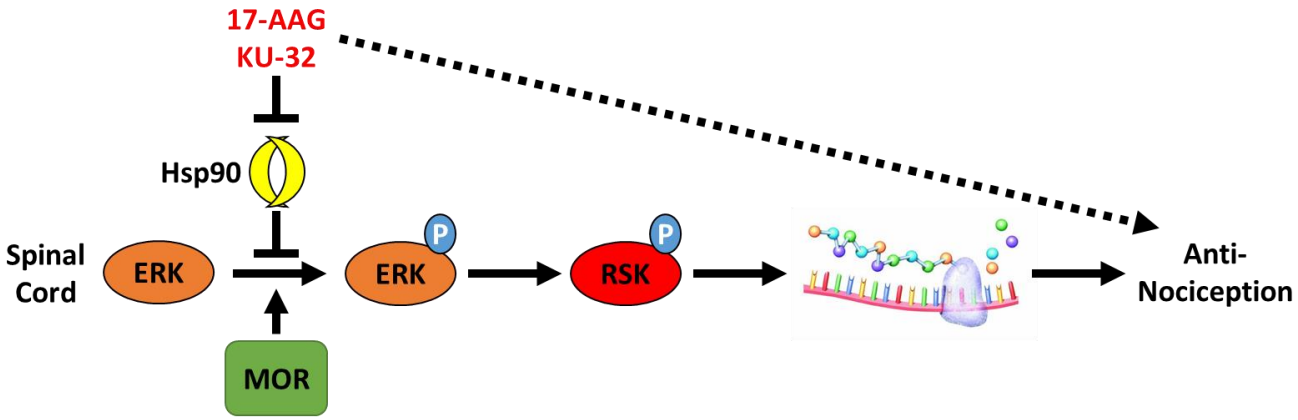

Figure 7 – Proposed model of Hsp90 regulation of opioid signaling in the spinal cord.

new proteins, and enhanced anti-nociception. Uncovering these additional mechanisms will lend great insight into how MOR signaling is organized in the spinal cord.

One potential clue to the unique organization of Hsp90 in the spinal cord is that we found that spinal Hsp90 inhibition does not result in Hsp70 upregulation, confirmed in multiple experiments. Hsp70 upregulation in response to Hsp90 inhibition has long been considered a canonical response, caused by the release of heat shock factor-1 when Hsp90 is inhibited; we and many others have shown in this paper and elsewhere that Hsp70 is upregulated in response to Hsp90 inhibition in numerous cell lines as well as brain tissue [104, 178]. Notably however we cannot find any reports of Hsp70 upregulation in wild type in vivo spinal cord after Hsp90 inhibitor treatment. Others have pointed out that Hsp90 inhibition does not always result in a heat shock response leading to Hsp70 upregulation [179]. It may be that Hsp90 in the spinal cord is organized differently at the molecular level than in the brain; perhaps it does not interact with heat shock factor-1 or similar proteins in the spinal cord. These differences may point to the mechanism by which Hsp90 has different signaling roles in brain vs. spinal cord.

Our observations are consistent with the ERK/RSK cascade enhancing opioid activation via rapid protein translation. Hsp90 and ERK have both been linked to the initiation of protein translation [160-163]. RSK phosphorylation by ERK has been shown to activate translation through a variety of substrates including eukaryotic translation initiation factor-4B (eIF4B), tuberous sclerosis complex-1/2 (TSC1/2), the 40S ribosomal subunit protein S6 (rpS6), glycogen synthase kinase-3 (GSK3β), and elongation factor-2 (EF2) kinase [165-171]. These studies provide plausible targets linking ERK/RSK to protein translation, but do not provide a potential mechanism for how protein translation enhances anti-nociception. Among the full list of proteins altered by 17-AAG treatment in our proteomic analysis, candidate proteins for this mechanism do occur (see

Supplementary Data). These include ion channels like KCNA4 and the CACNA2D1 subunit of the voltage gated calcium channel, and numerous signaling proteins and signaling protein regulators, such as PLCD3, PP1, RGS12, and GPR162. Alteration of the above-mentioned ion channels could lead to a reduction in action potential frequency and thus amplify the effects of MOR while the signaling protein regulators could indirectly lead to similar effects. These provide plausible future candidates to investigate that could link the protein translation we observe to enhanced anti-nociception. One finding which will guide such a search is that any candidate protein must have a rapid turnover half-life, since inhibition of translation within 30 minutes of opioid treatment abolished the response, suggesting the protein must be degraded sufficiently within that 30 minute window.

We also observed interesting systemic interactions above the level of molecular circuitry when investigating how Hsp90 inhibition in the brain and spinal cord interact. We found that brain inhibition dominated over spinal inhibition in terms of the overall behavioral output, with either systemic or combined i.c.v./i.t. inhibition. This occurred even with tail flick pain, in which brain inhibition showed no effect, but nonetheless caused a loss in spinal enhancement in tail flick anti-nociception. The brain has a well-established circuit of opioidergic descending modulation with cell bodies in the rostroventral medulla and other regions and synapsing on nociceptive modulatory circuits in the spinal cord [180]. It may be that descending modulatory neurons in the brain can override the spinal circuits when Hsp90 is inhibited in the brain. Lending some support to this hypothesis is our finding that spinal Hsp90 inhibition leads to enhanced ERK phosphorylation in lamina I/II of the dorsal horn of the spinal cord, which is a key target region for these descending neurons [181]. Investigating the circuit context in which Hsp90 regulates anti-nociception will provide key insights into how the molecular circuitry translates into a whole animal behavioral response.

In this study we demonstrate a spinal cord specific role for Hsp90 within MOR downstream signaling and in doing so, begin to elucidate MOR-dependent downstream mechanisms of ERK phosphorylation within the spinal cord which can impact systemic morphine-induced anti-nociception. We propose a mechanism in which Hsp90 serves as a brake on ERK phosphorylation within neurons in the spinal cord dorsal horn. Once the brake is removed by a spinal Hsp90 inhibitor, ERK phosphorylation is “unchained” and can contribute to MOR-agonist induced anti-nociception through RSK activation and rapid translation. This translation event must upregulate proteins which contribute to either hyperpolarization or the prevention of neurotransmitter release in primary or secondary nociceptive afferents within the spinal cord, further preventing the transmission of pain signals. This mechanism is not only significant in the context of molecular signaling, but there is also the potential to capitalize on these findings clinically by developing an opioid dose reduction strategy. Hsp90 inhibitors could be used to amplify morphine analgesia through the spinal cord without altering unwanted morphine side effects, many of which are evoked through brain regions such as the striatum (reward) or through the gut (constipation) and would not be affected by spinal cord treatment.

CHAPTER 5: IMPROVING THE THERAPUTIC INDEX OF SYSTEMIC MORPHINE THROUGH SPINAL CORD HSP90 INHIBITION

INTRODUCTION

Chronic pain is a condition which affects roughly 20% of the United States population [4]. Many of these patients lack adequately efficacious therapeutic options to manage their pain and therefore must turn to commonly prescribed opioids [182]. Continuous use of opioids for chronic pain management generates its own slew of additional problems in the form of constipation, tolerance, addiction, and respiratory depression which can lead to death [39]. It is therefore critical that the scientific community find new methods by which opioid pharmacology can be immediately improved, both enhancing analgesic efficacy and decreasing side effects. One such option for this is the modulation of opioid signal transduction through directly targeting signaling regulators with accompanying medications. One such target for this approach that we have identified is heat shock protein 90 (HSP90).

HSP90 is a chaperone protein which is involved in a variety of molecular and cellular processes, including but not limited to protein maturation, receptor translocation, transcription, translation, and kinase activation [97, 183]. HSP90 makes up ~2% of the total protein pool, which can be increased to ~6% under stressful conditions [184, 185]. The importance of HSP90 to cellular physiology is therefore not surprising, and there are likely many more functions which we are not yet aware of which may be dictated by cellular type, ongoing signal transduction, and/or the assembly of specific co-chaperone complexes. Due to the elevated expression of HSP90 in tumor cells, HSP90 has been primarily studied in the context of cancer, but recently there have emerged ongoing studies implicating HSP90 in mu opioid receptor (MOR) signal transduction [104, 143].

Our previous studies have demonstrated that intracerebroventricular (i.c.v.) administration of the HSP90 inhibitor 17-N-allylamino-17-demethoxygeldanamycin (17-AAG) prevents morphine anti-nociception in mice through an ERK dependent manner [104]. Contrary to these findings, we have additionally shown that 17-AAG treatment within the spinal cord causes an enhancement of systemic morphine anti-nociception in an ERK-RSK dependent manner **(Chapter 4)**. These contrasting results demonstrate that HSP90 has region-specific roles in the nervous system. In conjunction with these findings, novel HSP90 inhibitors such as KU-32 have recently been developed primarily as potential cancer related therapeutics [186, 187]. KU-32 is a novobiocin derivative which targets the C-terminal domain of HSP90, thereby modulating HSP90s function. These novel inhibitors provide additional tools, as well as novel approaches to dissect which functions of HSP90 are critical for modulating opioid signaling. We have previously demonstrated an equivalent effect of KU-32 to that of the earlier N-terminal ATP binding pocket inhibitor 17-AAG with regards to their effect on acute morphine induced anti-nociception **(Chapter 4),** [105].

Our findings in **Chapter 4** that spinal cord inhibition enhanced opioid anti-nociception suggested that we may be able to improve the therapeutic index of morphine using this mechanism. Since many side effects like constipation and reward/addiction are mediated through non-spinal regions, HSP90 inhibition in spinal cord would not be expected to impact them. The net effect may thus be to enhance opioid analgesia while keeping side effects the same, which could permit an opioid dose-reduction strategy.

This study set out to test this hypothesis by establishing dose response curves for morphine related anti-nociception and side effects with and without intrathecal KU-32 administration. In both acute and chronic pain models we demonstrate a dose dependent increase in morphine induced anti-nociception after i.t. KU-32 administration.

Further, we demonstrate no observable difference in the rewarding effects of morphine via conditioned place preference (CPP) and no observable difference in opioid induced constipation (OIC) via fecal pellet collection. With regards to the development of tolerance, we demonstrate that there is significant decrease in the development of tolerance with continuous i.t. KU-32 administration. Additionally, already established morphine tolerance can be retroactively reversed with i.t. KU-32 administration. These findings together suggest that spinal KU-32 treatment induces a leftward shift in the therapeutic window of morphine induced anti-nociception without altering side effects. This study in turn provides supporting evidence for a novel opioid dose reduction strategy through the spinal inhibition of HSP90 for more effective opioid pain treatment.

METHODS AND MATERIALS

Animals

Male and female CD-1 mice in age-matched controlled cohorts from 4–8 weeks of age were used for all behavioral experiments and were obtained from Charles River Laboratories (Wilmington, MA). CD-1 (a.k.a. ICR) mice are commonly used in opioid research as a line with a strong response to opioid drugs. Mice recovered for a minimum of 5 days after shipment before being used in experiments. Mice were housed no more than 5 mice per cage and kept in an AAALAC-accredited vivarium at the University of Arizona under temperature control and 12-h light/dark cycles. All mice were provided with standard lab chow and water available *ad libitum*. The animals were monitored daily, including after surgical procedures, by trained veterinary staff. All experiments performed were in accordance with IACUC-approved protocols at the University of Arizona.

Behavioral experiments

Prior to any behavioral experiment or testing, the animals were brought to the testing room in their home cages for at least 1 h for acclimation. Testing always occurred within the same approximate time of day between experiments, and environmental factors (noise, personnel, and scents) were minimized. All testing apparatus (cylinders, grid boxes, etc.) were cleaned between uses. The experimenter was blinded to treatment group by another laboratory member delivering coded drug vials, which were then decoded after collection of all data.

Paw incision and mechanical allodynia

Mechanical thresholds were determined prior to surgery using calibrated Von Frey filaments (Ugo Basile, Varese, Italy) with the up-down method and four measurements after the first response per mouse. The mice were housed in a homemade apparatus with Plexiglas walls and ceiling and a wire mesh floor (3-inch wide 4-inch long 3-inch high with 0.25- inch wire mesh). The surgery was then performed by anesthesia with ~2% isoflurane in standard air, preparation of the left plantar hind paw with iodine and 70% ethanol, and a 5-mm incision made through the skin and fascia with a no. 11 scalpel. The muscle was elevated with curved forceps leaving the origin and insertion intact, and the muscle was split lengthwise using the scalpel. The wound was then closed with 5-0 polyglycolic acid sutures. Mice were then injected i.t. and left to recover for 24 h. The next day, the mechanical threshold was again determined as described above. Mice were then injected with 1, 1.8 or 3.2 mg/kg morphine s.c., and mechanical thresholds were determined over a 3-hour time course. No animals were excluded from these studies.

Tail-flick assay

Pre-injection tail-flick baselines were determined in a 52 °C tail-flick assay with a 10-s cutoff time. The mice were then injected i.t. with 0.01 nmol KU-32 (obtained from Brain

Blagg, PhD; Department of Chemistry and Biochemistry, University of Notre Dame) or Vehicle (0.0025% DMSO in water) control with a 24-hour treatment time for all nociception experiments. 24-hours post-injection baselines were determined. The mice were then injected s.c. with 1, 3.2, 5.6, or 10mg/kg of morphine, and tail-flick latencies were determined over a 2-hour time course. For tolerance studies, baseline tail flick latencies were taken, and mice were then injected with i.t. with KU-32 with a 24-hour treatment time. 24 hours later mice were baselined again and then injected with 1, 3.2, or 10mg/kg s.c. morphine with one tail flick latency measured at 30 minutes post morphine. Mice were injected again with i.t. KU-32 and the process was repeated for an additional 7 days. For tolerance rescue experiments, mice underwent a full time course on day 1 with 10mg/kg morphine s.c. in the morning and a second injection of morphine in the afternoon. Days 2 and 3 consisted of morning and afternoon injections as well. On day 3 during the first injection, another full time course was taken to verify the development of tolerance. Mice received an i.t. injections of KU-32 or Vehicle after the second injection. On day 4 full time courses were taken again with 10 mg/kg s.c. morphine. No animals were excluded from these studies.

HIV peripheral neuropathy

Mechanical threshold baselines were measured prior to any treatment on the left hind paw using Von Frey filaments. HIV peripheral neuropathy was induced by intrathecal injection of gp120 protein (15 ng/μl in 0.1 M PBS and 0.1% BSA, 7-μl volume) using an established protocol [188] on days 1, 3, and 5. On day 20 a second mechanical threshold baseline was measured on the left hind paw using Von Frey filaments and then KU-32 was injected i.t with a 24-h treatment time. A third mechanical threshold was then measured on day 21 and morphine (1.8, 3.2, or 5.6 mg/kg s.c.) was then injected,

and mechanical thresholds were measured over a time course on the left hind paw. No animals were excluded from these studies.

Conditioned place preference

Conditioned place preference training, baseline runs, and post-training runs were all performed in Spatial Place Preference LE 896/898 rigs. Rigs were designed to consist of two chambers with one connecting chamber. Of the two conditioned chambers, one consisted of black and grey dotted walls with a textured floor. The other chamber consisted of black and grey striped walls with smooth floor. Chamber floors connected to a pressure sensor which transferred ongoing data to a computer running PPC WIN 2.0 software. Prior to preference training baselines were taken on day 0. Mice were placed in CPP chambers and allowed to roam freely for 15 minutes at ~7am. Chambers were cleaned thoroughly with VersaClean and allowed to dry in-between mice. Mice were then injected with i.t. KU-32 with a 24-hour treatment time. On day 1 mice were injected with i.t. KU-32 again and allowed to recover for 30 minutes. Mice were then injected s.c. with saline or morphine (3.2, 5.6, or 10mg/kg) at ~7am and placed in either stripe or dotted chambers. Half of each group paired morphine with the striped chamber and the other half to the dotted chamber. At ~12pm mice were then given a second injection of either saline or morphine which was paired to the opposite chamber. This training process was repeated for 4 days total which morning and noon pairings alternating each day. On day 5 mice were placed in CPP chambers and allowed to roam freely for 15 minutes at ~7am. Raw data in the form of seconds and percentage spent in chamber was exported from PPC WIN 2.0 as an excel file and transferred to GraphPad Prism for further analysis.

Opioid induced constipation

Prior to the experiment mice were injected with either KU-32 or vehicle i.t. and allowed to recover for 24 hours. 1, 3.2, or 10mg/kg s.c. morphine or saline was injected and followed by a 6-hour fecal production time course. During this time course the mice were housed in the Von Frey boxes used to collect the paw incision data above, which have a grate above a collection plate. The feces were counted and weighed in 1-hour bins and used to construct a cumulative plot. Morphine treated groups were normalized to saline groups and represented as a percentage at each timepoint. AUC values from these normalized values were also quantified for a further comparison.

Statistical analysis

All data were reported as the mean ± S.E.M. and normalized where appropriate as described above. The behavioral data were reported raw without maximum possible effect (MPE) or other normalization for the individual dose curves, but were normalized using MPE for dose/response curves. Biological and technical replicates are described in the figure legends. Comparisons of more than two groups were performed by two-way ANOVA with Sidak's post-hoc test. In all cases, significance was defined as $p < 0.05$. All graphing and statistical analyses were performed using GraphPad Prism 8.2 (San Diego, CA). Dose/response analysis was performed using linear regression to calculate A_{50} values, as previously described [104, 105].

RESULTS

The inhibition of HSP90 within the spinal cord has been previously demonstrated to enhance morphine induced anti-nociception within the thermal tail flick model and post-surgical paw incision model **(Chapter 4)**. To evaluate whether this effect occurs in a dose dependent manner within the thermal pain model, we performed tail flick assays in mice pre-treated with spinal KU-32 or vehicle and morphine doses of 1, 3.2, 5.6, and 10

mg/kg. We observed a significant increase in morphine induced anti-nociception at each dose with intrathecal KU-32 **(Fig. 1A-D)**. The resulting dose response curve yielded a 1.87 fold leftward shift in morphine potency within i.t. KU-32 treated mice **(Fig. 1E)**.

The thermal tail flick model has translational limitations as a relatively simplistic thermal and spinal reflex pain model. Therefore, we then aimed to evaluate the effects of i.t. KU-32 on a more complex acute pain model using the post-operative paw incision pain model. The resulting pain state before and after these surgeries can be evaluated using Von Frey filaments which yield a subsequent mechanical threshold. Mice which received a 24 hour pretreatment of i.t. KU-32 once again demonstrated enhanced morphine induced anti-nociception at 1, 1.8, and 3.2 mg/kg morphine doses **(Fig. 2A-C)**. Importantly, the pain state itself was not altered by KU-32, suggesting a downstream opioid specific anti-nociceptive effect. The resulting dose-response curve demonstrates a 2.29 fold leftward shift in morphine anti-nociception within the KU-32 treated mice **(Fig. 2D)**.

We demonstrated that spinal inhibition of HSP90 using KU-32 clearly enhances morphine anti-nociceptive potency in two acute pain models. Spinal HSP90 inhibition has thus far not been demonstrated to enhance morphine anti-nociception in a chronic pain model. Therefore, we aimed to assess the effects of i.t. KU-32 pretreatment on morphine anti-nociception within a HIV neuropathic pain model. This model achieves a neuropathic pain state through multiple i.t. injections of the HIV glycoprotein, gp120. After 21 days, a significant pain state is developed in mice which can then be evaluated using Von Frey filaments to obtain a mechanical threshold value. On day 20 mice were treated with i.t. KU-32 which demonstrated no significant effect on the pain state. Once again, KU-32 treated mice demonstrated an enhanced morphine induced anti-

Figure 1

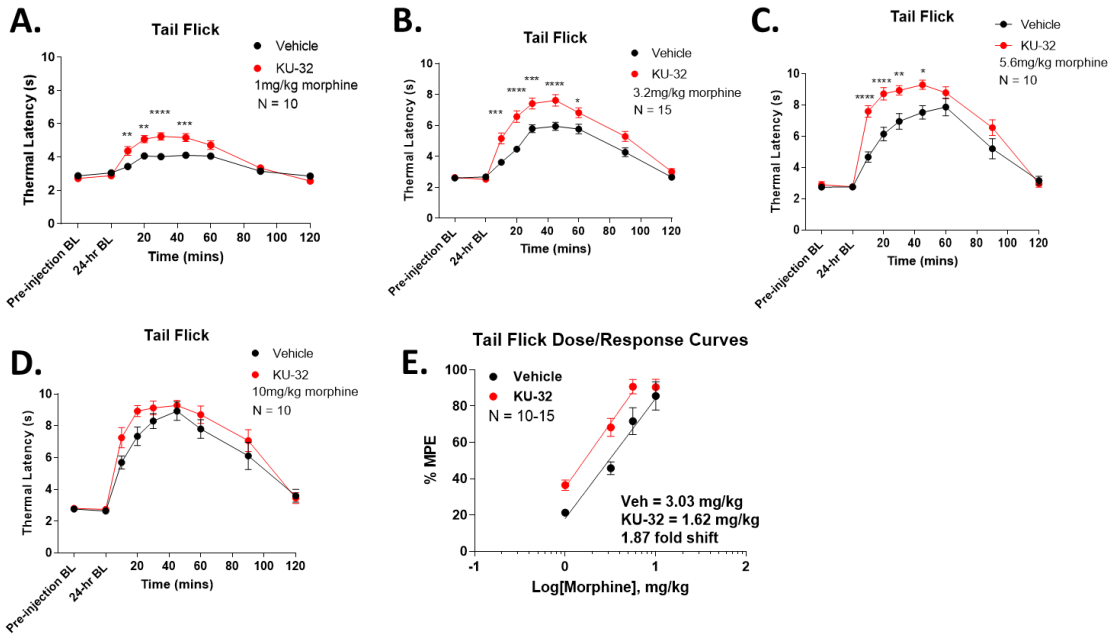

Figure 1 – Intrathecal KU-32 enhances morphine anti-nociception dose dependently in the tail flick model. Male and female CD-1 mice were injected as indicated with KU-32 (0.01 nmol) or Vehicle control by the i.t. route, followed by 24 hr recovery and then behavioral testing with or without morphine injection. Data reported as the mean ± SEM, with the sample size in mice/group noted on each graph. *, ***, **** = $p < 0.05$, 0.001, 0.0001 vs. same time point Vehicle group by 2 Way ANOVA with Sidak's post hoc test. **A-D)** Mice tested using the 52°C warm water tail flick assay with i.t. KU-32 and 1, 3.2, 5.6, and 10 mg/kg morphine s.c.; KU-32 caused a significant increase in anti-nociception. Two or three independent technical replicates each. **E)** Dose response curve demonstrating a 1.87 fold leftward shift in potency with KU-32 treated mice. A50 values: Vehicle = 3.03 mg/kg, KU-32 = 1.62 mg/kg.

Figure 2

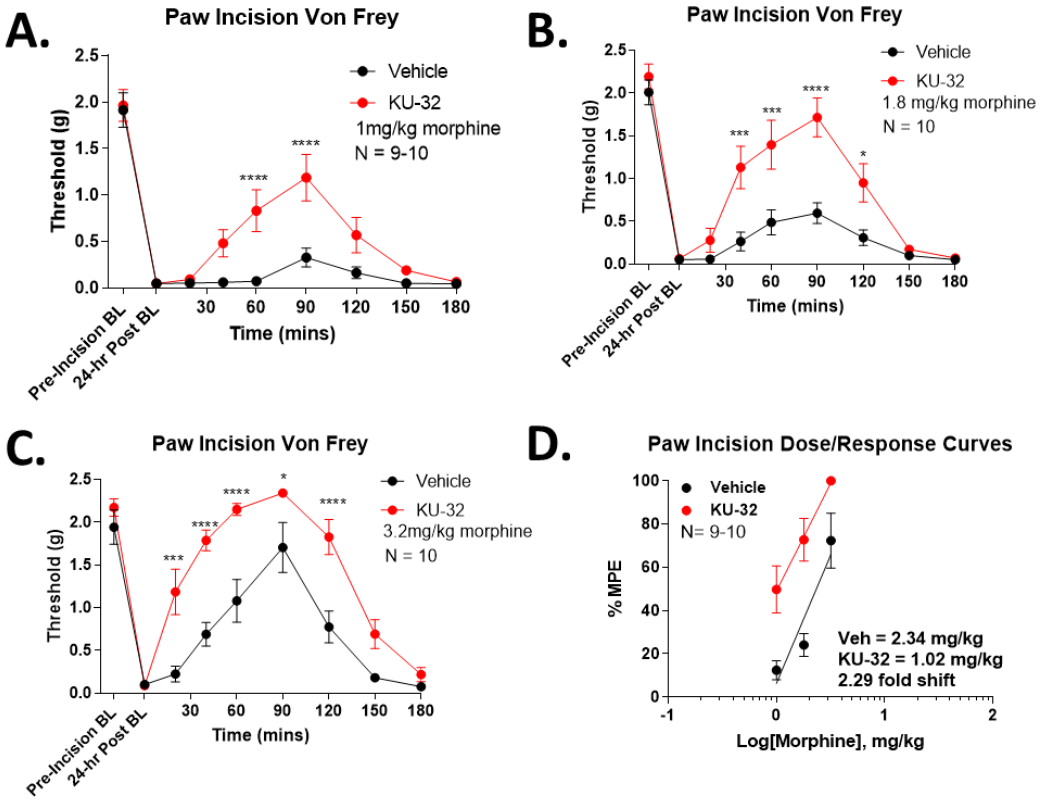

Figure 2 – Intrathecal KU-32 enhances morphine anti-nociception dose dependently in the post-operative paw incision model. Male and female CD-1 mice were injected as indicated with KU-32 (0.01 nmol) or Vehicle control by the i.t. route, followed by 24 hr recovery and then behavioral testing with or without morphine injection. Data reported as the mean ± SEM, with the sample size in mice/group noted on each graph. *, ***, **** = $p < 0.05$, 0.001, 0.0001 vs. same time point Vehicle group by 2 Way ANOVA with Sidak's post hoc test. **A-C)** Mice tested using a post-surgical paw incision model with i.t. KU-32 and 1, 1.8, and 3.2 mg/kg morphine s.c.; KU-32 caused a significant increase in anti-nociception. Two independent technical replicates each. **D)** Dose response curve demonstrating a 2.29 fold leftward shift in potency with KU-32 treated mice. A50 values: Vehicle = 2.34 mg/kg, KU-32 = 1.02 mg/kg.

nociception which occurred in a morphine dose dependent manner **(Fig. 3A-C)**. The resulting dose response curve again yielded a 3.26 fold leftward shift in morphine anti-nociceptive potency **(Fig. 3D)**.

Continuous administration of opioids such as morphine yield anti-nociceptive tolerance over time. This development of tolerance makes the treatment of chronic pain with opioids challenging in the long term, leading to dose escalation and increased side effects. The enhanced morphine induced anti-nociception caused by i.t. KU-32 pretreatment could also have impacts on the development of tolerance. To evaluate this, we used the thermal tail flick model to track peak thermal latencies after daily systemic morphine treatment over a 7 day period. Mice which received daily i.t. KU-32 still demonstrated an enhanced morphine induced anti-nociception throughout the 7 day period and still developed some, although less, anti-nociceptive tolerance at 1, 3.2, and 10mg/kg morphine doses **(Fig. 4A-C)**. Despite this apparent tolerance, the rate of tolerance development is significantly decreased, which can be seen from the difference of day 1 and day 4 in the resulting dose response curve, yielding a much smaller tolerance shift (Vehicle = 21 fold vs. KU-32 = 2.9 fold) in KU-32 treated mice **(Fig. 4D)**.

We have shown that spinal HSP90 inhibition using i.t. KU-32 enhances systemic morphine anti-nociception and reduces the development of tolerance. We also aimed to test whether this enhancement in morphine anti-nociception might still occur in a mouse which has already developed morphine anti-nociceptive tolerance. To test this, we developed morphine anti-nociceptive tolerance with twice daily injections of s.c. 10mg/kg morphine for 3 days. Morphine anti-nociception was evaluated before and after morphine tolerance development on days 1 and 3 using the thermal tail flick model **(Fig. 5A and B)**. On day 3 mice were then injected with i.t. KU-32 and were allowed to recover for 24 hours. Mice on day 4 were subjected to one additional morphine

Figure 3

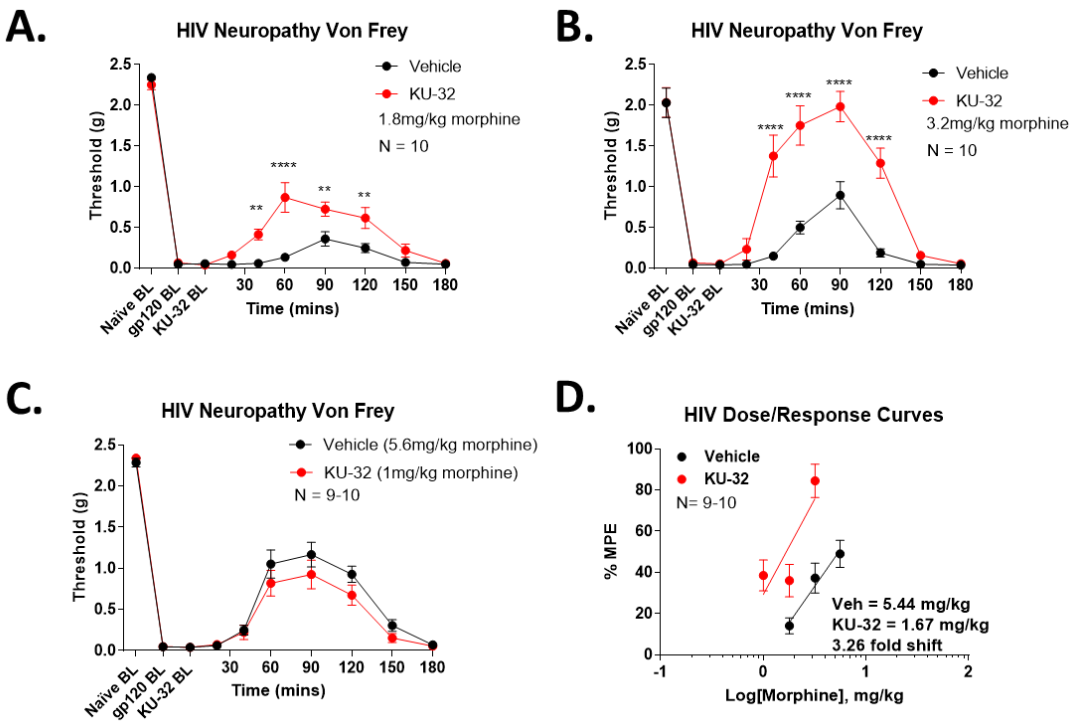

Figure 3 – Intrathecal KU-32 enhances morphine anti-nociception dose dependently in the HIV neuropathic pain model. Male and female CD-1 mice were injected as indicated with KU-32 (0.01 nmol) or Vehicle control by the i.t. route after establishment of the HIV neuropathic pain state, followed by 24 hr recovery and then behavioral testing with or without morphine injection. Data reported as the mean ± SEM, with the sample size in mice/group noted on each graph. *, ***, **** = $p < 0.05$, 0.001, 0.0001 vs. same time point Vehicle group by 2 Way ANOVA with Sidak's post hoc test. **A-C)** Mice tested using a HIV neuropathic pain model with i.t. KU-32 and 1, 1.8, 3.2, and 5.6 mg/kg morphine s.c.; KU-32 caused a significant increase in anti-nociception. Two independent technical replicates each. **D)** Dose response curve demonstrating a 3.26 fold a leftward shift in potency with KU-32 treated mice. A50 values: Vehicle = 6.44 mg/kg, KU-32 = 1.67 mg/kg.

Figure 4

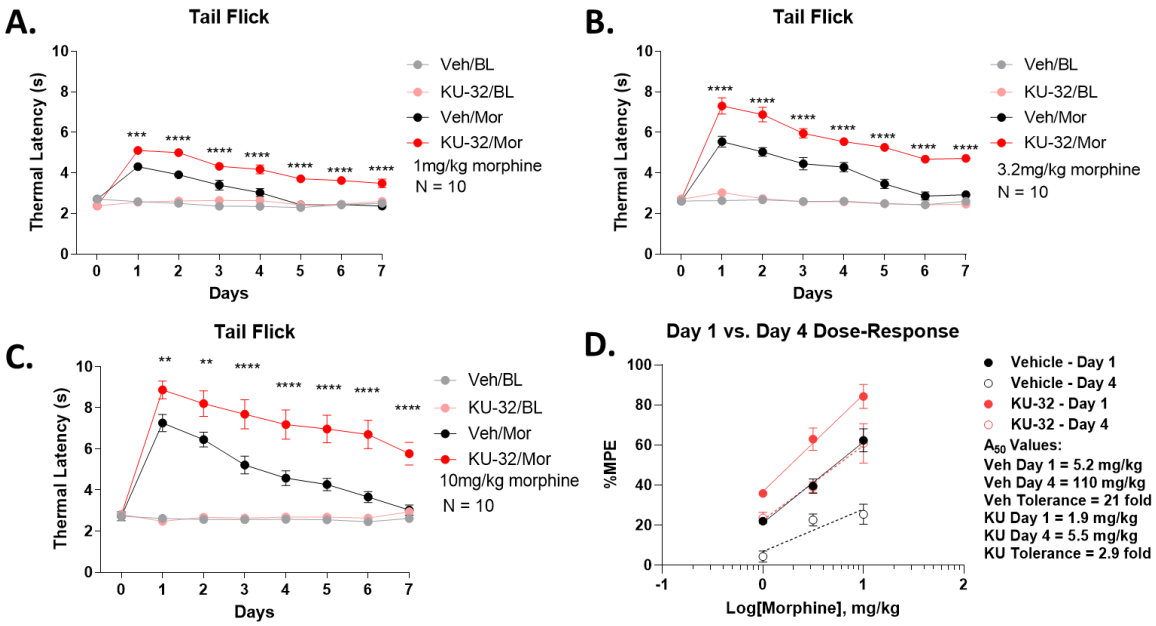

Figure 4 – Intrathecal KU-32 reduces morphine anti-nociceptive tolerance in the tail flick model. Male and female CD-1 mice were injected as indicated with KU-32 (0.01 nmol) or Vehicle control by the i.t. route daily, followed by 24 hr recovery and then behavioral testing with daily morphine injections s.c.. Data reported as the mean ± SEM, with the sample size in mice/group noted on each graph. *, ***, **** = $p < 0.05$, 0.001, 0.0001 vs. same time point Vehicle group by 2 Way ANOVA with Sidak's post hoc test. **A-C)** Mice tested using a tail flick model with daily i.t. KU-32 and daily 1, 3.2, and 10 mg/kg morphine s.c.; KU-32 still allows for a degree of morphine tolerance, but KU-32 treatment response is consistently elevated over Vehicle control. Two independent technical replicates each. **D)** Dose response curves for day 1 and day 4 show a smaller difference in the development of tolerance with KU-32 treated mice (Vehicle = 21 fold vs. KU-32 = 2.9 fold). A50 values: Vehicle day 1 = 5.2 mg/kg, KU-32 day 1= 1.9 mg/kg, Vehicle day 4 = 110 mg/kg, KU-32 = 5.5 mg/kg.

Figure 5

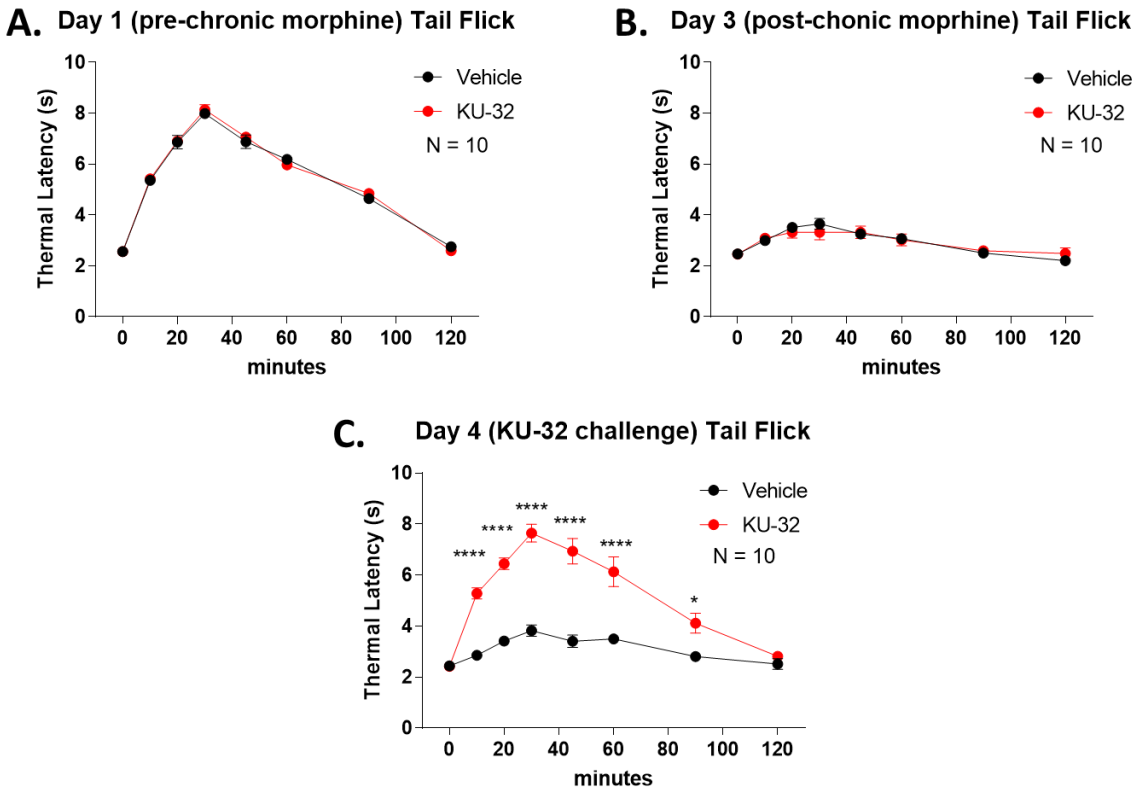

Figure 5 – Intrathecal KU-32 reverses morphine anti-nociceptive tolerance in the tail flick model. Male and female CD-1 mice were injected as indicated with KU-32 (0.01 nmol) or Vehicle control by the i.t. route after the development of tolerance on day 3, followed by 24 hr recovery and then behavioral testing with s.c. morphine on day 4 (day 1 and day 3 time courses are pre-KU-32 treatment). Data reported as the mean ± SEM, with the sample size in mice/group noted on each graph. *, ***, **** = $p < 0.05$, 0.001, 0.0001 vs. same time point Vehicle group by 2 Way ANOVA with Sidak's post hoc test. **A)** Mice tested using a tail flick model with 10mg/kg s.c. morphine on day 1, prior to chronic morphine treatment. Two independent technical replicates each. **B)** Mice tested using a tail flick model with 10mg/kg s.c. morphine after 3 days of twice daily 10mg/kg s.c. morphine. Two independent technical replicates each. **C)** Mice tested using a tail flick model with i.t. KU-32 and 10 mg/kg morphine s.c. after development of tolerance; KU-32 reverses morphine tolerance. Two independent technical replicates each.

treatment and anti-nociception was evaluated. Mice which received KU-32 demonstrated an antinociceptive profile similar to that of a pre-tolerant mouse, suggesting that established tolerance can be reversed by spinal HSP90 inhibition **(Fig. 5C)**.

We then aimed to assess additional morphine side effect profiles to confirm a lack of side effect differences with spinal KU-32 treatment. To evaluate morphine induced constipation, we collected fecal matter over a 6 hour time course after morphine treatment. To control for weight differences between male and female mice, fecal output after morphine treatment was normalized to saline treated mice. Mice which received intrathecal KU-32 demonstrated no significant difference in constipation at any morphine dose **(Fig 6A-C)**. This lack of difference was further demonstrated in the resulting dose response curve **(Fig. 6D)**. Morphine reward was evaluated using conditioned place preference at varying doses of morphine. Both vehicle and KU-32 treated mice demonstrated rewarding effects at 10mg/kg morphine which dose dependently reduced at 5.6 and 3.2 mg/kg morphine **(Fig. 7A-C)**. The resulting dose response curve demonstrates no difference between vehicle and KU-32 groups **(Fig. 7D)**.

DISCUSSION

HSP90 plays a critical role as a regulator of downstream MOR signal transduction within the brain and spinal cord [104] **(Chapter 4)**. This regulatory role has substantial impacts on morphine pain relief. In the brain, HSP90 is necessary for MOR agonist induced ERK phosphorylation to allow for morphine anti-nociception. In the spinal cord, HSP90 acts as a brake on ERK phosphorylation leading to a reduction of morphine anti-nociception. Therefore, the inhibition of HSP90 prevents morphine anti-nociception in the brain and enhances morphine anti-nociception in the spinal cord.

Figure 6

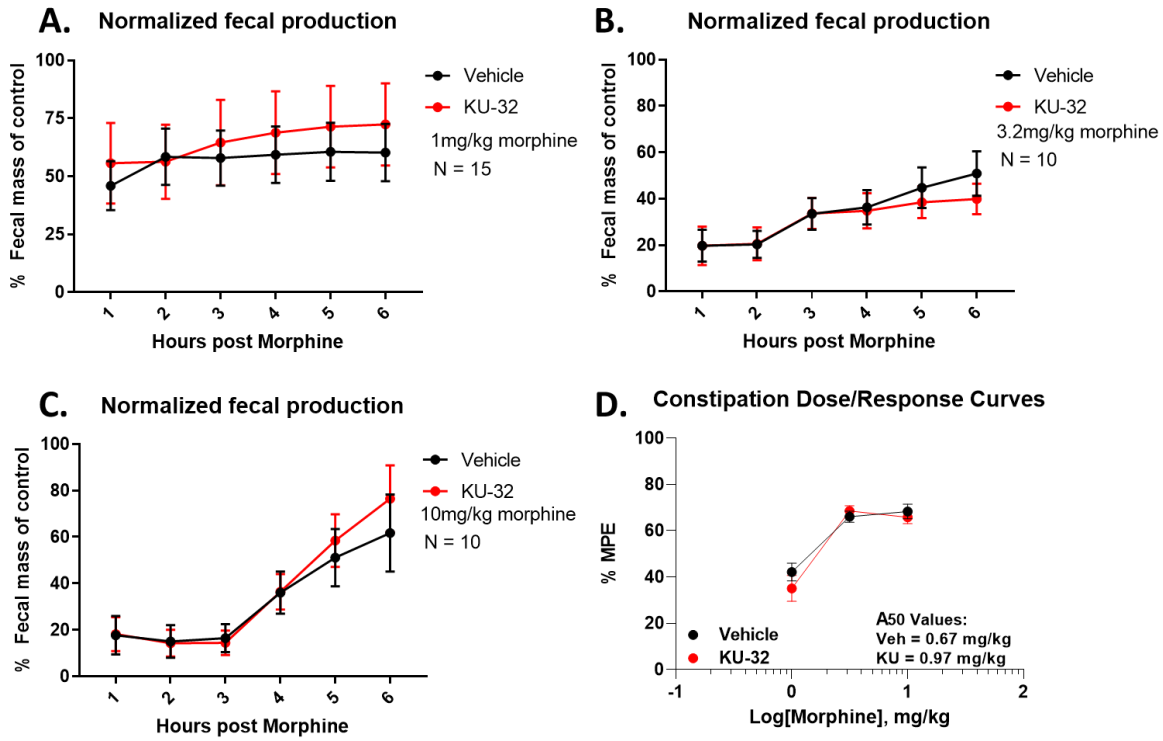

Figure 6 – Intrathecal KU-32 has no significant impact on morphine induced constipation. Male and female CD-1 mice were injected as indicated with KU-32 (0.01 nmol) or Vehicle control by the i.t. route, followed by 24 hr recovery and then behavioral testing with morphine injections s.c.. Data reported as the mean ± SEM, with the sample size in mice/group noted on each graph. *, ***, **** = $p < 0.05$, 0.001, 0.0001 vs. same time point Vehicle group by 2 Way ANOVA with Sidak's post hoc test. **A-C)** Fecal matter was collected and weighed with i.t. KU-32 and 1, 3.2, and 10 mg/kg morphine s.c. and normalized to saline controls; No significant difference between groups. Two or three independent technical replicates each. **D)** Dose response curves demonstrate no significant difference between groups. A50 values: Vehicle = 0.67 mg/kg, KU-32 = 0.97 mg/kg.

Figure 7

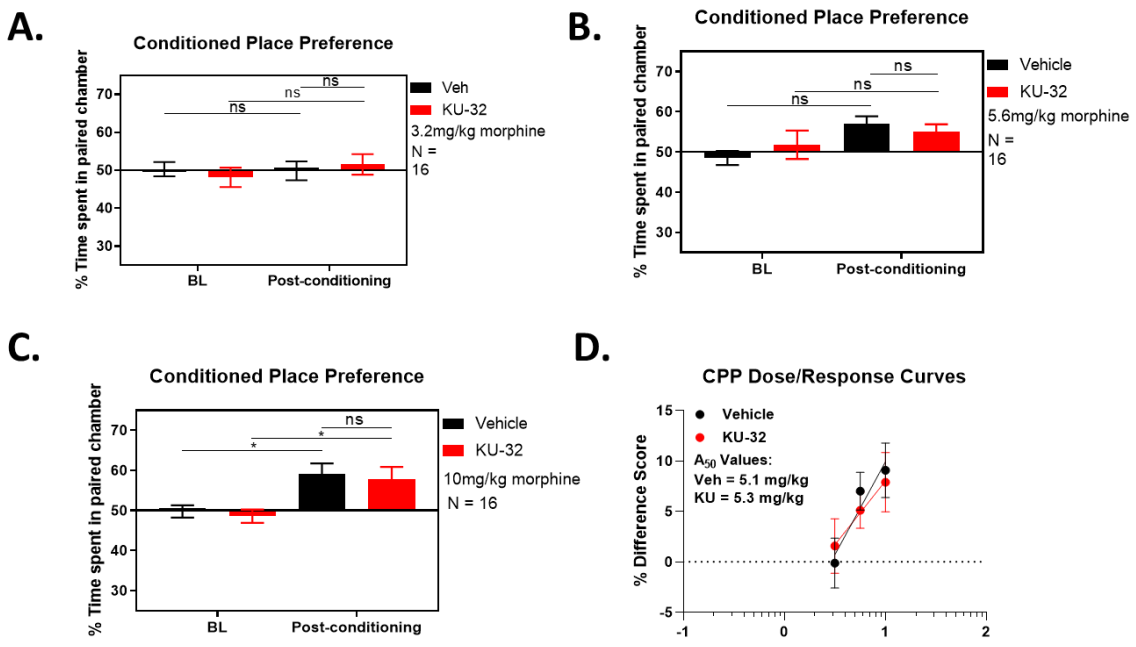

Figure 7 – Intrathecal KU-32 has no significant impact on morphine induced reward. Male and female CD-1 mice were injected as indicated with KU-32 (0.01 nmol) or Vehicle control daily by the i.t. route during CPP training to 3.2, 5.6, and 10mg/kg s.c. morphine, followed by one final day of CPP testing. Data reported as the mean ± SEM, with the sample size in mice/group noted on each graph. *, ***, **** = $p < 0.05$, 0.001, 0.0001 vs. same time point Vehicle group by 2 Way ANOVA with Tukey's post hoc test. **A-C)** CPP testing yielded no significant difference between groups in percent time spent in morphine paired chamber at any dose. A significant preference over baseline was only detected at 10 mg/kg morphine. Two independent technical replicates each. **D)** Dose response curves demonstrate no significant difference between groups. A50 values: Vehicle = 5.1 mg/kg, KU-32 = 5.3 mg/kg.

These opposing effects could be linked to differences in isoforms, chaperones, and other cellular contexts within the two regions of the CNS. Previous evidence for involvement of ERK pathways in pain have suggested this action through primarily transcriptional and post-translational regulation [189-191]. We have previously demonstrated that downstream ERK phosphorylation within pre and/or post-synaptic terminals induced by MOR activation paired with HSP90 inhibition within the spinal cord requires RSK activation and rapid translation to elicit enhanced anti-nociception **(Chapter 4)**. The specificity of ERK activation through the combination of a MOR agonist with an HSP90 inhibitor within the spinal cord may allow for a subsequently specific behavioral output which may be capitalized on to improve the therapeutic index of opioids such as morphine.

We have previously demonstrated that the N-terminal HSP90 inhibitor 17-AAG elicits an enhanced morphine anti-nociceptive profile when delivered intrathecally in mice at a 0.5 nmol dose **(Chapter 4)**. Novobiocin derived C-terminal HSP90 inhibitors such as KU-32 have shown promise in the treatment of bacterial infections, diabetic neuropathy, and chemotherapy induced cognitive impairment [192-194]. We show here that intrathecal administration of KU-32 achieves a comparable enhancement of morphine induced anti-nociception at a significantly lower dose (0.01nmol) when compared to 17-AAG.

In order to fully characterize the effects of i.t. KU-32 on morphine induced anti-nociception, we utilized two acute pain models and one chronic pain model with varying doses of morphine. In the thermal tail flick and post-operative paw incision pain models we observed a dose dependent enhancement of morphine anti-nociception and a subsequent leftward shift in morphine potency with i.t. KU-32. This effect was also

present when tested in the HIV neuropathic chronic pain model, suggesting a wide variety of pain states which i.t. KU-32 might be beneficially paired with opioid treatment.

The enhanced potency of morphine induced anti-nociception with i.t. KU-32 could drive a morphine dose reduction strategy if paired with a lack of enhanced morphine side effects. Both the CNS localization and molecular mechanism of opioid anti-nociceptive tolerance are still under extensive investigation [195-197]. Therefore, it is conceivable that i.t. KU-32 could mitigate or exacerbate morphine anti-nociceptive tolerance. We found that i.t. KU-32 administration reduced the development of tolerance and could recover anti-nociception in mice which have already developed tolerance. This may not necessarily be a direct reversal of tolerance itself, but rather an enhancement of spinal morphine induced anti-nociception despite the presence of CNS wide morphine tolerance detectable by the thermal tail flick model. Although spinal cord ERK signaling has been implicated in the development of morphine tolerance, these signaling events has thus far been primarily localized to microglia and astrocytes [176, 198, 199].

The localization and mechanisms of opioid induced constipation and reward are better understood in comparison to tolerance. Constipation is believed to be primarily localized to the enteric nervous system, while reward is believed to be localized to the mesolimbic dopamine pathway including the VTA and NAc [57, 200-203]. Therefore, i.t. injections of KU-32 are unlikely to impact these morphine induced side effects. Indeed, upon assessing these side effects with i.t. KU-32 we observe no significant difference compared to vehicle treated animals.

This study demonstrates an improved therapeutic index for morphine paired with intrathecal KU-32 administration. KU-32 treated mice display a dose dependent enhanced morphine induced anti-nociception in both acute and chronic pain models while improving anti-nociceptive tolerance development, without impacting reward or

constipation. Additionally, pre-developed tolerance was reversed in mice given i.t. KU-32. Overall spinal inhibition of HSP90 with compounds such as KU-32 may provide an alternative strategy for improving chronic morphine treatment in humans as a dose reduction strategy.

CHAPTER 6: NON-PHARMACOLOGICAL IMPROVEMENT OF THE THERAPUTIC INDEX OF MORPHINE: INTERMITTENT FASTING

INTRODUCTION

The opioid crisis has impacted the United States significantly, especially within the last decade, with roughly one hundred individuals dying each day due to opioid related overdoses [204]. This problem stems from many sources, including the abuse potential of opioids, the high prevalence of chronic pain within the United States, and the overprescribing of opioid analgesics within the clinic [182, 205]. Much of the effort to address this crisis revolves around the design and synthesis of novel compounds with lower abuse potential to replace current clinical opioids [206-208]. Some of these compounds are opioids which are designed to lack negative side effects, while others are non-opioid alternatives. The major issue with this approach is the long and typically unsuccessful process of clinical trials, with most compounds lacking efficacy and/or retaining the side effect profile of typical opioids. In the short-term these approaches do not address the immediate crisis of chronic pain patients within the clinic who must rely on opioid analgesics. Rather than forsake the current chronic pain patient population, it is prudent to develop alternative strategies for both chronic pain and opioid use management which can be quickly implemented.

Intermittent fasting (IF) or time restricted feeding is a method of food consumption which has recently grown in popularity as a weight management strategy [124]. There are many general schemes of IF. Some of the more popular schemes include: monthly fasting in which the individual goes without food for 3-5 days each month, weekly fasting in which the individual goes without food for 2 days each week, alternative day fasting in which the individual goes without food every other day, and daily fasting in which the individual goes

without food for 16-20 hours each day. The commonality between these schemes is the consistent and continuous period in which the individual goes without food. The idea behind eating in such a manner is to mimic our ancestors. There is a general consensus that human ancestors consumed food in an intermittent manner for hundreds of thousands of years due to the difficulty of food collection and preservation [209]. It is only within the last 100-200 years, in which the industrial age has given rise to an abundance of food, which has allowed for continuous feeding throughout the day [210]. This has occurred particularly within the United States and Western Europe which suffer the most with regards to obesity [211, 212]. From an evolutionary perspective it is plausible to hypothesize that our physiology evolved to operate most efficiently during long periods of fasts and that deviation from this pattern may explain many of the prevalent food-related pathologies within modern day society [213, 214]. For example, continuous insulin exposure due to standard American feeding patterns may result in tissue insulin resistance, leading to metabolic disease [215-217].

The health benefits of IF have been focused mostly on its positive effects on obesity and metabolic disorders, such as type 2 diabetes [123, 218-220]. These health benefits have also been extended to improvements in general homeostatic function and cognitive performance [221-224]. There is also evidence to support potential benefits in many pathological conditions including cardiovascular disease, neurological disorders, immunological disorders, and even cancer [118, 225-229]. Despite this literature, IF has not been tested as a strategy to improve opioid therapy.

It has previously been shown that endogenous opioid systems become active in the context of food consumption. The classic example being endogenous opioid release within the mesolimbic dopamine system to allow for food reward [230-232]. There are also studies which implicate the effects of certain “western” diets, which involve continuous

consumption of high fat content, on glutamatergic and opioid signaling [113-115]. In addition to these studies, new research has also found that acute (not intermittent) fasting alters mu opioid receptor (MOR) binding, signaling, and mRNA synthesis [233-235]. However, only one study has directly studied the impact of IF on opioid function. A 16-hour daily IF protocol resulted in a circadian shift in morphine anti-nociception via hot plate paw withdrawal in mice [125]. No other studies have addressed this question or investigated how IF might impact opioid pain therapy and side effects, although this approach has been suggested in the literature [127]. Considering the many interactions of food consumption with opioid systems and the general benefits shown for IF diets, we are interested in how IF might impact all aspects of opioid pharmacology. We are particularly interested in how IF might affect morphine analgesia, side effect profiles, and potential molecular mechanisms for these effects.

We thus established an 18/6 hour IF protocol by which male and female CD-1 mice underwent 18 hour fasting periods daily for one week while maintaining their body weight. After one week of this eating pattern, mice were then either given morphine acutely or chronically, and behavioral pain and side effect assays were performed. Acute morphine anti-nociception was strongly enhanced in both tail flick and post-operative paw incision pain models. Opioid induced constipation (OIC), the development of tolerance, and reward measured by conditioned place preference (CPP) were all reduced or completely blocked in IF mice. MOR function was measured by a ^{35}S-GTPγS coupling assay, which demonstrated increased MOR efficacy in spinal cord and no development of tolerance in the periaqueductal grey (PAG) brain region in IF mice. Western blots on spinal cord and PAG showed no significant differences in MOR expression, suggesting the observed functional benefits are independent of MOR expression. Overall this study demonstrates

a highly novel and strong benefit for IF in opioid therapy, the results of which could be quickly translated into clinical studies.

METHODS AND MATERIALS

Materials

Morphine sulfate pentahydrate was obtained from the NIDA Drug Supply Program. DAMGO (#11711) was obtained from Fisher Scientific (Hampton, NH). Morphine was prepared fresh prior to each experiment in USP saline or USP water (for i.c.v. and i.t. experiments). DAMGO was prepared as a 10 mM stock solution in water and stored at -20°C until use (single use aliquots). Saline or water vehicle controls were used in the experiments as described.

Animals

Male and female CD-1 mice were randomized to treatment group in age-matched controlled cohorts from 5–8 weeks of age for all behavioral experiments and were obtained from Charles River Laboratories (Wilmington, MA). CD-1 (a.k.a. ICR) mice are commonly used in opioid research as a line with a strong response to opioid drugs (e.g. [104, 148]). Mice were recovered for a minimum of 5 days after shipment before being used in experiments. Mice were housed 5 mice per cage and kept in an AAALAC-accredited vivarium at the University of Arizona under temperature control and 12-hr light/dark cycles. Control mice were provided with standard lab chow and water available *ad libitum*. IF mice were provided with 5 grams of food per mouse (25 grams total per cage) from 10AM to 4PM (6 hours). Any leftover food was removed at the end of this period and repeated the next day for 1-2 weeks. Mouse body mass was monitored to be sure body mass was maintained over the duration of the experiment. Acute 24 hour fasted mice had their food removed at 10AM with the following experiments occurring the next day at 10AM. Animals

were monitored daily, including after surgical procedures, by trained veterinary staff. All experiments performed were in accordance with IACUC-approved protocols at the University of Arizona, and by the standards of the NIH Guide for the Care and Use of Laboratory Animals.

Behavioral experiments

Prior to any behavioral experiment or testing, the animals were brought to the testing room in their home cages for at least 1 hr for acclimation. Testing always occurred within the same approximate time of day between experiments, and environmental factors (noise, personnel, and scents) were minimized. All testing apparatus (grid boxes, etc.) were cleaned between uses. The experimenter was blinded to treatment group by coding the identity of the treatment cages until after all data was collected.

Post-surgical paw incision and mechanical allodynia

Mechanical thresholds were determined prior to surgery using calibrated Von Frey filaments (Ugo Basile, Varese, Italy) with the up-down method and four measurements after the first response per mouse. The mice were housed in a homemade apparatus with Plexiglas walls and ceiling and a wire mesh floor (3-inch wide 4-inch long 3-inch high with 0.25- inch wire mesh). The surgery was then performed by anesthesia with ~2% isoflurane in standard air, preparation of the left plantar hind paw with iodine and 70% ethanol, and a 5-mm incision made through the skin and fascia with a no. 11 scalpel. The muscle was elevated with curved forceps leaving the origin and insertion intact, and the muscle was split lengthwise using the scalpel. The wound was then closed with 5-0 polyglycolic acid sutures. The next day, the mechanical threshold was again determined as described above. Mice were then injected with 3.2 mg/kg morphine s.c., and mechanical thresholds

were determined over a 3-hour time course. No animals were excluded from these studies. This method is also reported in our previous work [104, 236].

Tail-flick assay

Tail-flick baselines were determined in a 52°C warm water tail-flick assay with a 10 sec cutoff time. The mice were then injected s.c. with 3.2mg/kg of morphine, i.v. with 0.1 mg/kg morphine, i.t. with 0.1nmol morphine, or i.c.v with 0.5 nmol morphine in saline. The procedures for i.c.v. and i.t. injection are described in our previous work [104]. Tail-flick latencies were determined over a 2-hour time course. For tolerance studies, baseline tail flick latencies were taken, and mice were then injected with 10mg/kg s.c. morphine with one tail flick latency measured at 30 minutes post morphine. This process was then repeated for 7 days. No animals were excluded from these studies.

Opioid-induced constipation

IF mice were allowed food 2 hours prior to the OIC experiment. Morphine (10 mg/kg, s.c.) was injected followed by a 6 hour fecal production time course. During this time course the mice were housed in the Von Frey boxes used to collect the paw incision data above, which had a wire mesh floor above a collection plate. The feces were counted and weighed in 1 hour bins and used to construct a cumulative plot. Morphine treated groups were then normalized to saline groups and represented as a percentage at each timepoint. AUC values from these normalized values were also quantified for a further comparison using GraphPad Prism 8.2.

Conditioned place preference

CPP training, baseline runs, and post-training runs were all performed in Spatial Place Preference LE 896/898 rigs. Rigs were designed to consist of two chambers with

one connecting chamber. Of the two conditioned chambers, one consisted of black and grey dotted walls with a textured floor. The other chamber consisted of black and grey striped walls with a smooth floor. Chamber floors connected to a pressure sensor which transferred ongoing data to a computer running PPC WIN 2.0 software. Prior to preference training, unconditioned baselines were taken on day 0. Mice were placed in CPP chambers and allowed to roam freely for 15 minutes at ~10AM. Chambers were cleaned thoroughly with VersaClean and allowed to dry between mice. On day 1 of training mice were injected with 10mg/kg s.c. morphine at ~10AM and placed in either stripe or dotted chambers. Half of each group paired morphine with the striped chamber and the other half to the dotted chamber. At ~4PM mice were then given a second injection of saline which was paired to the opposite chamber. This training process was repeated for 4 days total with morning and afternoon pairings alternating each day. On day 5 mice were placed in CPP chambers and allowed to roam freely for 15 minutes at ~10AM. Raw data in the form of seconds and percentage spent in each chamber was exported from PPC WIN 2.0 as an Excel file and transferred to Prism 8.2 for further analysis.

Western blotting and analysis

Mouse spinal cord, PAG, and striatum protein lysates were prepared as previously reported [104] and quantified with a BCA protein quantitation assay using the manufacturer's protocol (Bio-Rad, Hercules, CA). The protein was run on precast Bolt gels (ThermoFisher, Waltham, MA) following the manufacturer's instructions. The gels were transferred to nitrocellulose membrane (Bio-Rad) using a wet transfer system (30 V, minimum of 1 h on ice). The blots were blocked with 5% nonfat dry milk in TBS and incubated with primary antibody in 5% BSA in TBS + 0.1% Tween-20(TBST) overnight rocking at 4°C. The blots were then washed three times for 5 min in TBST, incubated with secondary antibody (see below) in 5% milk in TBST for 1 hr of rocking at room

temperature, washed again, and imaged with a LiCor Fc infrared imaging system (LiCor, Lincoln, NE). The blots were then stripped with 25 mM glycine-HCl and 1% SDS, pH 2.0, for 30–60 min of rocking at room temperature prior to being washed and re-exposed to primary antibody. The resulting image bands were quantified using Scion Image (based on NIH Image). All images were quantified in the linear signal range. The MOR signal was normalized to GAPDH signal for spinal cord and PAG tissues, and β-actin for striatal tissue, with both measured from the same blot as the primary target. The normalized intensities were further normalized to a vehicle control present on the same blot.

Antibodies

The antibodies used were: GAPDH (ThermoFisher #MA5-15738, Lot PI209504, mouse, 1:1000), β-actin (Cell Signaling #3700S, Lot 17, mouse, 1:1000), MOR (Abcam #ab134054, Lot GR180137-4, rabbit, 1:1000), secondary GαM680 (LiCor #926-68020, Lot C50721-02, goat, 1:10,000–1:20,000), and secondary GαR800 (LiCor #926-32211, Lot C50602–05, goat, 1:10,000–1:20,000).

^{35}S-GTPγS coupling

^{35}S-GTPγS (#NEG030H250UC) was obtained from PerkinElmer (Waltham, MA). Guanosine diphosphate (GDP) was obtained from Sigma Aldrich (St. Louis, MO), stored at -20°C under desiccation, made fresh for each experiment, and discarded after 60 days. Standard chemicals and buffers were purchased from Fisher Scientific with a minimum purity of 95%. Our protocol for ^{35}S-GTPγS coupling is also reported in [237-240]. Mouse tissues were dounce homogenized in homogenization buffer containing: 20 mM HEPES pH 7.0, 100 mM NaCl, 2 mM $MgCl_2$, 1 mM EDTA, 1 mM DTT, and centrifuged at 20,000g for 20 minutes at 4°C. The resulting pellet was resuspended in assay buffer containing: 20 mM HEPES pH 7.0, 150 mM NaCl, 2 mM MgCl2,100 μM GDP. Concentration curves of

DAMGO or vehicle were combined with 15 µg of membrane protein and 25 pM ^{35}S-GTPγS (PerkinElmer) at a 200 µL volume using assay buffer. The reactions were incubated at RT for 2 hours. Reactions were terminated by rapid filtration through 96 well GF/B filter plates (PerkinElmer) using a 96 well format Brandel (Gaithersburg, MD) cell harvester. The plates were dried, 40 µL of Microscint PS (PerkinElmer) was added, and the data was collected using a 96 well format 6 detector MicroBeta2 scintillation counter (PerkinElmer). The resulting data was normalized to the stimulation caused by AL/Saline groups (100%) and vehicle (0%). The data was then fit with a 3 variable agonist curve, providing the potency (EC_{50}) and efficacy (E_{MAX}), using Prism 8.2 (GraphPad). The resulting data from N = 3 independent experiments performed at least in duplicate was reported as the mean with 95% confidence intervals (CI).

Statistical analysis

All data was reported as the mean ± SEM or 95% CI and normalized where appropriate as described above. The behavioral data were reported raw without maximum possible effect (MPE) or other normalization. Biological and technical replicates are described in the figure legends. Statistical comparisons were performed by Repeated Measures 2 Way ANOVA with Sidak's (paw incision, tail flick, weight, constipation) or Tukey's (CPP, Western) *post hoc* tests. Constipation AUC was compared by an Unpaired 2-Tailed *t* Test. In all cases, significance was defined as $p < 0.05$. For the ^{35}S-GTPγS experiments, potency and efficacy values were obtained from fitted curves from N = 3 animals performed in duplicate, reported as the mean with 95% CIs. Potency and efficacy values were considered significantly different if their 95% CIs did not overlap. All graphing and statistical analyses were performed using GraphPad Prism 8.2 (San Diego, CA). Approximately equal numbers of male and female CD-1 mice were used for each experiment. These were compared by 2 Way ANOVA with sex as a variable; no

differences were observed ($p > 0.05$) between male and female mice, so males and females were combined together and reported as one group in each experiment.

RESULTS

Daily intermittent fasting enhances morphine anti-nociception

Based on the human IF literature to model feasible translation, we chose a daily IF diet with an 18-hour fasting window and a 6-hour feeding window (10 AM – 4 PM, light cycle). Mice were housed in groups of 5 and provided with 5 grams of food per mouse during each feed period for 1 week. *Ad libitum* (AL) fed controls were provided free access to food 24 hours a day. The weight of each mouse was monitored on a daily basis before and after the feeding period. AL and IF mice were first subjected to the post-operative paw incision pain assay after 7 days of IF; mechanical thresholds were evaluated before and after paw incision surgeries, which demonstrated no significant difference between AL and IF groups (**Figure 1A-B**). Upon morphine treatment (3.2 mg/kg, s.c.), IF mice displayed an enhanced duration anti-nociception vs. AL controls; this was apparent both during the fasted state at 10 AM (**Figure 1A,** area under the curve [AUC] increase of 66.9%) and the fed state at 4 PM (**Figure 1B**, AUC increase of 80.9%). This experiment suggests that acute feeding status has no impact on anti-nociception, and that enhanced anti-nociception is due to the IF diet itself.

To investigate an alternative pain type, we performed the thermal tail flick pain model and assessed thermal latencies before and after morphine treatment (3.2 mg/kg, s.c.). IF baselines did not differ from that of their AL counterparts, but IF mice demonstrated a significantly enhanced efficacy of morphine induced anti-nociception, similar to that of the paw incision model (**Figure 1C**, AUC increase of 109%). This finding suggests that IF enhances anti-nociception over multiple pain models and modalities

Figure 1

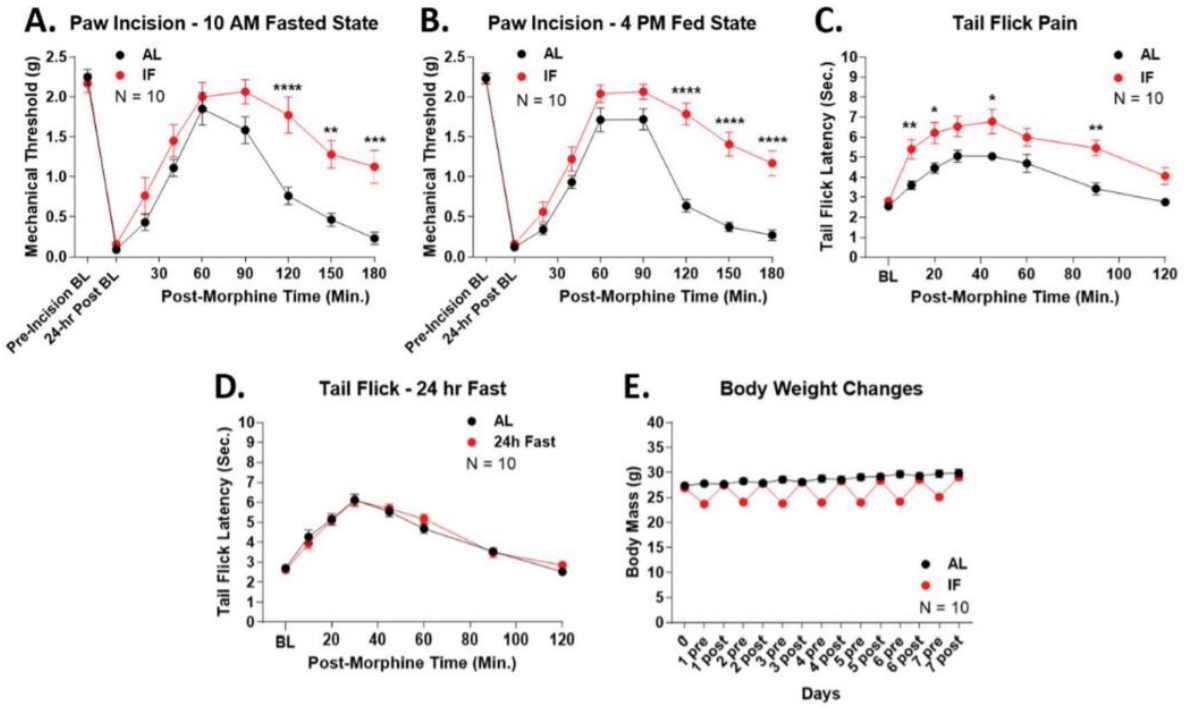

Figure 1 – Daily intermittent fasting enhances morphine anti-nociception. Male and female CD-1 mice were treated with an 18/6 hour intermittent fasting (IF) protocol for 7 days, along with *ad libitum* (AL)-fed controls. Data reported as the mean ± SEM with the sample size of mice/group noted in each graph. Each experiment had two independent technical replicates. *, **, ***, **** = $p < 0.05, 0.01, 0.001, 0.0001$ vs. same time point AL group by Repeated Measures 2 Way ANOVA with Sidak's *post hoc* test. **A)** Paw incision surgery performed on day 7 at 10 AM in the fasted state, with a 24 hour recovery and continued IF protocol. Pre- and post-surgery baselines were measured, and were not different. The mice were then injected at 10 AM on day 8 with 3.2 mg/kg, s.c. morphine with a 3 hour time course of mechanical allodynia measurement. IF enhanced morphine anti-nociception with an AUC increase of 66.9%. **B)** Paw incision performed as in **A**, except at 4 PM in the fed state. IF enhanced morphine anti-nociception with an AUC increase of 80.9%. **C)** Tail flick baselines were performed on day 7, which were not different between IF and AL mice. The mice were injected with 3.2 mg/kg, s.c. morphine and a 2 hour tail flick time course performed. IF enhanced morphine anti-nociception with an AUC increase of 109.0%. **D)** Naïve

mice were treated with an acute 24 hour fast, or AL controls. The tail flick assay was performed using 3.2 mg/kg, s.c. morphine. Baselines and morphine anti-nociception was not impacted by the acute fast ($p > 0.05$). **E)** Mouse body weights were recorded daily at 10 AM and 4 PM during the IF protocol (pre- and post-feeding). At 10 AM the IF groups had 2-4 g less body mass, however, body weights were the same as AL controls at the 4 PM fed period each day ($p > 0.05$). This suggests that the IF mice do not lose body mass during the protocol, and that the pre-feeding dip is due to the lack of bulk food mass in their GI tract after the 18 hour fasting period.

(naïve vs. post-surgical; thermal vs. mechanical). We also tested whether an acute fast for 24 hours could mimic these effects, or whether a sustained IF diet was necessary. We found that a 24 hour fast had no impact on baseline or morphine-induced responses in the tail flick assay, suggesting that a sustained IF diet is needed (**Figure 1D**). Lastly, we controlled for changes in weight which could impact opioid response. AL fed mice demonstrated a steady increase in body weight over the course of 7 days. Although IF mice demonstrated weight fluctuations of roughly 2-4 grams before and after eating, they also displayed a similar steady increase in body weight which was equivalent to that of the AL group at the end of each daily feed period (**Figure 1E**). This finding suggests that weight loss is not responsible for the enhanced morphine anti-nociception.

Daily intermittent fasting blocks morphine-induced reward

Opioid induced reward is a major contributing factor towards opioid addiction and dependence [42, 203]. IF has been shown to enhance brain plasticity, which might impact reward circuits and/or reward learning [127]. We thus utilized the well-established CPP assay to evaluate the effects of daily IF on morphine reward. AL mice demonstrated a significant preference for the morphine-paired (10 mg/kg, s.c.) chamber, which was absent in IF mice; neither group showed differences in baseline preference (**Figure 2A**). Food consumption is well-known to activate reward circuits, which might impact morphine reward; we thus measured morphine preference during fasted (10 AM) and fed (4 PM) states within IF mice. Both fasted and fed IF mice had no morphine preference, suggesting that blockade of morphine reward depends on sustained IF rather than acute feeding status (**Figure 2B**). The effects on morphine preference/reward were also consistent across the populations of each group, rather than being driven by outliers or extremes (**Figure 2C**). These observations thus suggest that IF mitigates or blocks morphine reward, which could be a unique translational tool to prevent pain patients from

Figure 2

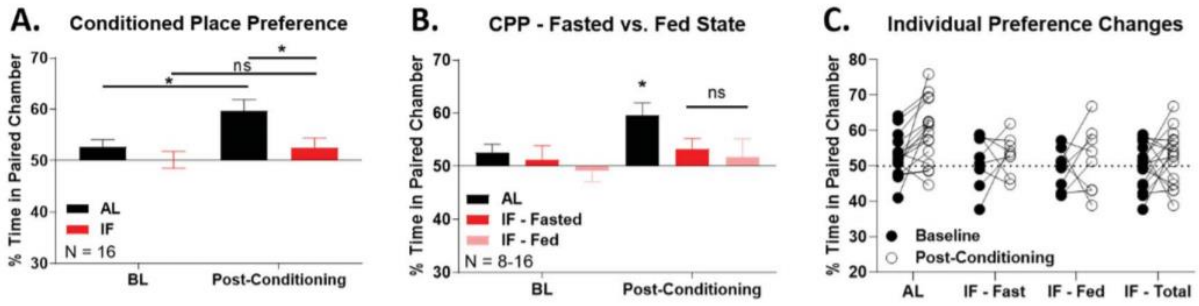

Figure 2 – Daily intermittent fasting blocks morphine-induced reward. Male and female CD-1 mice were treated with the IF or AL control protocol for 7 days, with CPP conditioning beginning on day 7 (see Methods for CPP protocol). All mice received 10 mg/kg s.c. morphine as the conditioning stimulus, with saline as the counter-balanced unconditioned stimulus. Data reported as the mean ± SEM of the % time spent in the paired (morphine) chamber. Sample sizes of mice/group noted in the graphs. * = $p < 0.05$ vs. indicated group by Repeated Measures 2 Way ANOVA with Tukey's *post hoc* test. Experiments performed in 2 independent technical replicates. **A)** Combined data from all mice. Baseline preference in either group was not different from the 50% mark. Morphine caused a significant preference in the AL group, which was not observed in the IF group. **B)** The IF data from **A** was split into 10 AM Fasted and 4 PM Fed groups (N = 8/each). Acute feeding status had no impact on morphine preference, with neither IF group showing a significant difference from baseline or each other ($p > 0.05$). **C)** The individual responses for each animal from each group are shown, baseline and post-conditioning. The population results suggest that the responses are consistent across each population, and are not being driven by outlie

transitioning to addiction during opioid treatment.

Daily intermittent fasting reduces morphine-induced tolerance and constipation

Opioid tolerance contributes to dose escalation, dependence, and addiction, while opioid-induced constipation has a strong negative impact on patient quality of life [241, 242]. We therefore investigated the effects of IF on these equally important aspects of morphine pharmacology. We induced morphine anti-nociceptive tolerance with daily 10mg/kg s.c. morphine injections followed by a thermal tail flick latency measurement 30 minutes after the injection. We observed a steady decline in thermal latencies in AL mice over a 7-day period, resulting in 94.6% tolerance; this tolerance was strongly reduced to 43.6% in IF mice (**Figure 3A**). We observed no differences in saline injected controls.

To assess IF's effects on constipation, we collected fecal matter produced from both AL and IF mice treated with either morphine or saline over a 6-hour time course. IF mice injected with saline produced more fecal matter over the 6 hour time course when compared to AL mice (**Figure S1**). To control for this difference, fecal production collected from mice injected with morphine was normalized to that of their saline counterparts. AL mice demonstrated a significant constipatory reduction in fecal output with morphine treatment which was significantly reduced by the IF diet (**Figure 3B-C**). Together these experiments suggest that IF enhances the therapeutic index of morphine, improving anti-nociception while reducing/blocking reward, tolerance, and constipation.

Altered pharmacokinetics do not explain enhancement of anti-nociception by IF

The pharmacokinetic profile of morphine has previously been shown to be altered in leptin deficient mice [243]. It is therefore possible that the altered pattern of leptin release in response to food intake with an IF diet could also cause pharmacokinetic differences which might account for the enhanced morphine induced anti-nociception observed. We thus injected equi-efficacious doses of morphine into AL and IF mice by

Figure 3

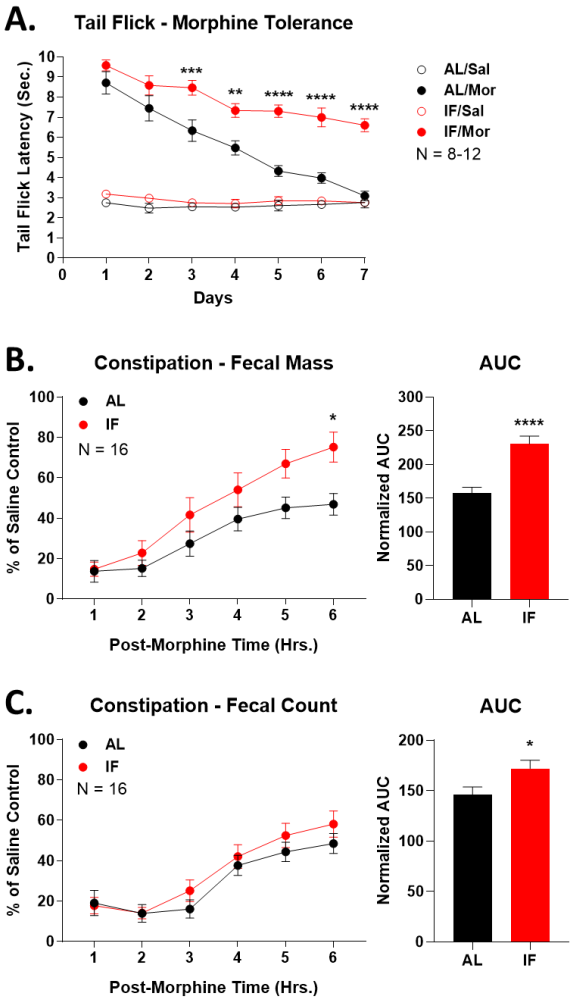

Figure 3 – Daily intermittent fasting reduces opioid tolerance and constipation. Male and female CD-1 mice were subjected to the 7 day IF protocol or AL control, with testing beginning on day 7. Data reported as the mean ± SEM, with sample sizes of mice/group noted in the graphs. 2-4 independent technical replicates performed for each experiment. *, **, ***, **** = $p < 0.05$, 0.01, 0.001, 0.0001 vs. same time point AL group by Repeated Measures 2 Way ANOVA with Sidak's *post hoc* test. **A)** Beginning on day 7, mice injected daily with 10 mg/kg morphine s.c. or saline control, with the IF or AL control protocol continuing with injections out to day 14. Tail flick latency measured 30 minutes after each daily injection and reported here. By day 7 (day 14 of total protocol), AL controls showed 94.6% tolerance, while IF mice showed 43.6% tolerance. **B)** On day 7, mice were injected with 10 mg/kg morphine s.c. or saline control with fecal mass in

grams measured over a 6 hour time course in a cumulative plot. The morphine treatment groups were normalized to % of saline control at each time point. AUC values were also reported for each group; **** = $p < 0.0001$ by Unpaired 2-Tailed *t* Test. **C)** The fecal count for **B** reported; * = $p < 0.05$ by Unpaired 2-Tailed *t* Test.

Figure 4

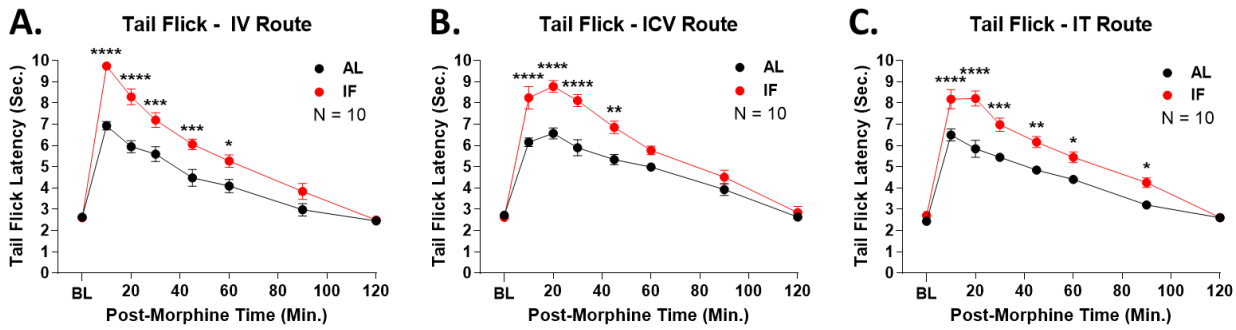

Figure 4 – Altered pharmacokinetics do not explain benefits of intermittent fasting. Male and female CD-1 mice treated with 7 day IF protocol or AL control. On day 7, mice injected with equi-efficacious doses of morphine as noted below, with a tail flick time course. Data reported as the mean ± SEM with the sample sizes noted in the graphs. Two independent technical replicates were performed for each experiment. *, **, ***, **** = $p < 0.05, 0.01, 0.001, 0.0001$ vs. same time point AL group by Repeated Measures 2 Way ANOVA with Sidak's *post hoc* test. **A)** 0.1 mg/kg morphine injected by the i.v. route. **B)** 0.5 nmol morphine injected by the i.c.v. route. **C)** 0.1 nmol morphine injected by the i.t. route. All 3 routes show equivalent enhancement of anti-nociception by IF, suggesting that IF does not alter morphine pharmacokinetics.

three different routes, intravenous (i.v., **Figure 4A**), intracerebroventricular (i.c.v., **Figure 4B**), and intrathecal (i.t., **Figure 4C**). Intravenous injection circumvents absorption into the bloodstream necessary in our previous s.c. injections, while i.c.v. and i.t. injection are direct into the CNS, bypassing distribution through the blood-brain-barrier. In all 3 cases, we observed an equivalent enhancement in morphine anti-nociception, very similar to the s.c. results in **Figure 1**. These experiments together suggest that absorption of morphine into the bloodstream and distribution of morphine into the CNS are not the primary contributing factors to the observed enhanced morphine induced anti-nociception in IF mice.

Daily intermittent fasting enhances receptor efficacy and blocks receptor tolerance in spinal cord and PAG

The majority of morphine's effects are elicited through the MOR, which is located in specific regions of the CNS including the PAG, rostroventral medulla, striatum, and spinal cord [244]. To evaluate the molecular function of MOR in these locations in IF mice, we harvested PAG, whole brain stem, whole striatum, and whole spinal cord tissue from AL and IF mice who underwent 1 additional week of their respective diet paired with daily injections of 10mg/kg morphine or saline s.c. e then performed ^{35}S-GTPyS coupling assays using DAMGO as a potent, selective MOR agonist. Use of the selective agonist DAMGO insures that resultant activity changes are specific to the MOR. IF mice treated with saline or morphine demonstrated an enhanced efficacy when compared to their AL counterparts specifically in spinal cord (**Figure 5A, Table 1**). Morphine treated AL PAG tissue samples demonstrated a reduction of efficacy (i.e. morphine tolerance) compared to their saline counterparts, which was blocked by IF treatment (**Figure 5B, Table 1**). MOR function in striatum was largely unchanged in any group, although there was significant variability within the IF/Morphine group (**Figure 5C**). Lastly, brain stem samples

Figure 5

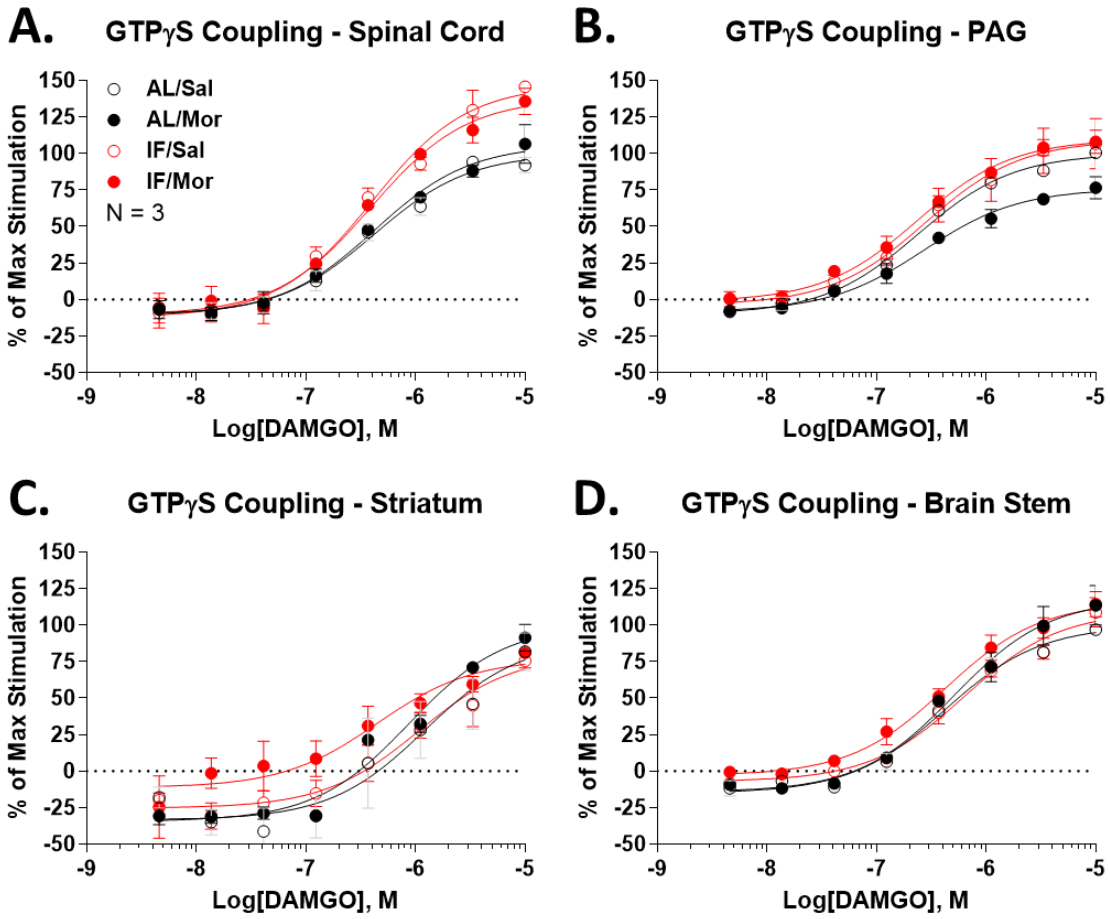

Figure 5 – Daily intermittent fasting enhances MOR efficacy and reduces tolerance in spinal cord and PAG. Male and female CD-1 mice were treated with IF or AL control for 7 days, with a further 7 days of daily morphine or saline injection with continued IF/AL protocol as in **Figure 3A** (14 days total). Spinal cord or brain regions were dissected and frozen, and used to perform DAMGO concentration-response curves using ^{35}S-GTPγS coupling (see Methods). Data normalized to the max stimulation of the AL/Saline group (100%) or Vehicle control (0%) and reported as the mean ± SEM of N=3 animals/group. 3 independent technical replicates performed for each experiment. Data fit using a 3 variable non-linear regression curve. **A)** Spinal cord. Both IF/Saline and IF/Morphine groups had increased efficacy (see **Table 1**). **B)** PAG. Morphine

treatment caused a loss of efficacy (tolerance) in the AL/Morphine group; this was not observed in the IF/Morphine group (see **Table 1**). **C)** Striatum. No differences between groups, although the IF/Morphine curve was more variable than the others. **D)** Brain stem. No differences between groups.

Table 1

	AL/Saline		AL/Morphine		IF/Saline		IF/Morphine	
	EC_{50} (nM)	E_{MAX} (%)	EC_{50} (nM)	E_{MAX} (%)	EC_{50} (nM)	E_{MAX} (%)	EC_{50} (nM)	E_{MAX} (%)
Spinal Cord	423 (273-659)	100 (90-111)	426 (257-716)	106 (95-119)	403 (248-663)	147* (132-163)	398 (251-635)	138* (124-153)
PAG	241 (188-308)	100 (95-105)	271 (165-446)	76* (69-84)	280 (127-629)	109 (94-127)	237 (156-359)	110 (102-118)
Striatum	1,220 (295-7,670)	90 (51-187)	883 (531-1,500)	100 (85-119)	1,070 (419-3,010)	80 (59-114)	449 (94-2,230)	77 (55-111)
Brain Stem	424 (306-590)	100 (92-108)	511 (304-871)	118 (104-134)	633 (400-1,020)	110 (98-123)	421 (264-675)	116 (105-128)

Table 1 – Daily intermittent fasting enhances MOR efficacy and reduces tolerance in spinal cord and PAG.

demonstrated no significant difference between AL and IF groups (**Figure 5D**). Although we did observe significant differences in efficacy as described above, there were no significant differences in potency in any tissue or group (**Table 1**). These observed differences in MOR function suggest a molecular mechanism linking IF with enhanced anti-nociception (spinal cord) and reduced anti-nociceptive tolerance (PAG).

Daily intermittent fasting does not alter MOR protein expression in spinal cord and PAG

We performed Western blot analysis to evaluate the role of MOR protein expression in the previously observed alterations in MOR function. Spinal cord and PAG demonstrated no observable difference in MOR expression in any treatment group (**Figure 6A-B**). Striatal samples demonstrated no significant differences in AL/Saline vs IF/Saline mice; interestingly, striatal samples taken from IF/Morphine mice demonstrated a significant reduction in MOR expression (**Figure 6C**). These results suggest that the enhanced efficacy and reduced tolerance observed in spinal cord and PAG are not due to changes in protein expression but are due to unit differences in receptor function. Our striatal results are more difficult to interpret; while no difference was observed in GTPγS function in this tissue, reduced receptor expression could have contributed to the high variability seen in this group in GTPγS. This reduction may also have contributed to the blocked morphine reward seen with IF treatment, as the striatum is a key region in the reward circuitry.

DISCUSSION

Despite the modern awareness of the opioid epidemic, opioid analgesics are still commonly prescribed for the treatment of acute and chronic pain. The majority of non-opioid pain medications simply lack the efficacy required for adequate pain relief in

Figure 6

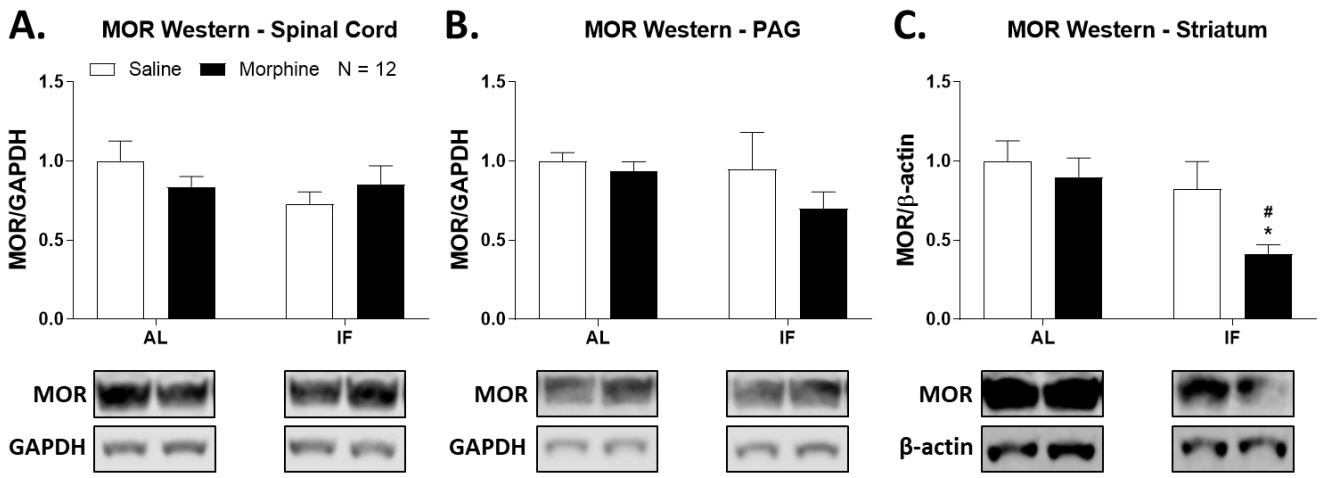

Figure 6 – Daily intermittent fasting does not change MOR protein expression in spinal cord and PAG. Male and female CD-1 mice treated with IF/AL and Morphine/Saline as in **Figures 3A, 5**. CNS regions analyzed for MOR protein expression by Western blot. MOR intensity normalized to GAPDH or β-actin intensity for each sample, and further normalized to the AL/Saline group, and reported as the mean ± SEM, with N = 12 mice/group. 4 independent technical replicates performed for the experiment. * = $p < 0.05$ vs. AL/Saline group; # = $p < 0.05$ vs. IF/Saline group; both by 2 Way ANOVA with Tukey's *post hoc* test. Representative blots for each group shown below each graph. **A)** Spinal cord – no MOR expression differences ($p > 0.05$). **B)** PAG – no MOR expression differences ($p > 0.05$). **C)** Striatum – MOR expression significantly decreased in IF/Morphine group.

moderate to severe pain conditions [245]. Today, roughly 19 to 43% of the United States adult population experiences chronic pain for which opioids cannot be prescribed due to insufficient efficacy and/or high side effects (i.e. poor therapeutic index) [4]. For the first time we demonstrate a non-pharmacological method of daily intermittent fasting (IF) which improved the therapeutic index of systemic morphine in mice. IF mice displayed an enhanced anti-nociceptive response in two different pain models, along with blocked reward and reduced tolerance and constipation. This finding suggests that IF could be used as an adjunct to opioid therapy as part of a dose reduction strategy. These findings together suggest IF may make opioid analgesic therapies safer and more effective for chronic pain patients, and may be useful in preventing the transition to addiction in chronic treatment patients. These findings are also easily translatable, as IF is well-established in the clinical literature, with relatively high compliance, low costs, and essentially no side effects.

Our findings also strongly distinguish IF from acute fasting and acute caloric restriction. The literature suggests that acute fasting and restriction causes a stress response in animals, deleteriously impacting opioid function and enhancing opioid reward, the opposite of what we observe [234, 246]. Our control experiments further support that IF is different from acute fasting and feeding states, as a 24 hour fast and daily fasting/fed states had no impact on opioid anti-nociception and reward (**Figures 1-2**). The literature and our findings thus suggest that specifically altering the timing of feeding over time is what induces long-lasting beneficial effects on opioid management of pain therapy, rather than caloric restriction, acute food-induced changes, or weight loss, which was also not impacted by IF in our study (**Figure 1E**).

This then leaves the question of what mechanisms link IF with beneficial changes to the opioid system. Our results suggest that morphine pharmacokinetics are not altered

by IF (**Figure 4**), leaving pharmacodynamics as the likely explanation. Supporting this finding, we found increased MOR efficacy in the spinal cord and blocked MOR tolerance in the PAG using ^{35}S-GTPγS coupling (**Figure 5, Table 1**). The enhanced spinal cord efficacy may be responsible for the enhanced behavioral efficacy seen in paw incision and tail flick (**Figure 1**), while the blocked PAG tolerance may relate to the decreased behavioral tolerance observed (**Figure 3A**). Supporting these hypotheses, other groups have found that altering PAG signaling (e.g. ERK MAPK, microglial activation) can block opioid tolerance [247, 248], while diabetes was shown to reduce opioid receptor coupling and thus opioid efficacy in the spinal cord [249]. Our results further suggest that unit receptor activity is altered in these tissues, since MOR protein expression is not altered in spinal cord and PAG (**Figure 6A-B**). Since we use a membrane preparation for our ^{35}S-GTPγS studies (see Methods) which strips away all soluble components, such as kinases, cytoskeletal elements, and similar, the change in receptor activity is likely due to alterations in the receptor itself. One likely candidate would be a persistent change in receptor phosphorylation by G Protein Receptor Kinases (GRK), which cause acute desensitization and internalization of the opioid receptors [133]. Future work should investigate these potential mechanisms.

Potential mechanisms for the blockade of opioid reward by IF are less certain. We did observe a decrease in MOR expression in the striatum when IF was combined with chronic morphine treatment (**Figure 6C**). This is the inverse of what was observed with acute food restriction, where striatal MOR signaling and opioid reward were both increased, suggesting this could be the mechanism for blocked reward with IF [246]. However, care should be taken in interpreting this data. Our ^{35}S-GTPγS coupling results showed no differences between groups in the striatum, albeit the IF/Morphine group was more variable than the rest (**Figure 5C, Table 1**). This mechanism will thus require more

investigation. Similarly, our results with IF and constipation have no obvious mechanistic hypothesis. However, since we did observe increased fecal production in IF/Saline mice (**Figure S1**), IF may act to generally promote GI motility, thus counteracting the constipatory effect of morphine. Considering the large clinical burden of opioid-induced constipation [242], this mechanism merits more clinical and basic science investigation.

Although our observations have resulted in mechanistic hypotheses at the MOR functional level, we still do not know what links IF with these receptor changes. Since we are the first study to investigate the impact of IF on opioid therapy, there are also few clues from the literature. However, an earlier study did show that glucocorticoids produced from the adrenal gland were necessary for IF to alter the entrainment of circadian MOR expression [125]. Another review of the IF literature has suggested that glucocorticoids could elicit changes in Brain Derived Neurotrophic Factor (BDNF) in the brain [127]; BDNF has been strongly linked to the regulation of opioid anti-nociception and side effects such as tolerance [247, 250]. An IF/glucocorticoid/BDNF axis could thus regulate the impact of IF on the opioid system. This and related mechanistic hypotheses must be pursued to improve our understanding of the beneficial impact of IF on opioid function and therapy and maximize our chances of successfully translating this technique to the clinic to improve opioid therapy for pain patients.

CHAPTER 7: GENERAL DISCUSSION AND CONCLUSIONS

Chronic pain and opioid abuse continue to plague the United States in massive proportions [1, 2, 49]. Despite this, opioids remain the most efficacious clinical analgesic in the majority of cases, regardless of their diminishing returns over continuous administration [50]. If side effect profiles for opioids can be improved, there may be a case to redeem the use of these compounds in chronic pain, as well as reduce addiction, abuse, and overdose rates. We identified a pharmacological and a non-pharmacological approach to the improvement of the therapeutic index of systemic morphine. By pharmacologically inhibiting HSP90 within the spinal cord, there is a specific increase to the potency of morphine. At the same time, the potency of morphine to produce reward and constipation is not changed, while anti-nociceptive tolerance is reduced. Shifting the analgesic potency to the left allows for a further separation from side effect dose ranges, thus permitting a dose-reduction strategy and improving the therapeutic index. Along with the translational impacts of this finding, there is also a contribution to our current understanding of downstream MOR signaling events, which may lead to additional drug discovery candidates.

With the aims of utilizing a physiological approach to opioid modulation, we demonstrated that one week of daily 18-hour fasts in mice augments the therapeutic potential of systemic morphine. IF mice demonstrate enhanced morphine induced anti-nociception and reduced reward, tolerance, and constipation. These surprising results could have tremendous translational implications for individuals seeking continuous and safer opioid medications at virtually no cost to the patient or healthcare provider. There are also a wide range of potential protein candidates which may explain the mechanism of this phenomenon and could serve as new drug discovery targets.

SPINAL CORD HSP90

Initially, we hypothesized that the inhibition of HSP90 with 17-AAG in the spinal cord would produce a similar reduction in morphine induced anti-nociception to that of HSP90 inhibition in the brain. To our surprise, we observed an enhancement of morphine induced anti-nociception when spinal cord HSP90 was inhibited. Typically, HSP90 inhibition via 17-AAG administration can be verified through an upregulation of HSP70, which is what we observed in the brain [104]. In the spinal cord, we observe no increase in HSP70. Therefore, we utilized an alternative site inhibitor, KU-32, which verified our behavioral effects. Another contrast between the brain and spinal cord is the effect rendered using the tail flick assay. Brain HSP90 inhibition yields no observable effects in this pain model, while spinal cord HSP90 inhibition demonstrates enhanced anti-nociception equivalent to the results of the post-operative pain model. Therefore, brain HSP90 appears to be pain type specific while spinal cord HSP90 affects different pain types more generally to a degree. This observation will require additional investigation, but several factors may be involved, including: the cell types which are affected, the difference in molecular actions of HSP90 within these two areas, and/or the location of HSP90 inhibition within the circuitry.

These differences between brain and spinal cord HSP90 inhibition resulted in a follow up question. What does systemic HSP90 inhibition and/or whole CNS HSP90 inhibition yield with respect to morphine anti-nociception? We therefore performed both systemic administration of 17-AAG and brain/spinal cord co-administration to address this question. Both systemic HSP90 inhibition and co-administration yield no significant differences in morphine anti-nociception within the tail flick model, but both reduce morphine anti-nociception in the post-operative paw incision pain model. We conclude

here that the actions of HSP90 within the brain override that of the spinal cord when both are inhibited. There are again several possibilities which might account for this observation. One explanation might be that the prevention of MOR-activated descending modulatory circuits within the brain allows for the activation of “on” cells which activate nociceptive circuits and override spinal cord mediated MOR activation. Another explanation might include HSP90’s role in pain processes within other areas of the brain. It is possible that the inhibition of HSP90 may have pro-nociceptive roles in areas such as the insula which again override HSP90 mechanisms within the spinal cord. These possible mechanisms will require further investigation for a more cohesive understanding.

Our initial behavioral data involving the inhibition of spinal cord HSP90 and increased morphine induced anti-nociception also prompted multiple mechanistic questions. What molecular function is HSP90 serving in the spinal cord which might account for these effects? In what cellular type is HSP90 inhibition yielding these molecular events? HSP90 has been shown to alter ERK phosphorylation levels, and we have previously demonstrated the necessity for HSP90 induced ERK phosphorylation to morphine anti-nociception in the brain [104, 251, 252]. Therefore, ERK may also play a role in within downstream MOR signaling within the spinal cord. We utilized both western blots and immunohistochemistry to assess ERK phosphorylation in mouse spinal cord. Interestingly, DAMGO on its own does not induce ERK phosphorylation in the spinal cord. DAMGO is known to produce ERK phosphorylation in a variety of cells in-vitro through downstream MOR signaling but specific spinal cord tissue DAMGO induced ERK phosphorylation has never been reported in the literature [173, 253-255]. 17-AAG treatment alone induces an increase in ERK phosphorylation which has been previously reported in cells [256]. More interesting is the even further increase in ERK

phosphorylation upon the co-administration of 17-AAG and DAMGO. We found that enhanced morphine induced anti-nociception through HSP90 inhibition could be rapidly reversed with the use of an ERK inhibitor, U0126, in either the tail flick or paw incision pain models. This ERK phosphorylation was further found to be localized to dendritic and/or axonal projections and not neuronal cell bodies within the dorsal horn of the spinal cord. With these findings, we propose that pre- and post-synaptic MOR induced ERK phosphorylation within the spinal cord enhances systemic MOR induced anti-nociception and that under naïve conditions HSP90 blocks this ERK phosphorylation from occurring. Many might find this proposition questionable due to previous studies suggesting a pro-nociceptive role for ERK phosphorylation [257, 258]. The majority of these studies suggest ERK's pro-nociceptive role is induced primarily through subsequent transcription [189]. Our immunohistochemical staining of phosphorylated ERK demonstrates that phosphorylated ERK, induced by HSP90 inhibition paired with MOR activation, is localized to dendritic and/or axonal projections and does not translocate to the nucleus within the cell body. Based on this observation, we believe the contrasting pro-nociceptive effect of ERK and MOR induced anti-nociceptive effects of ERK through HSP90 inhibition are context dependent and occur through different mechanisms.

These findings regarding ERK phosphorylation again prompt additional questions. How is HSP90 preventing ERK phosphorylation under naïve conditions? What is the substrate of ERK which is leading to enhanced morphine induced anti-nociception? The dendritic/axonal localization of our previous immunohistochemical staining of phosphorylated ERK within spinal cord samples provides a clue to the second question. Under this localization, ERK is likely to be affecting pre- and/or post-synaptic mechanisms of action potentials. In the case of MOR activation, this process can occur

through the activation of pre/post-synaptic GIRK channels and the inhibition of pre-synaptic N-type VG Ca^{++} channels. ERK may impact these processes either directly or indirectly, though previous studies suggest that proteins other than ERK are the primary regulators of these channels [71, 78, 259, 260]. Therefore, we directed our attention toward a function of ERK which is not through the process of transcription and not necessarily a direct mediator of GIRK channels or N-type VG Ca^{++} channels. This is still a large pool of possibilities, though ERK is known to activate both translation and post-translational modifications [189, 261]. ERK induced post-translational modification could impact GIRK channels and/or pre-synaptic N-type VG Ca^{++} channels directly but is also implicated in pro-nociception [189]. Therefore, we focused our attention on ERK induced translation which could produce any number of proteins which might impact the function of the two above mentioned channels including the channels themselves.

We began by asking the question, “is translation required for the enhanced morphine induced anti-nociception by spinally inhibited HSP90?”. To address this, we utilized a translational inhibitor which has been previously used in-vivo: cycloheximide [262, 263]. We administered cycloheximide intrathecally at a similar time course to that of our previous experiment with ERK inhibition. We observed a similar effect to the previous experiment in which the inhibition of translation rapidly reversed enhanced morphine induced anti-nociception via HSP90 inhibition. Though not significant, there does appear to be a bi-phasic response within our 17-AAG/cycloheximide/morphine tail flick latency profile which may be a product of cycloheximide pharmacodynamics and/or kinetics. This experiment only tells us that rapid translation is necessary for the effects of HSP90 on morphine induced anti-nociception, it does not tell us if it occurs as a result of ERK activation or vice versa. Therefore, we used western blots to evaluate ERK phosphorylation in spinal cords after the treatment of 17-AAG, DAMGO, and

cycloheximide. We observed no significant difference between cycloheximide and non-cycloheximide treated samples, and concluded that this translation event must occur post-ERK phosphorylation.

The requirement of rapid translation again leads to several new questions. How is ERK inducing translation? What is being translated to allow for enhanced morphine induced anti-nociception within the spinal cord? We utilized proteomics to identify key candidates which are upregulated after 17-AAG treatment within the spinal cord. Several candidates came to our attention based on the literature, but one in particular was an upregulation of RSK2. RSK2 is known to be involved in ERK induced translational activation, though increased RSK2 expression does not equate to activation or necessity [264, 265]. We also found that RSK1 and/or RSK2 activation is necessary for the enhanced morphine induced anti-nociception through HSP90 inhibition similar to that of ERK and translation using the a RSK1/2 selective irreversible inhibitor, Fmk. We then used western blot analysis to evaluate both RSK1 and RSK2 phosphorylation in mouse spinal cord after 17-AAG and DAMGO treatment. Both demonstrate a similar phosphorylation pattern to ERK phosphorylation. Again, we do not know where RSK phosphorylation occurs within this signaling pathway, but it is a known substrate of ERK leading to translational activation. Additional investigation will be necessary to confirm RSKs location within this molecular pathway.

We are steadily uncovering this novel downstream MOR signaling pathway within the spinal cord, but much more work must be done for a complete understanding. Many additional aspects will need to be addressed. The direct substrate of HSP90 blocking ERK activation is not known. We believe that this may be a phosphatase which is activated by HSP90 presumably in conjunction with other specific co-chaperones. HSP90 is known to directly activate phosphatases such as protein phosphatase 5 (PP5)

[266]. Therefore, phosphatases such as PP5 may be possible candidates for the inactivation of ERK in naïve spinal cord. There is also the matter of which protein upregulated by this ERK induced translational event contributes to morphine anti-nociception. This protein could fall under several categories. It could be a kinase such as PKA, PKC, and cyclin-dependent kinase 5. These kinases would allow for phosphorylation of the GIRK and/or N-type VG Ca^{++} channels and subsequent activation/inactivation respectively. An upregulated phosphatase could inhibit certain kinases to again allow for the respective modulation of these ion channels. It could also be a disruption in synaptic transmission machinery modulated by an upregulation of kinases, phosphatases, and/or synaptic proteins. Further proteomics and/or phospho-proteomics with 17-AAG/DAMGO treated spinal cords would be a good starting place to begin this investigation. Identifying specific HSP90 isoforms and co-chaperones may also differ from that of the brain and allow for further clues into HSP90 function within the spinal cord. If this is the case, specific inhibitors may be useful systemically in conjunction with systemic opioids to mimic the spinal inhibition phenotype and permit an opioid dose-reduction strategy. Furthering these studies may elucidate novel drug discovery targets, and are therefore of high impact for future pain medicine.

KU-32 is a novel C-terminal inhibitor which has shown promise in the treatment of diabetic neuropathy and chemotherapy induced cognitive impairment [192, 193]. We aimed to demonstrate the translational value of this drug, as an opioid modulator within the spinal cord, capable of improving the therapeutic index of clinical opioids such as morphine. We observed established systemic morphine dose response curves using tail flick, paw incision, and HIV neuropathic pain models. Tail flick is a simple assay which gives us a sense of how the drug impacts thermal nociception. Paw incision is relatively more complex, with mechanical and chemical inflammatory aspects of pain. The HIV

neuropathic pain model allows for the evaluation of clinical application of KU-32 paired with opioid treatment in a more complex chronic pain state. In all three pain states we observed a dose dependent increase in morphine anti-nociception paired with intrathecal KU-32 administration. This is recognized by a clear leftward shift in potency and respective ED_{50} values. Tail flick and paw incision pain models are more straight-forward to interpret and matches what we might hypothesize based on our previous behavioral and molecular studies. Interpreting the HIV neuropathic pain model is somewhat more convoluted. The pain model itself incorporates aspects of inflammatory pain and neuropathy [267]. Opioids are historically a poor option in the treatment of this pain type which also must be kept in mind moving forward [268]. Due to the homeostatic maintenance functions of HSP90, one might hypothesize HSP90 inhibition to promote neuropathy over the long term. Therefore, this aspect would be critical to further studies with KU-32 administration in these neuropathic pain models. Despite this, there remains an enhancement in morphine anti-nociception with spinal cord HSP90 inhibition within this pain model. I hypothesize that acute KU-32 inhibits HSP90 to promote MOR induced ERK phosphorylation, RSK phosphorylation and translation of critical proteins in surviving nociceptors to negate signal transmission stimulated by chemical inflammatory stimuli within the spinal cord. Additional research will be required to illuminate this further.

The enhanced morphine induced anti-nociception via intrathecal KU-32 administration only improves the therapeutic index of morphine if the side effect profiles are not subsequently enhanced. The administration of KU-32 was localized to the spinal cord, therefore we hypothesized that it would have no impact on side effects such as reward and constipation which are known to be localized to the mesolimbic system and enteric nervous system respectively [57, 269]. Upon evaluation of these side effects we

indeed observed no effect of intrathecal KU-32. The localization of tolerance on the other hand is less well known. One could hypothesize that MOR tolerance occurs equally at all regions which express MOR, but this is not the case [197]. For instance, endocytosis is thought to be a significant component of MOR tolerance and studies have demonstrated that morphine fails to induce MOR endocytosis within the spinal cord but does so efficiently within medium spiny striatal neurons [84]. MOR desensitization and resensitization are also thought to be significant components of MOR tolerance, and studies have demonstrated these this process occurs differently between different tissues [84]. Since morphine does not produce endocytosis within the spinal cord, it may be that enhancing morphine induced anti-nociception with KU-32 within this region does not increase tolerance. Upon evaluation, using continuous administration of morphine paired with tail flick latency acquisitions, we found that tolerance development still occurred in the presence of intrathecal KU-32, though potentially at a slightly slower rate at the highest morphine dose. Despite this, the efficacy of morphine is boosted in KU-32 treated animals and therefore the real-world application would appear as reduced tolerance. The finding that tolerance development is not largely impacted within our study suggests that spinal cord morphine induced anti-nociception may have a minimal role within global morphine analgesic tolerance. Therefore, it might be that the spinal cord mediated enhancement of morphine induced anti-nociception via KU-32 compensates for lost anti-nociception in an already developed model of tolerance. After establishing morphine tolerance in mice, we observed that intrathecal KU-32 administration recovered morphine anti-nociceptive to naïve levels. This finding could also suggest that morphine tolerance was somehow reversed but additional investigation would be required to address these interpretations. This could be achieved through location specific tolerance development via i.t., i.c.v. and/or brain microinjections of morphine, and subsequent evaluation of i.t. KU-32 on systemic morphine.

These pre-clinical studies provide evidence for the use of intrathecal administration of HSP90 inhibitors such as KU-32 in conjunction with morphine treatment as a dose reduction strategy, though there are some issues. Spinal injections of any kind are generally inconvenient for any human patient and therefore a systemic drug would be more desirable. We have already demonstrated that systemic 17-AAG blocks morphine anti-nociception similar to that of i.c.v. injections. We have also demonstrated the specific isoform HSP90α is responsible for these actions in the brain. If the results we have observed in the spinal cord are driven by an alternative HSP90 isoform, there is a case for the use of a systemic inhibitor. The results from the brain are also dependent on co-chaperones p23 and CDC37, and therefore if this differs in the spinal cord there may be a case for a selective co-chaperone systemic inhibitor to enhance morphine anti-nociception as well. Side effects with these systemic inhibitors would also be much more likely that spinal cord isolated inhibition and would have to be investigated. In particular, respiratory depression should be addressed, as it is the primary cause of death with opioid overdose. We know that HSP90 inhibition allows for enhanced morphine anti-nociception after a 24-hour duration, but we do not know the duration of this effect or if the enhancement can be achieved at an earlier timepoint. This follow up study would be crucial for the treatment of chronic pain in human patients, in terms of one long-lasting treatment vs many short-term treatments. Finally, we have only tested the effects of spinal HSP90 inhibition on morphine pharmacology. It is known that all opioid agonists are not created equal and have varying signaling, kinetic, and side effect profiles. It will be crucial to evaluate additional commonly prescribed opioids with spinal HSP90 inhibition as well.

INTERMITTENT FASTING

Intermittent fasting has been demonstrated to result in many positive physiological consequences such as increased insulin sensitivity and also to mitigate several negative physiological processes such as excess inflammation [209, 270]. These findings together have resulted in efforts to utilize intermittent fasting to improve and/or mitigate various pathologies [118]. Diet is known to impact the pharmacodynamics and pharmacokinetics of several drugs [271-273]. Since there are vast changes to physiology during intermittent fasting diets, IF is almost certain to impact the pharmacology of certain drugs as well. Based on previous literature, one class of drugs which is altered by intermittent fasting is opioids. Food reward is known to activate endogenous opioid release within the mesolimbic dopamine system which fasting directly alters [230]. Acute fasting has demonstrated alterations to MOR mRNA expression and binding [233, 235]. IF has been shown to promote anti-nociception through the endogenous kappa opioid system, while morphine has been shown to have circadian dependent increases to anti-nociception [125, 126]. We therefore hypothesized that 1 week of 18 hour daily intermittent fasting in mice would yield an enhancement to morphine induced anti-nociception and allow for a non-pharmacological morphine dose reduction strategy.

Caloric restriction is also known to impact opioid and reward systems [274, 275]. To differentiate between IF and caloric restriction, we aimed to achieve a time restriction diet without a loss of body weight in mice. Weights of IF mice fluctuate before and after the respective fasting period proportionally to the average food intake of an adult mouse. Weights after the feeding periods were equal to that of ad libitum (AL) fed controls and the IF mice even gained weight at an equivalent rate to that of AL mice in both males and females. It has been previously demonstrated that 2 weeks of daily 16 hour fasts in

mice enhances morphine induced anti-nociception via the hot plate pain assay [125]. We therefore aimed to achieve similar results with 1 week of daily 18 hour fasts in mice via the post-operative paw incision pain model and the thermal tail flick model. Unlike AL mice which are constitutively fed, IF mice have a fed state and a fasted state. To control for this paw incision experiments were performed both at the end of the fasted state and the fed state. Both states demonstrated an enhanced duration of morphine induced anti-nociception. In the tail flick model, we also observed an enhanced peak effect of morphine and though not significant a slight prolongation as well. It is possible that we have reached the stimulus threshold with the paw incision model and therefore additional testing may reveal enhanced efficacy in this model as well. We performed a 24 hour fast in mice to see if similar morphine antinociceptive enhancements could be achieved with an acute fast. These mice demonstrated no significant difference to non-fasted controls. Acute fasting within the literature commonly results in contrary results to that of intermittent fasting [276, 277]. This is likely due to the longer-term changes achieved with continuous intermittent fasting. These longer-term compensatory changes are likely not present in acute fasting and thus acute fasting is more similar to an acute stressful stimulus.

The prolonged and enhanced morphine induced anti-nociception with IF mice could be attributed to changes in pharmacokinetics and/or dynamics. Alternative routes of administration, i.v., i.c.v., and i.t., still resulted in an enhanced anti-nociceptive profile in IF mice and suggests that absorption and/or distribution are not driving the elevated potency and may be primarily due to differences in pharmacodynamics. With this said, the prolonged anti-nociceptive effect is absent in these animals which could be due to several factors. Differences in absorption and/or distribution due to IF may be the cause of the prolonged morphine induced anti-nociception but not the elevated potency. A full

pharmacokinetic profile would need to be obtained to directly address this observation. If this were the case, there are many possible factors which could lead to this effect. Morphine and/or its metabolites are a substrate for several transporters such as P-glycoprotein, OCT1, OATP1B1 and MRP2 and 3 [278, 279]. Differences in the expression of these transporters in IF would be likely candidates impacting morphine absorption and distribution into the CNS and the subsequent prolongation of morphine induced anti-nociception. Selective blockers and or CRISPR knockout mice could be utilized to investigate this possibility.

To begin to address differences in morphine pharmacodynamics with IF, we aimed to look at MOR functionality and expression in various CNS regions. In the spinal cord, MOR efficacy was enhanced in IF mice measured via the GTPyS assay without altering MOR expression measured via western blot. These two experiments together suggest that functionality must be enhanced through the membrane components of MOR signaling and not downstream signaling (since the GTPγS assay removes all soluble components). Two potential candidates are the phosphorylation of MOR and membrane cholesterol content. MOR phosphorylation directly impacts MOR internalization and reinsertion into the cell membrane, and cholesterol levels, which are shown to be altered in IF, can also impact the function of MOR [270, 280, 281]. IF did not alter MOR functionality within whole brain stem or PAG tissue samples, which informs the range of potential mechanisms. Additionally, PAG samples demonstrated no significant difference in MOR expression. IF has been previously demonstrated to increase MOR binding in mouse brain stem, though we did not look at expression within this region [125]. Although many regions in the brain stem express MOR, MOR functionality and/or expression may be differentially impacted by IF in different regions of the brain stem [282]. Therefore, these assays would have more relevance by looking

directly at areas such as the RVM which is involved in descending modulation of pain [27].

If IF enhances morphine induced anti-nociception, we might also expect it to enhance other aspects of morphine pharmacology as well. We began to address this by looking at morphine induced reward via conditioned place preference, constipation through fecal accumulation, and tolerance via tail flick. All of the assays indicated a general reduction in morphine side effects. There was no reward induction by morphine in IF mice, which was independent of fasted/fed state. Although we did not asses MOR function/expression within the VTA or NAc specifically, we did asses function/expression in whole striatal samples which demonstrated no significant difference with IF in function, though expression was significantly reduced in IF/morphine treated samples alone. Additionally, microdialysis studies will need to be performed to assess the direct effect of IF on morphine induced dopamine release. The reduction in morphine reward was surprising due to the increased anti-nociception, but other diets have also demonstrated to have impacts on opioid reward signaling within the mesolimbic pathway, altering reward function [113, 115]. Binge over-eating disorders can produce enhanced DAMGO induced reward and general sensitivity to reward [283]. It may be that the average constitutively fed individuals in Western culture may also experience some degree of opioid reward sensitivity. Within our IF model there is a daily 18-hour period in which this reward pathway cannot be activated. Therefore, IF may allow for a resetting of opioid machinery within the mesolimbic system and allow for a subsequently lessened degree of sensitivity to opioid reward. One possible mechanism for this may be related to ghrelin activity in the brain. Recent studies have demonstrated release and activity of ghrelin within non-hypothalamic regions of the CNS [284-286]. Additionally, ghrelin activation of GHS-R1α in the brain has been shown to produce endogenous opioid release, while

ghrelin antagonists blunt opioid induced reward [286-288]. Due to the elevated ghrelin levels during the prolonged fasting periods, it is possible that ghrelin is desensitizing opioid reward pathways and causing subsequent lack of morphine induced reward. This theory could be addressed with a similar CPP experiment in IF mice lacking the ghrelin or GHS-1Rα gene. Unfortunately, there are many other possibilities which may be of consequence with this phenomena, therefore larger genetic and proteomic studies may also be required to identify potential mechanisms.

The development of analgesic tolerance was reduced with a peak reduction of only 43.6% after 7 days in IF mice compared to 94.6% in AL mice. To identify potential mechanisms for this change in MOR tolerance, we measured MOR functionality and expression via GTPyS and Western blot respectively in IF mouse tissue after chronic morphine treatment. No differences in receptor tolerance were found in the brain stem, spinal cord, or striatum, but in the PAG, AL animals demonstrated an expression-independent significant reduction in MOR efficacy with chronic morphine treatment that was absent in IF mice. In other words, the MOR in PAG demonstrated apparent tolerance, which was blocked by IF treatment. MOR tolerance within the PAG has been demonstrated elsewhere [289, 290]. Although our functional data within the PAG matches our behavioral tolerance data, the spinal cord and brain stem functional data do not. With regards to the brain stem, it may be that evaluation of more specific regions such as the RVM may be necessary to detect any differences. Additionally, MOR desensitization and tolerance have been demonstrated to occur at varying rates if at all in different MOR expressing regions [80]. An absence of MOR tolerance in the spinal cord could be explained by this and/or it could also be due to changes in intracellular signaling, which could be assessed by probing for the activation of different MOR downstream molecules via western blot and/or IHC.

IF mice produced more fecal matter overall due to a larger recent food consumption and therefore, we normalized morphine treated mice to saline treated mice for both AL and IF groups. Although IF mice demonstrated equivalent early constipation to AL mice, they were able to recover significantly quicker with a 1.5-fold increased final output at the endo of the 6-hour time course compared to AL mice. This suggests that IF reduces morphine-induced constipation, which could be a potential treatment for this debilitating side effect. At this point in the study, we have not investigated any potential mechanisms for this behavioral effect. The likely site of action of this event is in the enteric nervous system. In general, opioids are known to suppress gastrointestinal motility by the suppression of neurotransmitter release from enteric musculomotor neurons [291]. MOR activation on excitatory musculomotor neurons prevents the release of acetylcholine (Ach) and/or substance P, preventing contraction of necessary smooth muscle [292-294]. MOR activation on inhibitory musculomotor neurons prevents vasoactive intestinal peptide (VIP) and/or nitric oxide (NO) release which allow for the relaxation of necessary smooth muscle [295, 296]. Together, these mechanisms interrupt peristaltic propulsion which results in constipation. Since MOR was not initially affected, I would hypothesize no immediate changes in MOR expression or function within enteric nervous system tissue samples, which could be evaluated via Western blot and GTPyS assays. Since constipation lasts for a shorter duration, I hypothesize that MOR internalization and desensitization occur at a quicker rate in IF animals. This could be measured via β-Arr recruitment assays in enteric nervous system tissue samples and internalization assays in enteric neuronal primary cell cultures from GFP-MOR labelled mice. Again, identifying the physiological source of these molecular changes may require an initial large scale proteomic and/or genetic analysis.

Since IF generates large scale physiological changes, it will be difficult to identify the mechanistic origins of the modifications of MOR functionality within various tissues. IF impacts regulatory release of several hormones including growth hormone, thyroid hormone, and orexin [297-299]. Therefore, it is likely one or more of these hormones are a catalyst for any eventual molecular changes in MOR function. These effects could be due to changes in cellular metabolism which can alter signaling, transcription, and enzymatic activity [300-302]. Nuclear hormone receptor activation can directly lead to the activation or inhibition of many transcription factors, ultimately impacting any cellular function [303]. Finally, activation of hormone receptors can also alter cellular signaling directly which may magnify or lessen MOR related effects [304, 305]. Moving forward, plasma levels of hormones and other messengers should be evaluated to identify possible candidates for further studies. Various other hormones and mimetics have also been already identified in the modulation of opioid induced effects [306, 307]. New drug discovery efforts may also be based on these IF studies in the future based on identified molecular mechanisms.

Finally, with few exceptions such as children, pregnant women, and type I diabetics, IF can be accomplished with relative ease and virtually no side effects. Additionally, IF can be achieved at virtually no cost within clinical trials. Therefore, small clinical trials can be quickly implemented with the aim of improving the therapeutic index of clinical opioids. Along with these studies, various clinical opioids are known to have different pharmacokinetic and dynamic profiles, which should be assessed in humans within these studies. The duration and onset of IF should also be explored to achieve desired effects. Finally, routes of administration may also impact the desired effects of IF on opioid pharmacology which should also be assessed. The preclinical investigation initiated here in mice paired with the future studies and the beginning of clinical trials in

humans, may suggest IF as a valid option for improving opioid pharmacology and possibly allow for future drug discovery efforts.

CLOSING STATEMENTS

We have identified two possible methods to potentially improve the therapeutic index of opioids. The first study implicates spinal cord HSP90 as a downstream MOR signaling modulator, which upon inhibition, allows for enhanced morphine induced anti-nociception with reduced or maintained side effects. Further molecular studies are in progress to identify more selective drug discovery targets which may have more clinical relevance in the future. Along with these studies, many selective HSP90 and other co-chaperone inhibitors are also under investigation to selectively enhance opioid anti-nociception and allow for a dose reduction strategy in patients. The second study demonstrates a non-pharmacological option of IF for improving opioid anti-nociception while simultaneously mitigating several side effects. Although there is a wide range of impacts to physiology via IF that allows for a diverse impact on MOR pharmacology, these wide ranged impacts may cause difficulties in the investigation and identification of the underlying molecular mechanisms. Therefore, along with preclinical studies, human clinical trials would provide more relevant findings with respect to the use of IF as a conjunctive therapy in opioid analgesic treatment.

REFERENCES

1. Henschke, N., S.J. Kamper, and C.G. Maher, *The epidemiology and economic consequences of pain.* Mayo Clin Proc, 2015. **90**(1): p. 139-47.
2. Phillips, C.J., *The Cost and Burden of Chronic Pain.* Reviews in pain, 2009. **3**(1): p. 2-5.
3. Gaskin, D.J. and P. Richard, *The Economic Costs of Pain in the United States.* The Journal of Pain, 2012. **13**(8): p. 715-724.
4. Pitcher, M.H., et al., *Prevalence and Profile of High-Impact Chronic Pain in the United States.* The Journal of Pain, 2019. **20**(2): p. 146-160.
5. Reid, M.C., C. Eccleston, and K. Pillemer, *Management of chronic pain in older adults.* BMJ (Clinical research ed.), 2015. **350**: p. h532-h532.
6. Treede, R.D., et al., *Chronic pain as a symptom or a disease: the IASP Classification of Chronic Pain for the International Classification of Diseases (ICD-11).* Pain, 2019. **160**(1): p. 19-27.
7. De Gregori, M., et al., *Combining pain therapy with lifestyle: the role of personalized nutrition and nutritional supplements according to the SIMPAR Feed Your Destiny approach.* Journal of pain research, 2016. **9**: p. 1179-1189.
8. Geneen, L.J., et al., *Physical activity and exercise for chronic pain in adults: an overview of Cochrane Reviews.* The Cochrane database of systematic reviews, 2017. **4**(4): p. CD011279-CD011279.
9. Antonaci, F., et al., *Recent advances in migraine therapy.* SpringerPlus, 2016. **5**: p. 637-637.
10. Colloca, L., et al., *Neuropathic pain.* Nature reviews. Disease primers, 2017. **3**: p. 17002-17002.
11. Dubin, A.E. and A. Patapoutian, *Nociceptors: the sensors of the pain pathway.* The Journal of clinical investigation, 2010. **120**(11): p. 3760-3772.
12. Volkers, L., Y. Mechioukhi, and B. Coste, *Piezo channels: from structure to function.* Pflugers Arch, 2015. **467**(1): p. 95-9.
13. Ramsey, I.S., M. Delling, and D.E. Clapham, *AN INTRODUCTION TO TRP CHANNELS.* Annual Review of Physiology, 2006. **68**(1): p. 619-647.
14. Surprenant, A. and R.A. North, *Signaling at Purinergic P2X Receptors.* Annual Review of Physiology, 2009. **71**(1): p. 333-359.
15. Cheng, Y.-R., B.-Y. Jiang, and C.-C. Chen, *Acid-sensing ion channels: dual function proteins for chemo-sensing and mechano-sensing.* Journal of Biomedical Science, 2018. **25**(1): p. 46.
16. Narumiya, S., Y. Sugimoto, and F. Ushikubi, *Prostanoid Receptors: Structures, Properties, and Functions.* Physiological Reviews, 1999. **79**(4): p. 1193-1226.
17. von Kügelgen, I. and K. Hoffmann, *Pharmacology and structure of P2Y receptors.* Neuropharmacology, 2016. **104**: p. 50-61.
18. Huang, Y. and A. Thathiah, *Regulation of neuronal communication by G protein-coupled receptors.* FEBS Letters, 2015. **589**(14): p. 1607-1619.
19. Beissner, F., et al., *Quick Discrimination of Adelta and C Fiber Mediated Pain Based on Three Verbal Descriptors.* PLOS ONE, 2010. **5**(9): p. e12944.
20. Basbaum, A.I., et al., *Cellular and molecular mechanisms of pain.* Cell, 2009. **139**(2): p. 267-284.

21. Willard, S.S. and S. Koochekpour, *Glutamate, glutamate receptors, and downstream signaling pathways.* International journal of biological sciences, 2013. **9**(9): p. 948-959.
22. Mantyh, P.W., *Neurobiology of substance P and the NK1 receptor.* J Clin Psychiatry, 2002. **63 Suppl 11**: p. 6-10.
23. Russell, F.A., et al., *Calcitonin gene-related peptide: physiology and pathophysiology.* Physiological reviews, 2014. **94**(4): p. 1099-1142.
24. D'Mello, R. and A.H. Dickenson, *Spinal cord mechanisms of pain.* BJA: British Journal of Anaesthesia, 2008. **101**(1): p. 8-16.
25. Ahmad, A.H. and C.B. Abdul Aziz, *The brain in pain.* The Malaysian journal of medical sciences : MJMS, 2014. **21**(Spec Issue): p. 46-54.
26. Millan, M.J., *Descending control of pain.* Progress in Neurobiology, 2002. **66**(6): p. 355-474.
27. Gebhart, G.F., *Descending modulation of pain.* Neuroscience & Biobehavioral Reviews, 2004. **27**(8): p. 729-737.
28. Bee, L.A. and A.H. Dickenson, *The importance of the descending monoamine system for the pain experience and its treatment.* F1000 medicine reports, 2009. **1**: p. 83.
29. Corder, G., et al., *Endogenous and Exogenous Opioids in Pain.* Annual review of neuroscience, 2018. **41**: p. 453-473.
30. Lau, B.K. and C.W. Vaughan, *Descending modulation of pain: the GABA disinhibition hypothesis of analgesia.* Current Opinion in Neurobiology, 2014. **29**: p. 159-164.
31. Ossipov, M.H., G.O. Dussor, and F. Porreca, *Central modulation of pain.* The Journal of clinical investigation, 2010. **120**(11): p. 3779-3787.
32. Treede, R.-D., et al., *A classification of chronic pain for ICD-11.* Pain, 2015. **156**(6): p. 1003-1007.
33. van Hecke, O., N. Torrance, and B.H. Smith, *Chronic pain epidemiology - where do lifestyle factors fit in?* British journal of pain, 2013. **7**(4): p. 209-217.
34. Mathur, S. and J. Sutton, *Personalized medicine could transform healthcare.* Biomedical reports, 2017. **7**(1): p. 3-5.
35. Bandyopadhyay, S., *An 8,000-year History of Use and Abuse of Opium and Opioids: How That Matters For A Successful Control Of The Epidemic ? (P4.9-055).* Neurology, 2019. **92**(15 Supplement): p. P4.9-055.
36. Norn, S., P.R. Kruse, and E. Kruse, *[History of opium poppy and morphine].* Dan Medicinhist Arbog, 2005. **33**: p. 171-84.
37. Zapata, L., et al., *Early Neolithic Agriculture in the Iberian Peninsula.* Journal of World Prehistory, 2004. **18**(4): p. 283-325.
38. Jones, M.R., et al., *A Brief History of the Opioid Epidemic and Strategies for Pain Medicine.* Pain and therapy, 2018. **7**(1): p. 13-21.
39. Benyamin, R., et al., *Opioid complications and side effects.* Pain Physician, 2008. **11**(2 Suppl): p. S105-20.
40. Rivat, C. and J. Ballantyne, *The dark side of opioids in pain management: basic science explains clinical observation.* PAIN Reports, 2016. **1**(2): p. e570.
41. Baldini, A., M. Von Korff, and E.H.B. Lin, *A Review of Potential Adverse Effects of Long-Term Opioid Therapy: A Practitioner's Guide.* The primary care companion for CNS disorders, 2012. **14**(3): p. PCC.11m01326.
42. Kosten, T.R. and T.P. George, *The neurobiology of opioid dependence: implications for treatment.* Science & practice perspectives, 2002. **1**(1): p. 13-20.

43. Cicero, T.J. and M.S. Ellis, *The prescription opioid epidemic: a review of qualitative studies on the progression from initial use to abuse.* Dialogues in clinical neuroscience, 2017. **19**(3): p. 259-269.
44. White, J.M. and R.J. Irvine, *Mechanisms of fatal opioid overdose.* Addiction, 1999. **94**(7): p. 961-72.
45. Soelberg, C.D., et al., *The US Opioid Crisis: Current Federal and State Legal Issues.* Anesth Analg, 2017. **125**(5): p. 1675-1681.
46. Stoicea, N., et al., *Current perspectives on the opioid crisis in the US healthcare system: A comprehensive literature review.* Medicine (Baltimore), 2019. **98**(20): p. e15425.
47. Van Zee, A., *The promotion and marketing of oxycontin: commercial triumph, public health tragedy.* American journal of public health, 2009. **99**(2): p. 221-227.
48. Onishi, E., et al., *Comparison of Opioid Prescribing Patterns in the United States and Japan: Primary Care Physicians' Attitudes and Perceptions.* The Journal of the American Board of Family Medicine, 2017. **30**(2): p. 248-254.
49. Gomes, T., et al., *The Burden of Opioid-Related Mortality in the United States.* JAMA Network Open, 2018. **1**(2): p. e180217-e180217.
50. Fields, H.L., *The doctor's dilemma: opiate analgesics and chronic pain.* Neuron, 2011. **69**(4): p. 591-594.
51. Chung, P.C.S., et al., *Delta opioid receptors expressed in forebrain GABAergic neurons are responsible for SNC80-induced seizures.* Behavioural brain research, 2015. **278**: p. 429-434.
52. Beck, T.C., et al., *Therapeutic Potential of Kappa Opioid Agonists.* Pharmaceuticals (Basel, Switzerland), 2019. **12**(2): p. 95.
53. Wang, D., et al., *Functional Divergence of Delta and Mu Opioid Receptor Organization in CNS Pain Circuits.* Neuron, 2018. **98**(1): p. 90-108.e5.
54. Lueptow, L.M., A.K. Fakira, and E.N. Bobeck, *The Contribution of the Descending Pain Modulatory Pathway in Opioid Tolerance.* Frontiers in neuroscience, 2018. **12**: p. 886-886.
55. Adams, M.L., et al., *The role of endogenous peptides in the action of opioid analgesics.* Ann Emerg Med, 1986. **15**(9): p. 1030-5.
56. Taddese, A., S.Y. Nah, and E.W. McCleskey, *Selective opioid inhibition of small nociceptive neurons.* Science, 1995. **270**(5240): p. 1366-9.
57. Fields, H.L. and E.B. Margolis, *Understanding opioid reward.* Trends Neurosci, 2015. **38**(4): p. 217-25.
58. Holzer, P., *Opioids and opioid receptors in the enteric nervous system: from a problem in opioid analgesia to a possible new prokinetic therapy in humans.* Neurosci Lett, 2004. **361**(1-3): p. 192-5.
59. Montandon, G. and R. Horner, *CrossTalk proposal: The preBotzinger complex is essential for the respiratory depression following systemic administration of opioid analgesics.* J Physiol, 2014. **592**(6): p. 1159-62.
60. Montandon, G. and R.L. Horner, *Role of the pre-Bötzinger Complex in opioid-induced respiratory depression in adult rats in-vivo.* The FASEB Journal, 2009. **23**(1_supplement): p. 960.5-960.5.
61. Goode, T.L. and R.B. Raffa, *An examination of the relationship between mu-opioid antinociceptive efficacy and G-protein coupling using pertussis and cholera toxins.* Life Sci, 1997. **60**(7): p. Pl107-13.
62. Gintzler, A.R. and S. Chakrabarti, *Chronic morphine-induced plasticity among signalling molecules.* Novartis Found Symp, 2004. **261**: p. 167-76; discussion 176-80, 191-3.

63. Tuteja, N., *Signaling through G protein coupled receptors.* Plant signaling & behavior, 2009. **4**(10): p. 942-947.
64. Syrovatkina, V., et al., *Regulation, Signaling, and Physiological Functions of G-Proteins.* Journal of molecular biology, 2016. **428**(19): p. 3850-3868.
65. Smrcka, A.V., *G protein βγ subunits: central mediators of G protein-coupled receptor signaling.* Cellular and molecular life sciences : CMLS, 2008. **65**(14): p. 2191-2214.
66. Milligan, G. and E. Kostenis, *Heterotrimeric G-proteins: a short history.* Br J Pharmacol, 2006. **147 Suppl 1**: p. S46-55.
67. Nobles, M., A. Benians, and A. Tinker, *Heterotrimeric G proteins precouple with G protein-coupled receptors in living cells.* Proc Natl Acad Sci U S A, 2005. **102**(51): p. 18706-11.
68. Yudin, Y. and T. Rohacs, *Inhibitory Gi/O-coupled receptors in somatosensory neurons: Potential therapeutic targets for novel analgesics.* Mol Pain, 2018. **14**: p. 1744806918763646.
69. Petit-Jacques, J., J.L. Sui, and D.E. Logothetis, *Synergistic activation of G protein-gated inwardly rectifying potassium channels by the betagamma subunits of G proteins and Na(+) and Mg(2+) ions.* J Gen Physiol, 1999. **114**(5): p. 673-84.
70. Zhao, Q., et al., *Interaction of G protein beta subunit with inward rectifier K(+) channel Kir3.* Mol Pharmacol, 2003. **64**(5): p. 1085-91.
71. Hell, J.W., et al., *Phosphorylation of presynaptic and postsynaptic calcium channels by cAMP-dependent protein kinase in hippocampal neurons.* The EMBO journal, 1995. **14**(13): p. 3036-3044.
72. Boyer, J.L., G.L. Waldo, and T.K. Harden, *Beta gamma-subunit activation of G-protein-regulated phospholipase C.* J Biol Chem, 1992. **267**(35): p. 25451-6.
73. Pumiglia, K.M., et al., *A direct interaction between G-protein beta gamma subunits and the Raf-1 protein kinase.* J Biol Chem, 1995. **270**(24): p. 14251-4.
74. Leopoldt, D., et al., *Gβγ Stimulates Phosphoinositide 3-Kinase-γ by Direct Interaction with Two Domains of the Catalytic p110 Subunit.* Journal of Biological Chemistry, 1998. **273**(12): p. 7024-7029.
75. Kim, D., et al., *G-protein beta gamma-subunits activate the cardiac muscarinic K+-channel via phospholipase A2.* Nature, 1989. **337**(6207): p. 557-60.
76. Menard, R.E. and R.R. Mattingly, *Gbetagamma subunits stimulate p21-activated kinase 1 (PAK1) through activation of PI3-kinase and Akt but act independently of Rac1/Cdc42.* FEBS Lett, 2004. **556**(1-3): p. 187-92.
77. Striessnig, J., *Getting a handle on Ca_V2.2 (N-type) voltage-gated Ca²⁺ channels.* Proceedings of the National Academy of Sciences, 2018. **115**(51): p. 12848-12850.
78. Lüscher, C. and P.A. Slesinger, *Emerging roles for G protein-gated inwardly rectifying potassium (GIRK) channels in health and disease.* Nature reviews. Neuroscience, 2010. **11**(5): p. 301-315.
79. Abdul Kadir, L., M. Stacey, and R. Barrett-Jolley, *Emerging Roles of the Membrane Potential: Action Beyond the Action Potential.* Frontiers in physiology, 2018. **9**: p. 1661-1661.
80. Dang, V.C. and M.J. Christie, *Mechanisms of rapid opioid receptor desensitization, resensitization and tolerance in brain neurons.* British journal of pharmacology, 2012. **165**(6): p. 1704-1716.
81. Lowe, J.D., et al., *Role of G Protein-Coupled Receptor Kinases 2 and 3 in mu-Opioid Receptor Desensitization and Internalization.* Mol Pharmacol, 2015. **88**(2): p. 347-56.

82. Zhang, J., et al., *Role for G protein-coupled receptor kinase in agonist-specific regulation of μ-opioid receptor responsiveness.* Proceedings of the National Academy of Sciences, 1998. **95**(12): p. 7157-7162.
83. Hu, Y.-B., et al., *The endosomal-lysosomal system: from acidification and cargo sorting to neurodegeneration.* Translational neurodegeneration, 2015. **4**: p. 18-18.
84. Williams, J.T., et al., *Regulation of μ-opioid receptors: desensitization, phosphorylation, internalization, and tolerance.* Pharmacological reviews, 2013. **65**(1): p. 223-254.
85. Ma, L. and G. Pei, *β-arrestin signaling and regulation of transcription.* Journal of Cell Science, 2007. **120**(2): p. 213-218.
86. Raehal, K.M. and L.M. Bohn, *β-arrestins: regulatory role and therapeutic potential in opioid and cannabinoid receptor-mediated analgesia.* Handbook of experimental pharmacology, 2014. **219**: p. 427-443.
87. Ehrlich, A.T., et al., *Biased Signaling of the Mu Opioid Receptor Revealed in Native Neurons.* iScience, 2019. **14**: p. 47-57.
88. Yekkirala, A.S., et al., *Breaking barriers to novel analgesic drug development.* Nature reviews. Drug discovery, 2017. **16**(8): p. 545-564.
89. Stanczyk, M.A. and R. Kandasamy, *Biased agonism: the quest for the analgesic holy grail.* Pain reports, 2018. **3**(3): p. e650-e650.
90. Portoghese, P.S., *From Models to Molecules: Opioid Receptor Dimers, Bivalent Ligands, and Selective Opioid Receptor Probes.* Journal of Medicinal Chemistry, 2001. **44**(14): p. 2259-2269.
91. Soltani, H. and A. Pardakhty, *Marketed New Drug Delivery Systems for Opioid Agonists/Antagonists Administration: A Rapid Overview.* Addiction & health, 2016. **8**(2): p. 115-122.
92. Mysels, D.J. and M.A. Sullivan, *The relationship between opioid and sugar intake: review of evidence and clinical applications.* Journal of opioid management, 2010. **6**(6): p. 445-452.
93. Berg, K.A., et al., *Rapid Modulation of μ-Opioid Receptor Signaling in Primary Sensory Neurons.* Journal of Pharmacology and Experimental Therapeutics, 2007. **321**(3): p. 839-847.
94. Wang, J., W. Yuan, and M.D. Li, *Genes and pathways co-associated with the exposure to multiple drugs of abuse, including alcohol, amphetamine/methamphetamine, cocaine, marijuana, morphine, and/or nicotine: a review of proteomics analyses.* Mol Neurobiol, 2011. **44**(3): p. 269-86.
95. Pratt, W.B. and D.O. Toft, *Regulation of signaling protein function and trafficking by the hsp90/hsp70-based chaperone machinery.* Exp Biol Med (Maywood), 2003. **228**(2): p. 111-33.
96. Chiosis, G., *Targeting chaperones in transformed systems--a focus on Hsp90 and cancer.* Expert Opin Ther Targets, 2006. **10**(1): p. 37-50.
97. Li, J. and J. Buchner, *Structure, function and regulation of the hsp90 machinery.* Biomed J, 2013. **36**(3): p. 106-17.
98. Sahasrabudhe, P., et al., *The Plasticity of the Hsp90 Co-chaperone System.* Mol Cell, 2017. **67**(6): p. 947-961.e5.
99. Jackson, S.E., *Hsp90: structure and function.* Top Curr Chem, 2013. **328**: p. 155-240.
100. Johnson, J.L., *Evolution and function of diverse Hsp90 homologs and cochaperone proteins.* Biochimica et Biophysica Acta (BBA) - Molecular Cell Research, 2012. **1823**(3): p. 607-613.

101. Vaughan, C.K., et al., *Hsp90-dependent activation of protein kinases is regulated by chaperone-targeted dephosphorylation of Cdc37.* Molecular cell, 2008. **31**(6): p. 886-895.
102. Sato, S., N. Fujita, and T. Tsuruo, *Modulation of Akt kinase activity by binding to Hsp90.* Proceedings of the National Academy of Sciences, 2000. **97**(20): p. 10832-10837.
103. Whitesell, L. and S.L. Lindquist, *HSP90 and the chaperoning of cancer.* Nat Rev Cancer, 2005. **5**(10): p. 761-72.
104. Lei, W., et al., *Heat-shock protein 90 (Hsp90) promotes opioid-induced anti-nociception by an ERK mitogen-activated protein kinase (MAPK) mechanism in mouse brain.* J Biol Chem, 2017. **292**(25): p. 10414-10428.
105. Lei, W., et al., *The Alpha Isoform of Heat Shock Protein 90 and the Co-chaperones p23 and Cdc37 Promote Opioid Anti-nociception in the Brain.* Frontiers in molecular neuroscience, 2019. **12**: p. 294-294.
106. Davidoff, F., *Focus on performance: the 21 century revolution in medical education.* Mens sana monographs, 2008. **6**(1): p. 29-40.
107. Mishra, S., *Does modern medicine increase life-expectancy: Quest for the Moon Rabbit?* Indian Heart Journal, 2016. **68**(1): p. 19-27.
108. Bodai, B.I., et al., *Lifestyle Medicine: A Brief Review of Its Dramatic Impact on Health and Survival.* Perm J, 2018. **22**: p. 17-025.
109. Roback, K., K. Dalal, and P. Carlsson, *Evaluation of health research: measuring costs and socioeconomic effects.* International journal of preventive medicine, 2011. **2**(4): p. 203-215.
110. Vina, J., et al., *Exercise acts as a drug; the pharmacological benefits of exercise.* British journal of pharmacology, 2012. **167**(1): p. 1-12.
111. Rao, T.S.S., et al., *Understanding nutrition, depression and mental illnesses.* Indian journal of psychiatry, 2008. **50**(2): p. 77-82.
112. Banks, S. and D.F. Dinges, *Behavioral and physiological consequences of sleep restriction.* Journal of clinical sleep medicine : JCSM : official publication of the American Academy of Sleep Medicine, 2007. **3**(5): p. 519-528.
113. Milanesi, L.H., et al., *Mediterranean X Western based diets: Opposite influences on opioid reinstatement.* Toxicol Lett, 2019. **308**: p. 7-16.
114. Nealon, C.M., et al., *Alterations in nociception and morphine antinociception in mice fed a high-fat diet.* Brain Res Bull, 2018. **138**: p. 64-72.
115. Fritz, B.M., et al., *A High-fat, High-sugar 'Western' Diet Alters Dorsal Striatal Glutamate, Opioid, and Dopamine Transmission in Mice.* Neuroscience, 2018. **372**: p. 1-15.
116. Kanarek, R.B., et al., *Dietary influences on morphine-induced analgesia in rats.* Pharmacol Biochem Behav, 1991. **38**(3): p. 681-4.
117. Gosnell, B.A. and A.S. Levine, *Reward systems and food intake: role of opioids.* Int J Obes (Lond), 2009. **33 Suppl 2**: p. S54-8.
118. Mattson, M.P., V.D. Longo, and M. Harvie, *Impact of intermittent fasting on health and disease processes.* Ageing Res Rev, 2017. **39**: p. 46-58.
119. Mattson, M.P., et al., *Meal frequency and timing in health and disease.* Proceedings of the National Academy of Sciences of the United States of America, 2014. **111**(47): p. 16647-16653.
120. Collier, R., *Intermittent fasting: the science of going without.* CMAJ : Canadian Medical Association journal = journal de l'Association medicale canadienne, 2013. **185**(9): p. E363-E364.

121. Templeman, I., et al., *The role of intermittent fasting and meal timing in weight management and metabolic health.* Proc Nutr Soc, 2019: p. 1-12.
122. Ganesan, K., Y. Habboush, and S. Sultan, *Intermittent Fasting: The Choice for a Healthier Lifestyle.* Cureus, 2018. **10**(7): p. e2947-e2947.
123. Li, G., et al., *Intermittent Fasting Promotes White Adipose Browning and Decreases Obesity by Shaping the Gut Microbiota.* Cell Metab, 2017. **26**(4): p. 672-685.e4.
124. Johnstone, A., *Fasting for weight loss: an effective strategy or latest dieting trend?* Int J Obes (Lond), 2015. **39**(5): p. 727-33.
125. Yoshida, M., et al., *Glucocorticoid is involved in food-entrainable rhythm of mu-opioid receptor expression in mouse brainstem and analgesic effect of morphine.* J Pharmacol Sci, 2006. **101**(1): p. 77-84.
126. de los Santos-Arteaga, M., et al., *Analgesia induced by dietary restriction is mediated by the kappa-opioid system.* J Neurosci, 2003. **23**(35): p. 11120-6.
127. Sibille, K.T., et al., *Increasing Neuroplasticity to Bolster Chronic Pain Treatment: A Role for Intermittent Fasting and Glucose Administration?* J Pain, 2016. **17**(3): p. 275-81.
128. Gaskin, D.J. and P. Richard, *The economic costs of pain in the United States.* J Pain, 2012. **13**(8): p. 715-24.
129. Johannes, C.B., et al., *The prevalence of chronic pain in United States adults: results of an Internet-based survey.* J Pain, 2010. **11**(11): p. 1230-9.
130. National Collaborating Centre for, C., *National Institute for Health and Clinical Excellence: Guidance*, in *Opioids in Palliative Care: Safe and Effective Prescribing of Strong Opioids for Pain in Palliative Care of Adults*. 2012, National Collaborating Centre for Cancer (UK)

131. Fields, H.L., *The doctor's dilemma: opiate analgesics and chronic pain.* Neuron, 2011. **69**(4): p. 591-4.
132. Goodyear, K., C.L. Haass-Koffler, and D. Chavanne, *Opioid use and stigma: The role of gender, language and precipitating events.* Drug Alcohol Depend, 2018. **185**: p. 339-346.
133. Al-Hasani, R. and M.R. Bruchas, *Molecular mechanisms of opioid receptor-dependent signaling and behavior.* Anesthesiology, 2011. **115**(6): p. 1363-81.
134. Madariaga-Mazon, A., et al., *Mu-Opioid receptor biased ligands: A safer and painless discovery of analgesics?* Drug Discov Today, 2017. **22**(11): p. 1719-1729.
135. Olson, K.M., et al., *Novel Molecular Strategies and Targets for Opioid Drug Discovery for the Treatment of Chronic Pain.* Yale J Biol Med, 2017. **90**(1): p. 97-110.
136. Villanueva, M.T., *Analgesia: Designing out opioid side effects.* Nat Rev Drug Discov, 2017. **16**(5): p. 311.
137. Liang, D.Y., et al., *Pharmacological Characters of Oliceridine, a mu-Opioid Receptor G-Protein[FIGURE DASH]Biased Ligand in Mice.* Anesth Analg, 2018.
138. Drieu la Rochelle, A., et al., *A bifunctional-biased mu-opioid agonist-neuropeptide FF receptor antagonist as analgesic with improved acute and chronic side effects.* Pain, 2018.
139. Manglik, A., et al., *Structure-based discovery of opioid analgesics with reduced side effects.* Nature, 2016. **537**(7619): p. 185-190.
140. Wang, Y., et al., *Modulation of mTOR Activity by mu-Opioid Receptor is Dependent upon the Association of Receptor and FK506-Binding Protein 12.* CNS Neurosci Ther, 2015. **21**(7): p. 591-8.

141. Bao, Y., et al., *Engagement of signaling pathways of protease-activated receptor 2 and mu-opioid receptor in bone cancer pain and morphine tolerance.* Int J Cancer, 2015. **137**(6): p. 1475-83.
142. Eckl, J.M. and K. Richter, *Functions of the Hsp90 chaperone system: lifting client proteins to new heights.* Int J Biochem Mol Biol, 2013. **4**(4): p. 157-65.
143. Kaigorodova, E.V. and M.V. Bogatyuk, *Heat shock proteins as prognostic markers of cancer.* Curr Cancer Drug Targets, 2014. **14**(8): p. 713-26.
144. Schulz, R. and U.M. Moll, *Targeting the heat shock protein 90: a rational way to inhibit macrophage migration inhibitory factor function in cancer.* Curr Opin Oncol, 2014. **26**(1): p. 108-13.
145. Jhaveri, K., et al., *Heat shock protein 90 inhibitors in the treatment of cancer: current status and future directions.* Expert Opin Investig Drugs, 2014. **23**(5): p. 611-28.
146. Streicher, J.M., *The Role of Heat Shock Proteins in Regulating Receptor Signal Transduction.* Mol Pharmacol, 2019. **95**(5): p. 468-474.
147. Burlison, J.A., et al., *Novobiocin: redesigning a DNA gyrase inhibitor for selective inhibition of hsp90.* J Am Chem Soc, 2006. **128**(48): p. 15529-36.
148. Ananthan, S., et al., *14-Alkoxy- and 14-acyloxypyridomorphinans: mu agonist/delta antagonist opioid analgesics with diminished tolerance and dependence side effects.* J Med Chem, 2012. **55**(19): p. 8350-63.
149. Chaplan, S.R., et al., *Quantitative assessment of tactile allodynia in the rat paw.* J Neurosci Methods, 1994. **53**(1): p. 55-63.
150. Kruse, R., et al., *Characterization of the CLASP2 Protein Interaction Network Identifies SOGA1 as a Microtubule-Associated Protein.* Mol Cell Proteomics, 2017. **16**(10): p. 1718-1735.
151. Parker, S.S., et al., *Insulin Induces Microtubule Stabilization and Regulates the Microtubule Plus-end Tracking Protein Network in Adipocytes.* Mol Cell Proteomics, 2019. **18**(7): p. 1363-1381.
152. Deutsch, E.W., et al., *The ProteomeXchange consortium in 2017: supporting the cultural change in proteomics public data deposition.* Nucleic Acids Res, 2017. **45**(D1): p. D1100-D1106.
153. Perez-Riverol, Y., et al., *The PRIDE database and related tools and resources in 2019: improving support for quantification data.* Nucleic Acids Res, 2019. **47**(D1): p. D442-D450.
154. Chiosis, G., C.A. Dickey, and J.L. Johnson, *A global view of Hsp90 functions.* Nat Struct Mol Biol, 2013. **20**(1): p. 1-4.
155. McClellan, A.J., et al., *Diverse cellular functions of the Hsp90 molecular chaperone uncovered using systems approaches.* Cell, 2007. **131**(1): p. 121-35.
156. Thanomkitti, K., et al., *Molecular functional analyses revealed essential roles of HSP90 and lamin A/C in growth, migration, and self-aggregation of dermal papilla cells.* Cell Death Discov, 2018. **4**: p. 53.
157. Ansar, S., et al., *A non-toxic Hsp90 inhibitor protects neurons from Abeta-induced toxicity.* Bioorg Med Chem Lett, 2007. **17**(7): p. 1984-90.
158. Smith, V., et al., *Comparison of 17-dimethylaminoethylamino-17-demethoxy-geldanamycin (17DMAG) and 17-allylamino-17-demethoxygeldanamycin (17AAG) in vitro: effects on Hsp90 and client proteins in melanoma models.* Cancer Chemother Pharmacol, 2005. **56**(2): p. 126-37.

159. Kwon, H.M., et al., *Geldanamycin protects rat brain through overexpression of HSP70 and reducing brain edema after cerebral focal ischemia.* Neurol Res, 2008. **30**(7): p. 740-5.
160. Cargnello, M. and P.P. Roux, *Activation and function of the MAPKs and their substrates, the MAPK-activated protein kinases.* Microbiol Mol Biol Rev, 2011. **75**(1): p. 50-83.
161. Gehart, H., et al., *MAPK signalling in cellular metabolism: stress or wellness?* EMBO Rep, 2010. **11**(11): p. 834-40.
162. Pal, J.K., *Hsp90 regulates protein synthesis by activating the heme-regulated eukaryotic initiation factor 2α (eIF-2α) kinase in rabbit reticulocyte lysates.* Journal of Biosciences, 1998. **23**(4): p. 353-360.
163. Uma, S., et al., *Hsp90 is obligatory for the heme-regulated eIF-2alpha kinase to acquire and maintain an activable conformation.* J Biol Chem, 1997. **272**(17): p. 11648-56.
164. Darcq, E., et al., *RSK2 signaling in medial habenula contributes to acute morphine analgesia.* Neuropsychopharmacology, 2012. **37**(5): p. 1288-96.
165. Roux, P.P., et al., *Tumor-promoting phorbol esters and activated Ras inactivate the tuberous sclerosis tumor suppressor complex via p90 ribosomal S6 kinase.* Proc Natl Acad Sci U S A, 2004. **101**(37): p. 13489-94.
166. Shahbazian, D., et al., *The mTOR/PI3K and MAPK pathways converge on eIF4B to control its phosphorylation and activity.* Embo j, 2006. **25**(12): p. 2781-91.
167. Roux, P.P., et al., *RAS/ERK signaling promotes site-specific ribosomal protein S6 phosphorylation via RSK and stimulates cap-dependent translation.* J Biol Chem, 2007. **282**(19): p. 14056-64.
168. Sutherland, C., I.A. Leighton, and P. Cohen, *Inactivation of glycogen synthase kinase-3 beta by phosphorylation: new kinase connections in insulin and growth-factor signalling.* Biochem J, 1993. **296 (Pt 1)**: p. 15-9.
169. Cohen, P. and S. Frame, *The renaissance of GSK3.* Nature Reviews Molecular Cell Biology, 2001. **2**(10): p. 769-776.
170. Wang, X., et al., *Regulation of elongation factor 2 kinase by p90(RSK1) and p70 S6 kinase.* Embo j, 2001. **20**(16): p. 4370-9.
171. Anjum, R. and J. Blenis, *The RSK family of kinases: emerging roles in cellular signalling.* Nat Rev Mol Cell Biol, 2008. **9**(10): p. 747-58.
172. Macey, T.A., J.D. Lowe, and C. Chavkin, *Mu opioid receptor activation of ERK1/2 is GRK3 and arrestin dependent in striatal neurons.* The Journal of biological chemistry, 2006. **281**(45): p. 34515-34524.
173. Duraffourd, C., et al., *Opioid-induced mitogen-activated protein kinase signaling in rat enteric neurons following chronic morphine treatment.* PLoS One, 2014. **9**(10): p. e110230.
174. Gutstein, H.B., et al., *Opioid effects on mitogen-activated protein kinase signaling cascades.* Anesthesiology, 1997. **87**(5): p. 1118-26.
175. Schmidt, H., et al., *Involvement of mitogen-activated protein kinase in agonist-induced phosphorylation of the mu-opioid receptor in HEK 293 cells.* J Neurochem, 2000. **74**(1): p. 414-22.
176. Chen, Y., C. Geis, and C. Sommer, *Activation of TRPV1 contributes to morphine tolerance: involvement of the mitogen-activated protein kinase signaling pathway.* J Neurosci, 2008. **28**(22): p. 5836-45.
177. Popiolek-Barczyk, K., et al., *Inhibition of intracellular signaling pathways NF-kappaB and MEK1/2 attenuates neuropathic pain development and enhances morphine analgesia.* Pharmacol Rep, 2014. **66**(5): p. 845-51.

178. Kim, N., J.Y. Kim, and M.A. Yenari, *Pharmacological induction of the 70-kDa heat shock protein protects against brain injury.* Neuroscience, 2015. **284**: p. 912-9.
179. Wang, Y. and S.R. McAlpine, *Heat-shock protein 90 inhibitors: will they ever succeed as chemotherapeutics?* Future Med Chem, 2015. **7**(2): p. 87-90.
180. Ossipov, M.H., et al., *Spinal and supraspinal mechanisms of neuropathic pain.* Ann N Y Acad Sci, 2000. **909**: p. 12-24.
181. Heinricher, M.M., et al., *Descending control of nociception: Specificity, recruitment and plasticity.* Brain Res Rev, 2009. **60**(1): p. 214-25.
182. Voon, P., M. Karamouzian, and T. Kerr, *Chronic pain and opioid misuse: a review of reviews.* Subst Abuse Treat Prev Policy, 2017. **12**(1): p. 36.
183. Eckl, J.M. and K. Richter, *Functions of the Hsp90 chaperone system: lifting client proteins to new heights.* International journal of biochemistry and molecular biology, 2013. **4**(4): p. 157-165.
184. Taipale, M., D.F. Jarosz, and S. Lindquist, *HSP90 at the hub of protein homeostasis: emerging mechanistic insights.* Nature Reviews Molecular Cell Biology, 2010. **11**(7): p. 515-528.
185. Mansfield, A.S., et al., *48 - New Targets for Therapy in Lung Cancer*, in *IASLC Thoracic Oncology (Second Edition)*, H.I. Pass, D. Ball, and G.V. Scagliotti, Editors. 2018, Content Repository Only!: Philadelphia. p. 479-489.e6.
186. Forsberg, L.K., et al., *Development of noviomimetics that modulate molecular chaperones and manifest neuroprotective effects.* Eur J Med Chem, 2018. **143**: p. 1428-1435.
187. Zhao, H., et al., *Novologues containing a benzamide side chain manifest anti-proliferative activity against two breast cancer cell lines.* Bioorg Med Chem Lett, 2014. **24**(15): p. 3633-7.
188. Yuan, S.-B., et al., *Gp120 in the pathogenesis of human immunodeficiency virus–associated pain.* Annals of Neurology, 2014. **75**(6): p. 837-850.
189. Ji, R.R., et al., *MAP kinase and pain.* Brain Res Rev, 2009. **60**(1): p. 135-48.
190. Imbe, H., et al., *Activation of mitogen-activated protein kinase in descending pain modulatory system.* Journal of signal transduction, 2011. **2011**: p. 468061-468061.
191. Qu, Y.J., et al., *MAPK Pathways Are Involved in Neuropathic Pain in Rats with Chronic Compression of the Dorsal Root Ganglion.* Evid Based Complement Alternat Med, 2016. **2016**: p. 6153215.
192. Sofis, M.J., et al., *KU32 prevents 5-fluorouracil induced cognitive impairment.* Behavioural brain research, 2017. **329**: p. 186-190.
193. Farmer, K., et al., *KU-32, a novel drug for diabetic neuropathy, is safe for human islets and improves in vitro insulin secretion and viability.* Exp Diabetes Res, 2012. **2012**: p. 671673.
194. Donnelly, A. and B.S.J. Blagg, *Novobiocin and additional inhibitors of the Hsp90 C-terminal nucleotide-binding pocket.* Current medicinal chemistry, 2008. **15**(26): p. 2702-2717.
195. Martyn, J.A.J., J. Mao, and E.A. Bittner, *Opioid Tolerance in Critical Illness.* N Engl J Med, 2019. **380**(4): p. 365-378.
196. Sim-Selley, L.J., et al., *Region-dependent attenuation of mu opioid receptor-mediated G-protein activation in mouse CNS as a function of morphine tolerance.* Br J Pharmacol, 2007. **151**(8): p. 1324-33.

197. Dumas, E.O. and G.M. Pollack, *Opioid tolerance development: a pharmacokinetic/pharmacodynamic perspective.* The AAPS journal, 2008. **10**(4): p. 537-551.
198. Berta, T., et al., *Tissue plasminogen activator contributes to morphine tolerance and induces mechanical allodynia via astrocytic IL-1beta and ERK signaling in the spinal cord of mice.* Neuroscience, 2013. **247**: p. 376-85.
199. Wang, Z., et al., *Cell-type specific activation of p38 and ERK mediates calcitonin gene-related peptide involvement in tolerance to morphine-induced analgesia.* Faseb j, 2009. **23**(8): p. 2576-86.
200. Brock, C., et al., *Opioid-induced bowel dysfunction: pathophysiology and management.* Drugs, 2012. **72**(14): p. 1847-65.
201. Kumar, L., C. Barker, and A. Emmanuel, *Opioid-induced constipation: pathophysiology, clinical consequences, and management.* Gastroenterol Res Pract, 2014. **2014**: p. 141737.
202. Nelson, A.D. and M. Camilleri, *Opioid-induced constipation: advances and clinical guidance.* Therapeutic advances in chronic disease, 2016. **7**(2): p. 121-134.
203. Le Merrer, J., et al., *Reward processing by the opioid system in the brain.* Physiological reviews, 2009. **89**(4): p. 1379-1412.
204. Schiller, E.Y. and O.J. Mechanic, *Opioid Overdose*, in *StatPearls*. 2019, StatPearls Publishing

StatPearls Publishing LLC.: Treasure Island (FL).
205. Manchikanti, L., et al., *Opioid epidemic in the United States.* Pain Physician, 2012. **15**(3 Suppl): p. Es9-38.
206. Nicol, A.L., R.W. Hurley, and H.T. Benzon, *Alternatives to Opioids in the Pharmacologic Management of Chronic Pain Syndromes: A Narrative Review of Randomized, Controlled, and Blinded Clinical Trials.* Anesth Analg, 2017. **125**(5): p. 1682-1703.
207. Reiman, A., M. Welty, and P. Solomon, *Cannabis as a Substitute for Opioid-Based Pain Medication: Patient Self-Report.* Cannabis Cannabinoid Res, 2017. **2**(1): p. 160-166.
208. Knezevic, N.N., A. Yekkirala, and T.L. Yaksh, *Basic/Translational Development of Forthcoming Opioid- and Nonopioid-Targeted Pain Therapeutics.* Anesth Analg, 2017. **125**(5): p. 1714-1732.
209. Anton, S.D., et al., *Flipping the Metabolic Switch: Understanding and Applying the Health Benefits of Fasting.* Obesity (Silver Spring, Md.), 2018. **26**(2): p. 254-268.
210. Wallinga, D., *Today's Food System: How Healthy Is It?* Journal of hunger & environmental nutrition, 2009. **4**(3-4): p. 251-281.
211. Cuschieri, S. and J. Mamo, *Getting to grips with the obesity epidemic in Europe.* SAGE open medicine, 2016. **4**: p. 2050312116670406-2050312116670406.
212. Imes, C.C. and L.E. Burke, *The Obesity Epidemic: The United States as a Cautionary Tale for the Rest of the World.* Current epidemiology reports, 2014. **1**(2): p. 82-88.
213. Mattson, M.P., *Lifelong brain health is a lifelong challenge: from evolutionary principles to empirical evidence.* Ageing Res Rev, 2015. **20**: p. 37-45.
214. Fontana, L. and L. Partridge, *Promoting health and longevity through diet: from model organisms to humans.* Cell, 2015. **161**(1): p. 106-118.
215. Sutton, E.F., et al., *Early Time-Restricted Feeding Improves Insulin Sensitivity, Blood Pressure, and Oxidative Stress Even without Weight Loss in Men with Prediabetes.* Cell metabolism, 2018. **27**(6): p. 1212-1221.e3.

216. Barzilai, N., et al., *Caloric restriction reverses hepatic insulin resistance in aging rats by decreasing visceral fat.* J Clin Invest, 1998. **101**(7): p. 1353-61.
217. Klempel, M.C., et al., *Intermittent fasting combined with calorie restriction is effective for weight loss and cardio-protection in obese women.* Nutr J, 2012. **11**: p. 98.
218. Antoni, R., et al., *Effects of intermittent fasting on glucose and lipid metabolism.* Proc Nutr Soc, 2017. **76**(3): p. 361-368.
219. Barnosky, A.R., et al., *Intermittent fasting vs daily calorie restriction for type 2 diabetes prevention: a review of human findings.* Transl Res, 2014. **164**(4): p. 302-11.
220. Li, C., et al., *Effects of A One-week Fasting Therapy in Patients with Type-2 Diabetes Mellitus and Metabolic Syndrome - A Randomized Controlled Explorative Study.* Exp Clin Endocrinol Diabetes, 2017. **125**(9): p. 618-624.
221. Kim, K.H., et al., *Intermittent fasting promotes adipose thermogenesis and metabolic homeostasis via VEGF-mediated alternative activation of macrophage.* Cell Res, 2017. **27**(11): p. 1309-1326.
222. Zhang, S., et al., *Aging and Intermittent Fasting Impact on Transcriptional Regulation and Physiological Responses of Adult Drosophila Neuronal and Muscle Tissues.* Int J Mol Sci, 2018. **19**(4).
223. Cherif, A., et al., *Effects of Intermittent Fasting, Caloric Restriction, and Ramadan Intermittent Fasting on Cognitive Performance at Rest and During Exercise in Adults.* Sports Med, 2016. **46**(1): p. 35-47.
224. Brandhorst, S., et al., *A Periodic Diet that Mimics Fasting Promotes Multi-System Regeneration, Enhanced Cognitive Performance, and Healthspan.* Cell Metab, 2015. **22**(1): p. 86-99.
225. Wei, M., et al., *Fasting-mimicking diet and markers/risk factors for aging, diabetes, cancer, and cardiovascular disease.* Sci Transl Med, 2017. **9**(377).
226. Fann, D.Y., et al., *Positive effects of intermittent fasting in ischemic stroke.* Exp Gerontol, 2017. **89**: p. 93-102.
227. Mattson, M.P. and R. Wan, *Beneficial effects of intermittent fasting and caloric restriction on the cardiovascular and cerebrovascular systems.* J Nutr Biochem, 2005. **16**(3): p. 129-37.
228. Shin, B.K., et al., *Intermittent fasting protects against the deterioration of cognitive function, energy metabolism and dyslipidemia in Alzheimer's disease-induced estrogen deficient rats.* Exp Biol Med (Maywood), 2018. **243**(4): p. 334-343.
229. Razeghi Jahromi, S., et al., *Effects of Intermittent Fasting on Experimental Autoimune Encephalomyelitis in C57BL/6 Mice.* Iran J Allergy Asthma Immunol, 2016. **15**(3): p. 212-9.
230. Berridge, K.C., *Food reward: brain substrates of wanting and liking.* Neurosci Biobehav Rev, 1996. **20**(1): p. 1-25.
231. Morales, I., et al., *Involvement of opioid signaling in food preference and motivation: Studies in laboratory animals.* Prog Brain Res, 2016. **229**: p. 159-187.
232. Bodnar, R.J., *Endogenous opioids and feeding behavior: a 30-year historical perspective.* Peptides, 2004. **25**(4): p. 697-725.
233. Barnes, M.J., S.D. Primeaux, and G.A. Bray, *Food deprivation increases the mRNA expression of micro-opioid receptors in the ventral medial hypothalamus and arcuate nucleus.* Am J Physiol Regul Integr Comp Physiol, 2008. **295**(5): p. R1385-90.
234. Scheggi, S., et al., *Fasting biases mu-opioid receptors toward beta-arrestin2-dependent signaling in the accumbens shell.* Neuroscience, 2017. **352**: p. 19-29.

235. Bencherif, B., et al., *Regional mu-opioid receptor binding in insular cortex is decreased in bulimia nervosa and correlates inversely with fasting behavior.* J Nucl Med, 2005. **46**(8): p. 1349-51.
236. Lei, W., et al., *A Novel Mu-Delta Opioid Agonist Demonstrates Enhanced Efficacy with Reduced Tolerance and Dependence in Mouse Neuropathic Pain Models.* J Pain, 2019.
237. Olson, K.M., et al., *Comprehensive molecular pharmacology screening reveals potential new receptor interactions for clinically relevant opioids.* PLoS One, 2019. **14**(6): p. e0217371.
238. Olson, K.M., et al., *Synthesis and Evaluation of a Novel Bivalent Selective Antagonist for the Mu-Delta Opioid Receptor Heterodimer that Reduces Morphine Withdrawal in Mice.* J Med Chem, 2018. **61**(14): p. 6075-6086.
239. Stefanucci, A., et al., *Fluorescent-labeled bioconjugates of the opioid peptides biphalin and DPDPE incorporating fluorescein-maleimide linkers.* Future Med Chem, 2017. **9**(9): p. 859-869.
240. Ramos-Colon, C.N., et al., *Structure-Activity Relationships of [des-Arg(7)]Dynorphin A Analogues at the kappa Opioid Receptor.* J Med Chem, 2016. **59**(22): p. 10291-10298.
241. Williams, J.T., et al., *Regulation of mu-opioid receptors: desensitization, phosphorylation, internalization, and tolerance.* Pharmacol Rev, 2013. **65**(1): p. 223-54.
242. Streicher, J.M. and E.J. Bilsky, *Peripherally Acting micro-Opioid Receptor Antagonists for the Treatment of Opioid-Related Side Effects: Mechanism of Action and Clinical Implications.* J Pharm Pract, 2017: p. 897190017732263.
243. Dalesio, N.M., et al., *Effects of Obesity and Leptin Deficiency on Morphine Pharmacokinetics in a Mouse Model.* Anesth Analg, 2016. **123**(6): p. 1611-1617.
244. Benarroch, E.E., *Endogenous opioid systems: current concepts and clinical correlations.* Neurology, 2012. **79**(8): p. 807-14.
245. Kroenke, K., E.E. Krebs, and M.J. Bair, *Pharmacotherapy of chronic pain: a synthesis of recommendations from systematic reviews.* Gen Hosp Psychiatry, 2009. **31**(3): p. 206-19.
246. Jung, C., et al., *Effects of food restriction on expression of place conditioning and biochemical correlates in rat nucleus accumbens.* Psychopharmacology (Berl), 2016. **233**(17): p. 3161-72.
247. Matsushita, Y., et al., *Microglia activation precedes the anti-opioid BDNF and NMDA receptor mechanisms underlying morphine analgesic tolerance.* Curr Pharm Des, 2013. **19**(42): p. 7355-61.
248. Macey, T.A., et al., *Extracellular signal-regulated kinase 1/2 activation counteracts morphine tolerance in the periaqueductal gray of the rat.* J Pharmacol Exp Ther, 2009. **331**(2): p. 412-8.
249. Shaqura, M., et al., *Reduced number, G protein coupling, and antinociceptive efficacy of spinal mu-opioid receptors in diabetic rats are reversed by nerve growth factor.* J Pain, 2013. **14**(7): p. 720-30.
250. Moy, J.K., et al., *eIF4E phosphorylation regulates ongoing pain, independently of inflammation, and hyperalgesic priming in the mouse CFA model.* Neurobiol Pain, 2018. **4**: p. 45-50.
251. Dou, F., L.D. Yuan, and J.J. Zhu, *Heat shock protein 90 indirectly regulates ERK activity by affecting Raf protein metabolism.* Acta Biochim Biophys Sin (Shanghai), 2005. **37**(7): p. 501-5.
252. Piatelli, M.J., C. Doughty, and T.C. Chiles, *Requirement for a hsp90 chaperone-dependent MEK1/2-ERK pathway for B cell antigen receptor-induced cyclin D2 expression in mature B lymphocytes.* J Biol Chem, 2002. **277**(14): p. 12144-50.

253. Rozenfeld, R. and L.A. Devi, *Receptor heterodimerization leads to a switch in signaling: beta-arrestin2-mediated ERK activation by mu-delta opioid receptor heterodimers.* FASEB journal : official publication of the Federation of American Societies for Experimental Biology, 2007. **21**(10): p. 2455-2465.
254. Gutstein, Howard B., MD, et al., *Opioid Effects on Mitogen-activated Protein Kinase Signaling Cascades* Anesthesiology: The Journal of the American Society of Anesthesiologists, 1997. **87**(5): p. 1118-1126.
255. Belcheva, M.M., et al., *Mu and kappa opioid receptors activate ERK/MAPK via different protein kinase C isoforms and secondary messengers in astrocytes.* J Biol Chem, 2005. **280**(30): p. 27662-9.
256. Koga, F., et al., *Hsp90 inhibition transiently activates Src kinase and promotes Src-dependent Akt and Erk activation.* Proceedings of the National Academy of Sciences, 2006. **103**(30): p. 11318-11322.
257. Komatsu, T., et al., *Inhibition of ERK phosphorylation by substance P N-terminal fragment decreases capsaicin-induced nociceptive response.* Neuropharmacology, 2011. **61**(4): p. 608-13.
258. Kingwell, K., *MAPK inhibitor shows promise in clinical trial for neuropathic pain.* Nature Reviews Neurology, 2011. **7**(7): p. 360-360.
259. Su, S.C., et al., *Regulation of N-type voltage-gated calcium channels and presynaptic function by cyclin-dependent kinase 5.* Neuron, 2012. **75**(4): p. 675-687.
260. Herlitze, S., et al., *Allosteric modulation of Ca²⁺ channels by G proteins, voltage-dependent facilitation, protein kinase C, and Ca_vβ subunits.* Proceedings of the National Academy of Sciences, 2001. **98**(8): p. 4699-4704.
261. Roux, P.P. and I. Topisirovic, *Regulation of mRNA translation by signaling pathways.* Cold Spring Harbor perspectives in biology, 2012. **4**(11): p. a012252.
262. Freedman, L.S., M.E. Judge, and D. Quartermain, *Effects of cycloheximide, a protein synthesis inhibitor, on mouse brain catecholamine biochemistry.* Pharmacology Biochemistry and Behavior, 1982. **17**(2): p. 187-191.
263. Morales-Corraliza, J., et al., *In Vivo Turnover of Tau and APP Metabolites in the Brains of Wild-Type and Tg2576 Mice: Greater Stability of sAPP in the β-Amyloid Depositing Mice.* PLOS ONE, 2009. **4**(9): p. e7134.
264. Roux, P.P., et al., *RAS/ERK signaling promotes site-specific ribosomal protein S6 phosphorylation via RSK and stimulates cap-dependent translation.* The Journal of biological chemistry, 2007. **282**(19): p. 14056-14064.
265. Cargnello, M. and P.P. Roux, *Activation and Function of the MAPKs and Their Substrates, the MAPK-Activated Protein Kinases.* Microbiology and Molecular Biology Reviews, 2011. **75**(1): p. 50-83.
266. Haslbeck, V., et al., *The activity of protein phosphatase 5 towards native clients is modulated by the middle- and C-terminal domains of Hsp90.* Scientific Reports, 2015. **5**(1): p. 17058.
267. Hao, S., *The Molecular and Pharmacological Mechanisms of HIV-Related Neuropathic Pain.* Current neuropharmacology, 2013. **11**(5): p. 499-512.
268. Liu, B., X. Liu, and S.-J. Tang, *Interactions of Opioids and HIV Infection in the Pathogenesis of Chronic Pain.* Frontiers in microbiology, 2016. **7**: p. 103-103.
269. Farmer, A.D., et al., *Pathophysiology and management of opioid-induced constipation: European expert consensus statement.* United European gastroenterology journal, 2019. **7**(1): p. 7-20.

270. Malinowski, B., et al., *Intermittent Fasting in Cardiovascular Disorders-An Overview.* Nutrients, 2019. **11**(3): p. 673.
271. Anderson, K.E., *Influences of diet and nutrition on clinical pharmacokinetics.* Clin Pharmacokinet, 1988. **14**(6): p. 325-46.
272. Perez-Pitarch, A., et al., *Impact of Undernutrition on the Pharmacokinetics and Pharmacodynamics of Anticancer Drugs: A Literature Review.* Nutr Cancer, 2017. **69**(4): p. 555-563.
273. Johansson, S.A., et al., *Effect of Food Intake on the Pharmacodynamics of Tenapanor: A Phase 1 Study.* Clinical pharmacology in drug development, 2017. **6**(5): p. 457-465.
274. Cintron-Colon, R., et al., *Activation of Kappa Opioid Receptor Regulates the Hypothermic Response to Calorie Restriction and Limits Body Weight Loss.* Current Biology, 2019.
275. Stice, E., K. Burger, and S. Yokum, *Caloric deprivation increases responsivity of attention and reward brain regions to intake, anticipated intake, and images of palatable foods.* NeuroImage, 2013. **67**: p. 322-330.
276. Shojaie, M., F. Ghanbari, and N. Shojaie, *Intermittent fasting could ameliorate cognitive function against distress by regulation of inflammatory response pathway.* Journal of Advanced Research, 2017. **8**(6): p. 697-701.
277. Krause, J.S., et al., *Effects of short-term fasting on stress physiology, body condition, and locomotor activity in wintering male white-crowned sparrows.* Physiology & Behavior, 2017. **177**: p. 282-290.
278. Mooij, M.G., et al., *Development of Human Membrane Transporters: Drug Disposition and Pharmacogenetics.* Clinical Pharmacokinetics, 2016. **55**(5): p. 507-524.
279. Mercer, S.L. and A. Coop, *Opioid analgesics and P-glycoprotein efflux transporters: a potential systems-level contribution to analgesic tolerance.* Current topics in medicinal chemistry, 2011. **11**(9): p. 1157-1164.
280. Zheng, H., et al., *Cholesterol level influences opioid signaling in cell models and analgesia in mice and humans.* Journal of lipid research, 2012. **53**(6): p. 1153-1162.
281. Bowman, S.L., et al., *Cell-autonomous regulation of Mu-opioid receptor recycling by substance P.* Cell Rep, 2015. **10**(11): p. 1925-36.
282. Erbs, E., et al., *A mu-delta opioid receptor brain atlas reveals neuronal co-occurrence in subcortical networks.* Brain structure & function, 2015. **220**(2): p. 677-702.
283. Giuliano, C. and P. Cottone, *The role of the opioid system in binge eating disorder.* CNS spectrums, 2015. **20**(6): p. 537-545.
284. Cabral, A., et al., *Is Ghrelin Synthesized in the Central Nervous System?* International journal of molecular sciences, 2017. **18**(3): p. 638.
285. Ferrini, F., et al., *Ghrelin in central neurons.* Current neuropharmacology, 2009. **7**(1): p. 37-49.
286. Wu, B., et al., *The antinociceptive effects and molecular mechanisms of ghrelin(1-7)-NH2 at the supraspinal level in acute pain in mice.* Brain Res Bull, 2019. **146**: p. 112-123.
287. Engel, J.A., I. Nylander, and E. Jerlhag, *A ghrelin receptor (GHS-R1A) antagonist attenuates the rewarding properties of morphine and increases opioid peptide levels in reward areas in mice.* Eur Neuropsychopharmacol, 2015. **25**(12): p. 2364-71.
288. Pirzadeh, S., et al., *Effects of Intracerebroventricular and Intra-Arcuate Nucleus Injection of Ghrelin on Pain Behavioral Responses and Met-Enkephalin and β-Endorphin Concentrations in the Periaqueductal Gray Area in Rats.* International journal of molecular sciences, 2019. **20**(10): p. 2475.

289. Tortorici, V., C.S. Robbins, and M.M. Morgan, *Tolerance to the antinociceptive effect of morphine microinjections into the ventral but not lateral-dorsal periaqueductal gray of the rat.* Behav Neurosci, 1999. **113**(4): p. 833-9.
290. Morgan, M.M., C.C. Clayton, and J.S. Boyer-Quick, *Differential susceptibility of the PAG and RVM to tolerance to the antinociceptive effect of morphine in the rat.* Pain, 2005. **113**(1-2): p. 91-8.
291. Wood, J.D. and J.J. Galligan, *Function of opioids in the enteric nervous system.* Neurogastroenterology & Motility, 2004. **16**(s2): p. 17-28.
292. Niel, J.P., *[Role of substance P in the nervous system control of digestive motility].* Arch Int Physiol Biochim Biophys, 1991. **99**(5): p. A65-76.
293. Nishiwaki, H., et al., *Possible role of potassium channels in mu-receptor-mediated inhibition and muscarinic autoinhibition in acetylcholine release from myenteric plexus of guinea pig ileum.* Jpn J Pharmacol, 2000. **82**(4): p. 343-9.
294. Paton, W.D., *The action of morphine and related substances on contraction and on acetylcholine output of coaxially stimulated guinea-pig ileum. 1956.* Br J Pharmacol, 1997. **120**(4 Suppl): p. 123-31; discussion 121-2.
295. Galligan, J.J. and H.I. Akbarali, *Molecular physiology of enteric opioid receptors.* American journal of gastroenterology supplements (Print), 2014. **2**(1): p. 17-21.
296. Galligan, J.J. and C. Sternini, *Insights into the Role of Opioid Receptors in the GI Tract: Experimental Evidence and Therapeutic Relevance.* Handb Exp Pharmacol, 2017. **239**: p. 363-378.
297. Ho, K.Y., et al., *Fasting enhances growth hormone secretion and amplifies the complex rhythms of growth hormone secretion in man.* The Journal of clinical investigation, 1988. **81**(4): p. 968-975.
298. Harvie, M. and A. Howell, *Potential Benefits and Harms of Intermittent Energy Restriction and Intermittent Fasting Amongst Obese, Overweight and Normal Weight Subjects-A Narrative Review of Human and Animal Evidence.* Behavioral sciences (Basel, Switzerland), 2017. **7**(1): p. 4.
299. Ravussin, E., et al., *Early Time-Restricted Feeding Reduces Appetite and Increases Fat Oxidation But Does Not Affect Energy Expenditure in Humans.* Obesity (Silver Spring), 2019. **27**(8): p. 1244-1254.
300. Husted, A.S., et al., *GPCR-Mediated Signaling of Metabolites.* Cell Metab, 2017. **25**(4): p. 777-796.
301. Sweetlove, L.J., et al., *The Mitochondrion: An Integration Point of Cellular Metabolism and Signalling.* Critical Reviews in Plant Sciences, 2007. **26**(1): p. 17-43.
302. van der Knaap, J.A. and C.P. Verrijzer, *Undercover: gene control by metabolites and metabolic enzymes.* Genes Dev, 2016. **30**(21): p. 2345-2369.
303. Huang, P., V. Chandra, and F. Rastinejad, *Structural overview of the nuclear receptor superfamily: insights into physiology and therapeutics.* Annual review of physiology, 2010. **72**: p. 247-272.
304. Zhang, Q., et al., *The Role of Endocrine G Protein-Coupled Receptors in Ovarian Cancer Progression.* Frontiers in endocrinology, 2017. **8**: p. 66-66.
305. Wang, D., et al., *G-protein-coupled receptor controls steroid hormone signaling in cell membrane.* Scientific Reports, 2015. **5**(1): p. 8675.
306. Kasson, B.G. and R. George, *Endocrine influences on the actions of morphine. I. Alteration of target gland hormones.* J Pharmacol Exp Ther, 1983. **224**(2): p. 273-81.
307. Sianati, S., et al., *Effects of female sex hormones on morphine dependence.* Annals of General Psychiatry, 2008. **7**(1): p. S264.